11-5-2017

# A decision support system for ship’s energy efficient operation: based on artificial neural network method

Yasser Bayoumy Abdelwahab Farag

**WORLD MARITIME UNIVERSITY**
Malmö, Sweden

# A DECISION SUPPORT SYSTEM FOR SHIP'S ENERGY EFFICIENT OPERATION

## Based on ANN problem case

**By**

**YASSER B. A. FARAG**

**The Arab Republic of Egypt**

A dissertation submitted to the World Maritime University in partial fulfillment of the requirements for the award of the degree of

**MASTER OF SCIENCE**
**In**
**MARITIME AFFAIRS**

**(MARITIME ENERGY MANAGEMENT)**

*2017*

I certify that all the material in the dissertation that is not my work has been identified and that no material is included for which a degree previously been conferred on me.

The contents of this dissertation reflect my own personal views and are necessarily endorsed by the university.

(Signature): ……………………………………..

(Date): ……………………………………………

**Supervised by:**

**World Maritime University**

# *Abstract*


The technical upgrades are not the only way to achieve improvements in ship's energy efficiency, changing the crew operation behavior on board can gain cost-free energy savings. These potential behavioral savings need to be guided by analyzing the ship operational data and distinguish the inherent opportunities in the ship dynamic operating environment. However, achieving an optimized energy-efficient performance for ship's operation is an enormous challenge that requires a robust mechanism decision support system for the ship operators.

The thesis aims to employ a non-classical methodology for the ship performance prediction; to develop a Decision Support System for energy efficient ship operation.

The study has proposed an operational Decision Support System (DSS) that comprises mainly two primary components, the ship performance prediction Model (PPM) and the ship Performance Optimization Model (POM). The (PPM) employed Artificial Neural Network and Multi regression analysis methodologies. The (ANN) model has been developed by intensive dataset rather Noon Reports as opposed to previously published studies.

The proposed (DSS) has been tested with three case studies, to assess its applicability, the results are presented for evaluation.



**Keywords:** Ship Energy Efficiency, Operational Measures, Fuel Savings, GHG emissions, Ship Performance Optimization, Decision Support System, Multiple Regression analysis, Artificial Neural Network

# *Acknowledgment*

*I owe my deepest gratitude to my precious wife; Marwa for her unconditional support throughout our journey, thank you for being the inspiration I needed. I also grateful to my boys Ammar, Omar, Anas and Abdullah for enduring me while I was hectic for the past 14 months, and they never complained.*

*I am grateful to NAPA for providing me with their precious data that made this research possible. Special thanks to Mr. Ilie George Adrian how endured my endless emails.*

*Then, my two favorites, they were my mentors; they directed me in my research activities; one taught me inquisitiveness, the other taught me problem-solving. Thank you, Prof. A.Olcer and Prof. M.A. Qotb for educating me.*

*I appreciate the support the Arab Academy For Science, Technology and Maritime Transportation ( AASTMT) provided me through the last year of my MSc study. I also appreciate the sacrifices my colleagues made in the Maritime Upgrading Studies Institute to cover my absence for such a long period, without your assistance, I would not be here in the first place.*

*Last but not least, I want to express my appreciation to the first class of MEM specialization, teaching staff and the students. Everday I had learned something new from you in this journey. I wish you all the best in your lives.*

# *Table of Contents*

# *List of Figures*

# *List of Tables*

# *Abbreviations and symbols*

| | |
|---|---|
| UN | United Nation |
| GHG | Green House Gases |
| IMO | International Maritime Organization |
| MEPC | Maritime Environment Protection Committee |
| UNFCCC | United Nations Framework Climate Change Convention |
| MARPOL | The International |
| EEDI | Energy Efficiency Design Index |
| EEOI | Energy Efficiency Operational Indicator |
| ANN | Artificial Neural Network |
| DSS | Decision Support System |
| HFO | Heavy Fuel Oil |
| USD | United States Dollar |
| CO2 | Carbon Dioxide |
| RFR | Required Freight Rate |
| SOG | Speed Over Ground |
| B.S.F.C | Brake Specific Fuel Consumption |
| mt | Metric ton |
| kn | Knot |
| kW | Kilo Watt |
| nm | Nautical miles |
| JIT | Just In Time |
| CSR | Continuous Service Rating |
| CFD | Computational Fluid Dynamic |
| OEEM | Operational Energy Efficiency Measure |
| ITTC | International Towing Tank Conference |
| M.R | Multiple Regression Analysis |

| | |
|---|---|
| PPM | Performance Prediction Model |
| VOM | Voyage Optimization Management |
| POM | Performance Optimization Model |
| NR | Noon Report |
| CM | Continuous Monitoring |
| AIS | Automatic identification system |

# Chapter 1.

# Introduction

## 1.1 Background

The maritime transport is undoubtedly indispensable for securing a sustainable future of the global economy. In 2015 ships carried more than 10 billion tonnes of cargo by volume and 2.2 billion passengers, all these figures secured the maritime transport a place as the most energy-efficient mode of transporting mass freight. Moreover, based on the data collected between 1980 and 2014, a growth of international seaborne trade by 265% had observed during that period (UNCTAD, 2016, p. 7). With that critical role shipping plays, its share of global GHG emissions represents 2.5% of global GHG emissions with around 1000 million tonnes annually according to the (Third IMO GHG study 2014). However, referring to the same study, the shipping share in the global carbon dioxide emissions has projected to increase from 50% to 250% as a result of the seaborne trade expected expansion and other industries emission reductions. All of that may explain why the International Maritime Organization (IMO) chose early to join the global efforts to achieve the UNFCC primary objective of maintaining GHG concentrations at a safe level to prevent any further dangerous anthropogenic effect with the climate system (UNFCCC, Art. 2).

By the entry into force of MARPOL Annex VI, Chapter IV, on the 1st of January 2013, the IMO established the first mandatory global regime controlling the GHG emissions among the entire transport sector.The new chapter included the new design and operational standards for new and existing ships. The Energy Efficiency Design Index (EEDI) set for new ships as a technical measure, the Ship Energy Efficiency Plan (SEEMP) for all ships as an operational measure and the Energy Efficiency Operational indication (EEOI) set to be voluntarily applied (Haag, Kleverlaan, & Dispert, 2015). Additionally, the IMO's Marine Environment Protection Committee (MEPC) adopted mandatory requirements for establishing a new data collection (expected to enter into force on 1st of March 2018) for ships bunker fuel consumption as a step of building a global database to monitor and verify the precise effectiveness of the applied control measures. MEPC also approved a new roadmap (from 2017 through to 2023), to develop a new comprehensive IMO strategy on GHG emissions reduction from ships. (International Maritime Organization, 2016).

As a result, the shipping industry is currently stacking between the hammer of reducing its emissions in an energy efficient way, and an anvil of being sustainable as it should be. In the recent years, the industry has gone through many solutions. The up to now developed solutions are belonging to three categories; energy efficiency enhancement measures, the adoption of renewable sources and introducing innovative solutions to ship's design. The energy efficiency improvement measures differ in its approaches, merely focusing on the main goal of reducing the ship fuel consumption. The proposed solutions include the hull form optimisation, propeller configuration to lightweight construction for new building ships. While the existing ships solutions embrace solutions for machinery system, energy saving devices or ship operation management & optimisation (ABS, 2015).

Meanwhile, for a large vessel, a ship may consume daily up to 100 ton of marine heavy fuel oil (HFO) costing 500 to 600 USD per ton at current fuel prices, representing around 50% of the ship operating expenses; which explains the dominance of bunker fuel cost in the ship operating expenses. (Christiansen, Fagerholt, Nygreen, & Ronen, 2013). Additionally, the released emissions are directly proportional to the amount of bunker fuel consumed, for example, the mentioned ship with each HFO ton consumed emits approximately 3.1144 ton-$CO_2$/ton-fuel (Psaraftis & Kontovas, April 2009) with daily $CO_2$ emissions of 311.4 ton. Therefore, the saving of ship's bunker fuel consumption will reduce both the ship operational cost and its released emissions.

All of that led the shipping companies to aim to reduce their fleet fuel consumption to cope with the increasingly stringent environmental protection regulations and hence improve their competitive advantage in the market. Such an aim requires a behavioral's transformation of how their fleet operates with the day to day operational decisions. However, the needed transformation demanded a deep analysis of the operational data combined with the available practical alternatives and validated prediction methods for the effect of applying each alternative. Besides, many recent publications highlighted the need for a full-scale ship performance analysis. The Ship performance analysis mainly associated with the ship speed-power interaction from one side and corresponding fuel consumption from the other side. Such an approach could provide for instance the platform needed to predict the required ship propulsion power at various routes, weather conditions, the resulted speed loss and hence the appropriate action necessary to achieve better performance (Bialystocki & Konovessis, 2016).

To sum up, the need for the appropriation of this approach becomes even more compelling with the new IMO data collection scheme, where an extensive data set related to each sea voyage will be available and ready for deep analysis and hence achieve a higher shipping energy efficiency performance.

## *1.2 The dissertation*

The rationale behind this thesis is related to both environmental and economic aspects. The environmental perspective mainly based on the direct relationship between energy efficiency as a measure and ship's emission reduction, especially the GHG emissions. The IMO's environmental protection regulations are becoming stricter year after year which justifies the need for a more energy efficient shipping operations.

The economic perspective based on the fact that fuel cost represents more than 50% of the ship's operational cost. Despite the current relatively low ship's bunker prices, the fuel prices historically showed volatile behavior and projected to increase in the future.

### 1.2.1 Dissertation objectives

***The main research objectives of this dissertation are :***

1. Employ a non-classical methodology to predict the ship power performance in seaways to;
2. Develop a ship performance prediction model that can predict the ship performance in various seaways scenarios, and
3. Build a ship performance optimization model that can solve single-objective optimization problems, then
4. Integrate both models into an operation Decision Support System to maximize the ship energy efficiency during a sea voyage.

The system should be able to provide the ship's operators with a means to set the voyage energy efficiency objective and advise the optimum operational variables that lead to minimizing the power requirements, the least fuel consumption, thereby less emissions.

### 1.2.2 Methodology

The non-classical approach employed in this study based on the adaptation of Artificial Neural Network (ANN) to predict the ship power requirements at seaways combined with the use of Multi Regression (M.R) analysis to obtain other performance variables to conclude a precise forecast for the ship fuel consumption. Then, assessing the ship performance with various voyage scenarios to recommend the best available solutions for the ship operator.

In this dissertation, different software utilized to model the proposed system. A licensed version of Microsoft Office Excel used for organizing, calculating and processing the obtained data set. Then, A licensed version of Matlab used to develop the ANN and M.R models. So finally, an Oracle Crystal Ball software employed to design the optimization model.

### *1.2.3 Dataset*

The research was limited to the obtained data from NAPA. Only two detailed sea voyages data sets ( in Excel sheet format) for a particular ship were available for this study due to their legal commitment to their clients and AIS provider. However, the given data sets were quite enough to present an ideal model of the proposed system under the specified conditions.

### *1.2.4 Dissertation outline*

- ***Chapter 2*** describes the factors influencing the ship's fuel consumption during a seaway voyage. The chapter also analyzes the effect of these factors on the ship fuel consumption. The chapter illustrates the available operational energy efficiency measures in the context of the dissertation flow. Measures like slow steaming, draught optimisation, route and weather routing are discussed in details.
- ***Chapter 3*** demonstrates in details the developed research methodology supported by a presentation of the designed models for the proposed DSS. The chapter further explains how the data sets have been managed, analyzed and processed. Then, a description of the developed DSS accompanied by a discussion of how the system components integrated together to achieve the main objective behind it. Finally, the effect of the voyage environmental state on the ship performance has been analyzed and linked to the discussion established in the previous chapter.
- ***Chapter 5*** illustrates three case studies premeditated to validate the DSS to improve the ship performance in a sea voyage. The obtained result analyzed, justified, and discussed case by case in the context of the dissertation's main objective.

- ***Chapter 6*** sums up the thesis conclusion and lessons learned throughout the research followed by recommendations for the subject related future research.

Finally, **Figure 1-1** shows the dissertation workflow in stepwise illustration.

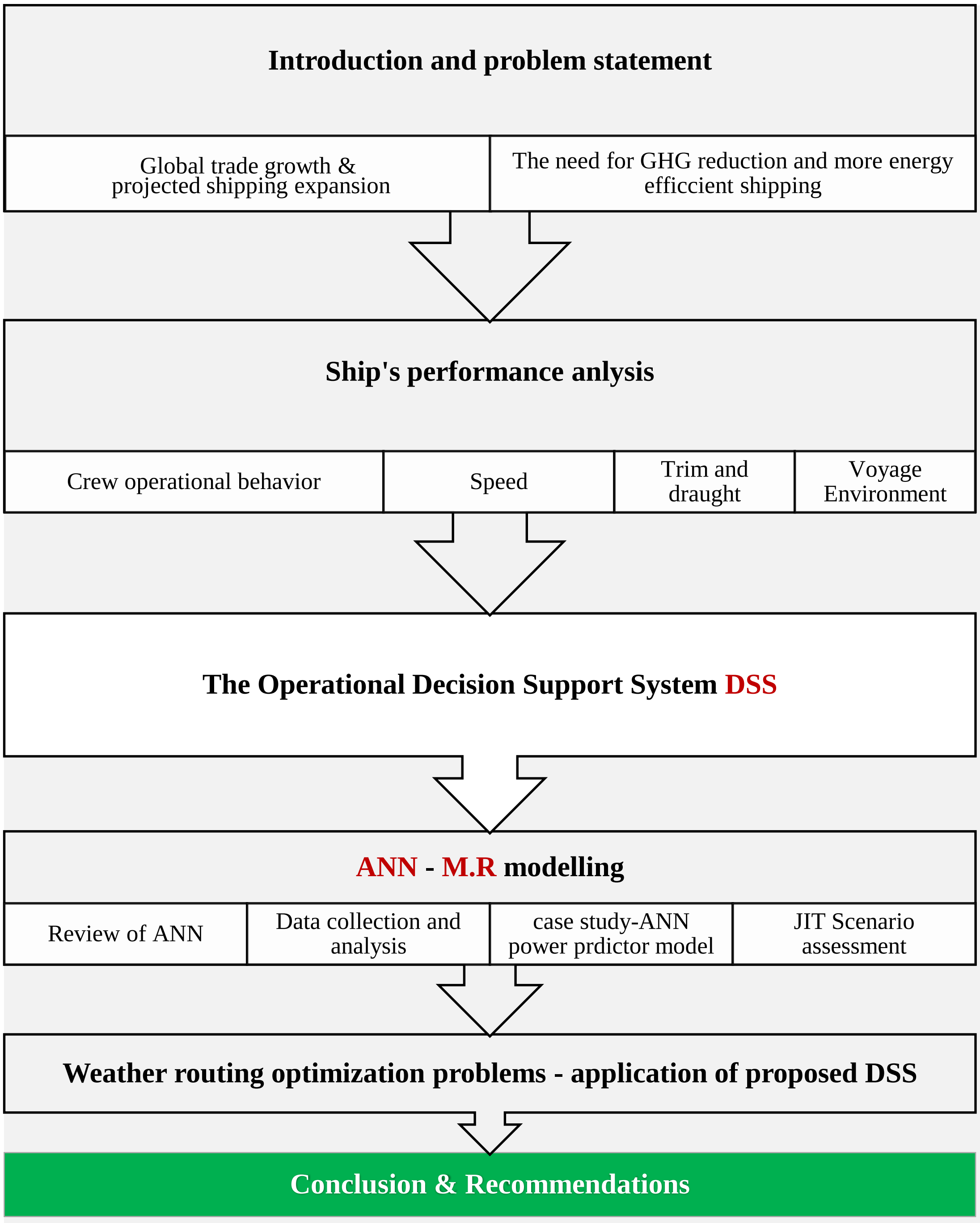


***Figure 1-1*** *Dissertation workflow*

# *Chapter 2.*

# *Energy efficiency operational measures*

## *2.1 introduction*

The variables that influence the ship's performance during a sea voyage are numerous. These variables are ship's specific and vary according to the voyage executed seaway. Some of these variables are controllable like ship's speed, draught, trim, engine condition, and Hull cleanliness, while other variables are uncontrollable such as weather condition and shallow water effect (Pedersen & Larsen, 2009). However, the weather and route optimization techniques can improve ship performance to accommodate these uncontrollable variables.

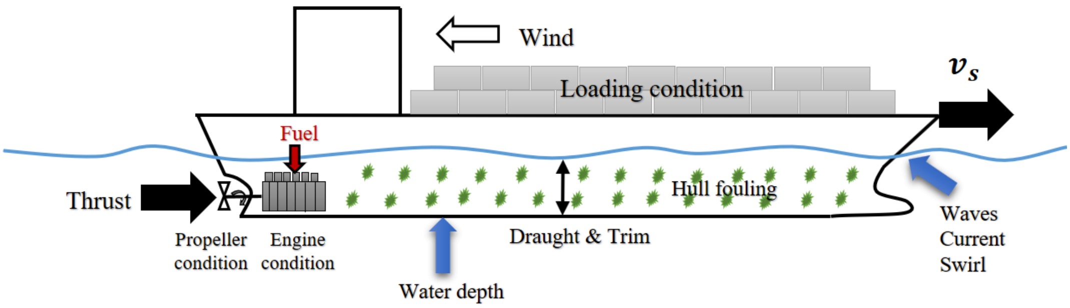


***Figure 2-1** Factors affecting ship's fuel consumption*

The operational energy saving techniques differ from one operator to another based on their operational mode. Ship's operational modes can be divided into three categories;

liner; industrial; and tramp shipping. Liner shipping usually has a fixed route with predetermined schedules to maximize profit, more like a public bus service. While industrial owned ships, both the ship and the cargo are owned and controlled by the same operator aiming to minimize the transportation cost of their cargo as much as possible. Meanwhile, tramp shipping operation is more likely similar to private taxi services; ships follow the available cargoes to maximise their profit.

Each operational mode has its own characteristics that influence their operational behavior. For instance, LNG shipping in tramp mode has an insufficient number of berths and ships arrival has to be coordinated due to the hazardous cargo nature (Christiansen, Fagerholt, Nygreen, & Ronen, 2013).

The second IMO GHG study had proposed different technologies and practices that valid for all ships to improve their energy efficiency. These OEEMs focus on three dimensions, fleet management, voyage optimization and energy management. The assessed potential CO2 emissions reductions are illustrated in **Table 2-1.** (Second IMO GHG study 2009)

***Table 2-1*** *Potential CO2 emissions reduction assessment from shipping by using operational measures, Source: (Second IMO GHG study 2009)*

| ***Operational Energy Efficiency Measure OEEM*** | ***Saving (%) of CO2/tonne.mile*** | ***combined*** |
|---|---|---|
| Fleet Management, logistics and incentives | 5-50%** | |
| Voyage Optimisation | 1-10% | 5-50%** |
| Energy Management | 1-10% | |

*** Reduction at this level may require speed reduction*

Notwithstanding of the mentioned study assessment, and according to the energy management report released from DNV-GL, most shipping companies are selecting their energy-efficiency measures EEMs based on financial considerations like payback period, vessel age, investment and ongoing costs. The report also revealed that more than the half of surveyed companies were driven by information availability of the selected EEM which reflects the lack of trusted information and verification data for some these measures. On the answer to another survey question, where the candidate can choose three answers about the top techniques that contributed the most of the company fleet's fuel reduction in 2014, 68% of the examined companies chose by far slow steaming, then 44% went for hull and propeller cleaning. Both selected measures represent the traditional measures used in the industry. It can be concluded from above discussion that the uncertainty is still dominating further techniques like trim optimisation or hull retrofitting for example (DNV-GL, 2015).

The chapter will discuss in more details the available OEEMs to maximize the ship energy efficiency, their potential savings and the challenges for their application. Some measures will have more focus than others to line up with the scope of this dissertation and the chosen case study scenarios in the following chapters.

## *2.2 Fleet Management*

According to the second IMO GHG study, Fleet management concept is a more logistic measure that depends on distributing as much as possible seaborne cargo through larger ships, while the smaller sized ships should be used to assist in onward distribution. Larger ships have much less specific fuel consumption than smaller vessels, and hence it is more energy efficient. The concept also includes the speed reduction combined with extending the voyage time and better-synchronized port scheduling time with economic incentives. Such measures combined according to the study could achieve globally up to 50% fuel consumption and CO2 emissions reduction, **Table 2-1** (Second IMO GHG study 2009).

### *2.2.1 Ship's speed*

Fuel cost represents from 50 to 60% of the total operating cost of ships according to the World Shipping Council report in 2008. The fuel consumption is known to be the third power function of ships speed. In simple words, if ship's speed increased two times, the power requirements to achieve such a speed will increase six times. In contrast, the speed reduction of 10% will reduce the fuel consumption by about 27% (Besikci, Arsalan, & Olcer, 2014) (Second IMO GHG study 2009). Therefore, many international shipping companies had employed slow steaming to reduce their operating cost, especially during economic crisis times.

**Figure 2-2** illustrates the M/T Orthis Speed Over Ground (SOG) relationship with the propulsion power delivered to the propeller during an individual voyage and a loading condition. The curve shows propulsion power nonlinearity relation to the change of ship speed.

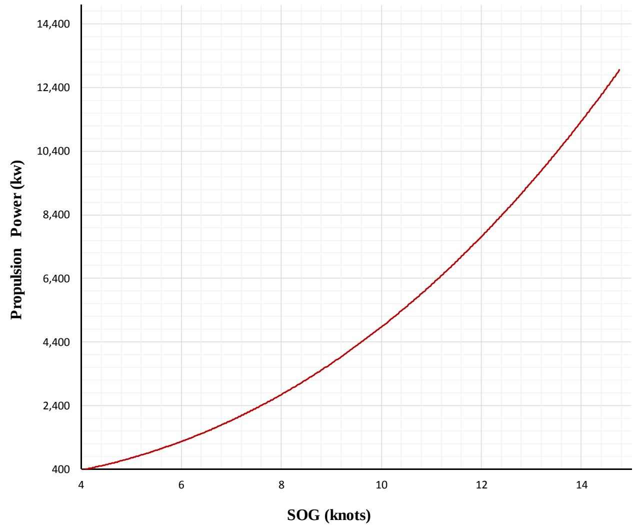


***Figure 2-2** Actual voyage Speed and Propulsion Power relationship at different seaway conditions - [ MT/ Orthis, 2017]*

Meanwhile, The Brake Specific Fuel Consumption (B.S.F.C) decreases as the engine brake power output rises as **Figure 2-3** shows due to better achieved thermal efficiency (up to a certain limit) at higher engine speeds. However, the total ship fuel consumption indeed increases in a nonlinear proportion as illustrated in **Table 2-2 & Figure 2-3.**

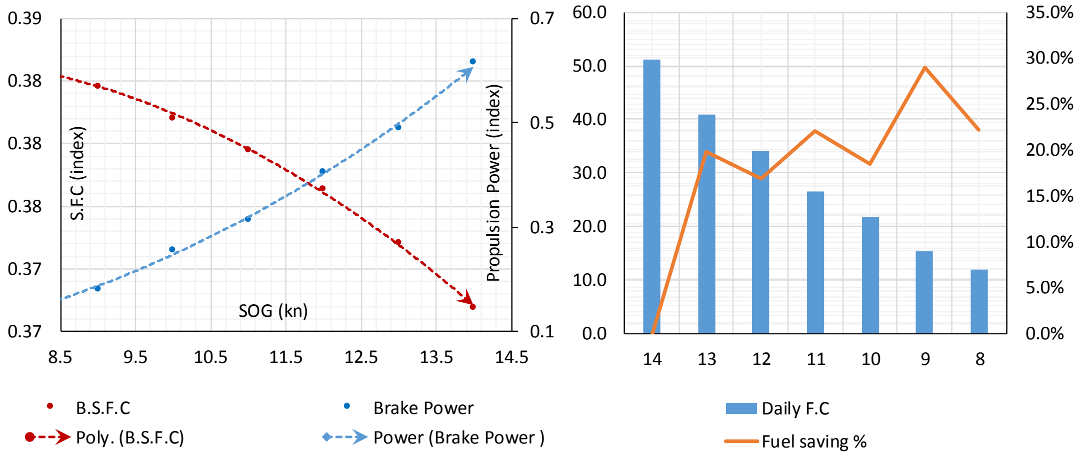


***Figure 2-3** Relationship of Brake Power and B.S.F.C with ship SOG for M/T Orthis at particular voyage [by author, MT/ Orthis, 2017]*

For example, At a ship's speed of 12 kn, the corresponding average brake power was around 7600 kW, while at 13 kn the required propulsion power would be around 9200 kW with an increase of 21.3% of power. The propulsion power for 14 kn speed was 11,600 kW with a power increase of 25.8% which illustrates the nonlinear relationship between the ship's speed change and the associated power requirements.

***Table 2-2*** *Comparison of power and fuel savings at different ship SOG reductions [by author, MT/ Orthis, 2017]*

| Ship SOG (kn) | *Average Brake Power (kW) | *Average B.S.F.C (gr/kW.hr) | ** Daily F.C (mt) | Speed reduction % | Power saving % | Fuel saving % |
|---|---|---|---|---|---|---|
| 14 | 11594.5 | 183.6 | 51.1 | | Base case | |
| 13 | 9222.4 | 185.2 | 41.0 | 7.7% | 20.5% | 19.8% |
| 12 | 7611.6 | 186.4 | 34.1 | 8.3% | 17.5% | 16.9% |
| 11 | 5900.0 | 187.4 | 26.5 | 9.1% | 22.5% | 22.1% |
| 10 | 4790.3 | 188.1 | 21.6 | 10.0% | 18.8% | 18.5% |
| 9 | 3388.1 | 188.9 | 15.4 | 11.1% | 29.3% | 29.0% |
| 8 | 2630.5 | 189.3 | 12.0 | 12.5% | 22.4% | 22.2% |

* Average values taken as the corresponding power values differ according to the seaway conditions
** All values of F.C and power values are dependence on the voyage, loading, and hull fouling conditions.

Chang and Chang (2013) had studied the influence of a speed reduction of 10%, 20%, and 30% of different sized bulk carriers (Chan & Chia-Hong, 2013). They investigated the fuel consumption reduction, CO2 emission reductions, and resulted fleet operating cost. The results showed that Speed reductions of 10 %, 20%, and 30% reduced fuel consumption by 27.1%, 48.8%, and 60.3% and CO2 emissions by 19%, 36%, and 51%, respectively. However, the study concluded that despite the fuel cost savings, the operational cost due to low-speed charter contract increased. For fleet operations, a fleet of 9 Capesize vessels operating at 14.53 knots, more ships are required as illustrated in **Figure 2-4** with each speed reduction scenario.

Moreover, the second IMO GHG study highlighted that a global reduction in the scheduled speed would certainly increase the industry's energy efficiency. If 10 percent reduction of global maritime speeds, carbon dioxide savings would rise to 19 percent, but such a reduction will result in more ships demanded by the market

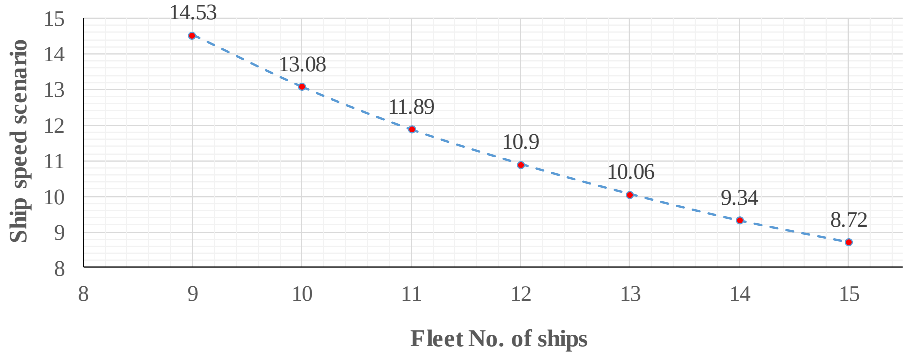


***Figure 2-4*** *Fleet's number of ships required for each speed reduction scenario, source: (Chan & Chia-Hong, 2013)*

It is imperative at this point to distinguish the difference between the speed optimisation as a design measure and slow steaming as an operational decision. While design speed is initially chosen by ship's owner after an economic analysis as will discuss below, speed optimization is more technical related with a precise fine-tuning of hull-propeller-engine interrelation. Slow steaming from the other hand, refers to running a ship at a significantly lower speed than its design speed combined with a derated main engine with some of its parts exchanged with retrofitted ones to suit the new operational speed (MAN, 2012).

## 2.2.2 *Speed optimisation as a design measure*

Ship's Speed as a parameter is a dominant aspect of the ship in its design phase. Ship's design speed determination mainly is governed by several factors representing the expected operational map of the ship. These factors include but are not limited to market condition; operation mode; required speed to maintain regular service; needed sea margins for the planned service; cargo value; maximising efficiency; current and future forecast fuel price; and regulatory requirements such as EEDI.

The optimum design speed estimation usually calculated from an economic analysis such as Required Freight Rate (RFR) analysis. The RFR analysis for an individual service considers the annual expected cargo quantity, a target fuel cost, number of ships to meet freight demand at some speed, capital costs, and operating expenses. Such an analysis provides a convenient way to evaluate a range of designs economic efficiency. By performing RFR analysis for a range of potential fuel costs, optimum outset speed could quickly be concluded (ABS, 2015).

For example, Maersk's mew 18,000 TEU 'Triple-E' container ships have less design speed of 17.8 knots from the industry's normal range of 23 knots. Maersk claims that by such a speed optimization, a reduction of 20% less CO2 per container is obtained from their previous largest container vessel, the Emma Maersk (MAERSK, 2014).

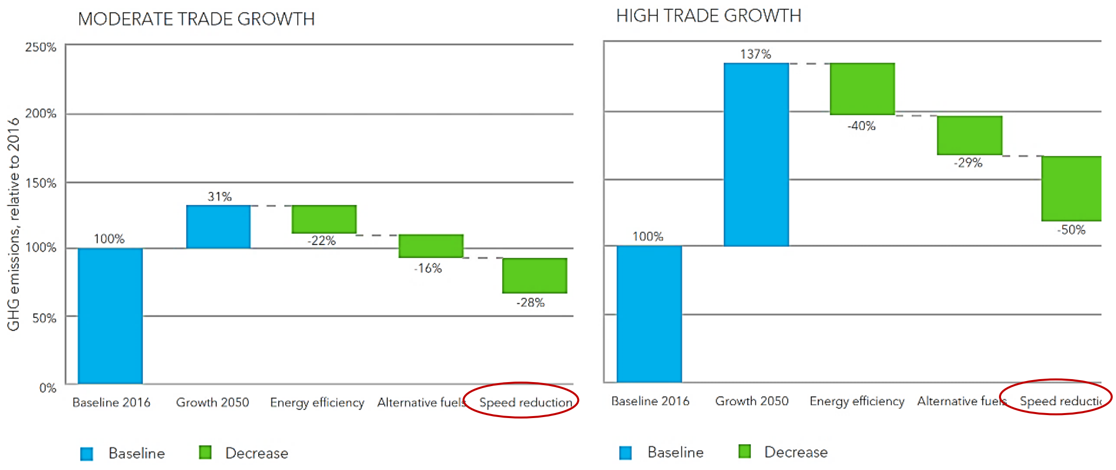


***Figure 2-5*** *Comparison of GHG emissions under high and moderate trade growth scenarios, and varying uptake of different measures, (DNV-GL-2017)*

In a recent study published by DNV-GL analyzes the current GHG emissions from global shipping and aims to explore the possibilities for realistic reduction towards 2050, the study used two scenarios for predicting the models result. A moderate and high trade growth models developed with different measures of reducing GHG emissions. The study claims that the rate of global growth will directly determine the sea trade, and hence to a large extent the fleet growth, fuel consumption and emissions in the next few decades. The study results used to evaluate the uptake of applying energy efficiency, alternative fuels and speed reduction measures. The speed reduction assumed to commence from 2020 and to increase gradually to reach a level of 20% reduction by 2050. **Figure 2-5** shows that under the moderate growth scenario, the emissions' level in 2050 will be significantly lower than the high growth scenario when the same measures are applied. In both scenarios, the speed reduction has the highest potentiality among other measures to reduce global maritime GHG emissions (DNV-GL, June, 2017).

However, low-powered ship designs may seem attractive from an economic and environmental point of view, but it still has to align with the minimum power requirements to fulfill the safety criteria especially in high seas regions. Such a trade-off between economics, environment, and safety must be dealt with carefully from both ship owners and ship designers.

### *2.2.3 Slow steaming*

It is common sense that ships with slower speeds consume less than faster ships. This simple logic historically drove existing ship's operators to use it, especially during market failures or sudden fuel price rise to reduce their operational cost and minimise their loss.

At ship lower speeds, the frictional resistance dominates, and the propulsion power is proportional to the third power of speed. The wave making resistance increases with higher speeds to become prominent, and the additional resistance makes the demand of power greater than the third power of speed. Thus, speed reduction for faster ships like container results in a considerable energy saving. However, ships speed from an operational point of view is highly sensitive to transport capacity and freight rates as increasing ship speed is a standard procedure to meet a shortage in transport capacity or greater rates (Second IMO GHG study 2009). Therefore, it can be justly stated that economic considerations mainly drive operational speed in the first place.

## *2.3 Voyage optimization*

Voyage optimization could be defined as the optimization of ship's operations that the master can achieve within the constraints that imposed by logistics, scheduling, contractual arrangements and other limitations. It includes measures such as Just In time arrival (JIT), weather routing, trim and ballast optimization. The potential CO2 emissions savings if these measures applied up to 10% (Second IMO GHG study 2009) (ABS, 2015).

### *2.3.1 Just In Time arrival (JIT)*

It is fundamentally uneconomical practice for a ship to steam at high speed to its destination where it has to drop an anchor or drift for days waiting for cargo handling permission. The second IMO GHG study stated based on the IMO 2000 study that a saving between 1 to 5 % could be achieved by applying just in time arrival. However, it stipulated the potential saving to several economic considerations, like contractual agreements and incentives and penalties for inefficient arrival.

The ship speed decision may not be an absolute operational choice as it depends on the charter party nature. For instance, time charter party, the speed, and fuel cost are managed by the charterer, and consequently the delay consequences. While in voyage charter party, the ship operator sets ship’s speed and also eligible to demurrage in case of port operation delay due to overcrowding. In such a scenario, ship operator will accelerate his ship if he has a new cargo order or at least to be compensated by the demurrage, especially that often demurrage rates are higher than extra fuel cost. Therefore, with voyage charter party, the ship's operator intends to sail at high speed and to arrive as early as possible (Second IMO GHG study 2009).

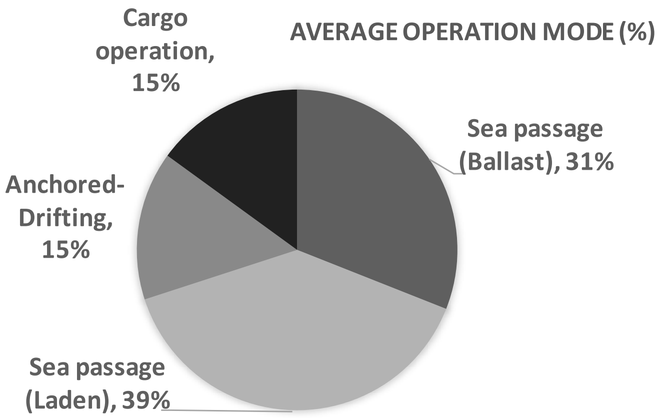


***Figure 2-6*** *Typical Vessel Operational Profile by Mode (Target, 2014, p. 22)*

**Figure 2-6** demonstrates the operational profile of a bulk carrier based on one-year voyage data providing the ship various operating modes by percentage. Anchorage and drifting time represented 15% of the ship total time. This proportion could be justified by several reasons like congestion at cargo handling terminals, delays due to weather conditions, storage space or cargo availability. From above, we conclude that the potential energy savings from voyage optimization are a case specific. The potential savings are directly related to the ship type, its operational profile, and the ship contractual nature which could cause split incentives between different contract parties (Target, 2014). To sum up, obtaining an energy efficiency gain from such a measure necessitates the complete cooperation of various key players including ship's operator (or the charter), ship's master, port authorities in addition to the promotion of energy awareness amongst all of them.

### *2.3.2 Wheather routing*

Ships are designed to transport cargo and people from one port to another safely. The ship through its sea voyage has to navigate with sufficient speed and intact stability in a volatile weather environment. Another crucial determinant added to ship's mission in recent years, to be energy efficient and cope with national and international environmental regulations. From a naval architecture viewpoint, the main concern is to design a ship floats upright in the calm water and to ensure its stability characteristics in different seaway conditions within an acceptable safety margin (Bhattacharyya, 1978). From an energy-efficiency viewpoint, the foremost objective is to minimise the ship energy consumption and to advocate weather variables to achieve such a goal.

Traditionally, during the ship design phase, the calm water state's resistance calculations are the main concerns of the ship's designer. There are several reasons behind that approach; first, the shipyard's guarantee usually is based on calm water performance. Second, the added resistance due to sea state is comparatively small to the total resistance, normally less than 10 %. Third, the speed loss estimation due to weather impact is complicated with a high uncertainty level. Finally, the architect trade-off alternatives for performance improvement in high seas are usually confined or overridden by other safety-related constraints. Thus, performance drop in Seaways typically judged for by applying a sea margin with a traditional value between 10 and 25%. This sea margin mimics the power raise for hull fouling and weather impact (ABS, 2015). Usually, the sea margin is chosen based on ship's type, the predicted trade routes, owner expertise and the importance of maintaining ship's operation schedule.

When the ship is sailing with full-power against a severe weather, the resistance increment causes a speed loss, a rise in fuel consumption and an extended voyage time. Thus, if the ship tends to maintain the same engine RPM and torque, the engine tends to be overloaded with a high probability of violent slamming, propeller rise, racing and high accelerations induced by pitch and roll motions. The Ship's master in such a condition has to commence a slowdown governed by the engine load diagram and allowable sea margin (Basic Principles of ship propulsion).

The weather routing could be categorized into two types, route optimization, and in-operation speed optimization. The route optimization tends to select alternative waypoints with more favorable conditions with reference to weather hindcast data. Meanwhile, in-operation speed optimization between two seaway points refers to deriving the most optimum speed to accommodate Main Engine's load within the allowable sea margin, the vessel loading condition, and hull roughness status. The weather optimization problem may have multiple criteria such as; ship's safety, passenger comfort, arrival time and ship's fuel consumption. Consequently, it may require a multi-objective optimization approach to solve it (Perera & Soares, 2017).

Therefore, each criterion should be weighted to the ship operator preferences. For instance, some shipping companies favor arriving on time with shorter transit time over fuel consumption reduction. For other companies, having a higher environmental ranking is much more valuable. Consequently, the objective should be set according to the operators' preferences based on their ultimate aims. Finally, The main challenges for the optimization process as many studies revealed are weather forecast accuracy, ship performance model quality, and the availability of alternative route especially in short voyages or restricted seaways (Bal Besikci, Arslan, Turan, & Olcer, 2016) (ABS, 2015) (Perera & Soares, 2017) (Lu, Turan, Boulougouris, Banks, & Incecik, 2015).

### *2.3.3 Trim optimization*

Traditionally, the ship's hull form is designed at various drafts values with zero trim assumption. The flow pattern at ship's bow and stern then tuned with care to achieve as minimum resistance as possible. Any change to the ship's trim than the design point will positively or negatively affect the ship resistance. The still water ship resistance according to ITTC standards can be expressed by the following equation (ITTC, 2014):

$$R_T = {}^1/_2 \,.\, \rho . V_s{}^2 . S . C_T \qquad (1)$$

Therefore, the ship total resistance ($\boldsymbol{R_T}$) is a function of the ship speed ($\boldsymbol{V_s}$), the wetted service area ($\boldsymbol{S}$), total resistance coefficient ($\boldsymbol{C_T}$), and sea water density ($\boldsymbol{\rho}$). The wetted surface area and total resistance coeffecient are influenced by ship's trim and have to be reduced to obtain a gain from trim optimization (Reichel, Minchev, & Larsen, 2014).

The technical reports had evaluated the potential saving of trim optimization between 1 to 2 % of the ship's fuel consumption. Such a gain can justify ship owner's investment in model tests, CFD simulation or full-scale measures. Additionally, the payback-time could be within months especially for ships with high-power consumption and long voyages range (ABS, 2015).

## *2.4 Other operational measures*

### *2.4.1 Autopilot settings optimization*

It is well-known from a naval architecture basics, that rudder movement adds drag to the ship hull and increases the ship's total resistance (Bhattacharyya, 1978) (MAN). Conventional autopilot systems built on the direct linear relation between rudder angle and ship's heading change rate. These systems aim to maintain ship's course using a simple proportional action on the heading error angle. Such a relation may be suitable for stable hull forms and small rudder angle. Technically, a good performance autopilot system should produce no more than six to ten small rudder movements per minute (ABS, 2015). If the ship during its voyage exposed to severe weather conditions, it may require large rudder angle with more frequent rudder movements to maintain its course.

For optimal energy efficient use of the autopilot system, a fine tuning of its parameters is required with best practice in shipboard procedures. The crew should be aware of how to configure the system settings. The shipboard procedure should include recommendations for an optimal number of rudder movements and corresponding angles in various loading and weather situations in line with the system manufacturer instructions. **Figure 2-7** illustrates two system configurations. Ship 1 with the track control activated that tends to generate very steady course line but will use excessive large angle rudder with high-frequency movements, which result in high resistance and higher fuel consumption. In ship 2, the system configured with a small deviation in ships course that allowed the system to use a smoother rudder movements to maintain the set course line. The second adaptive system has less resistance and is more energy efficient (DNV-GL, GLOMEEP, 2014).

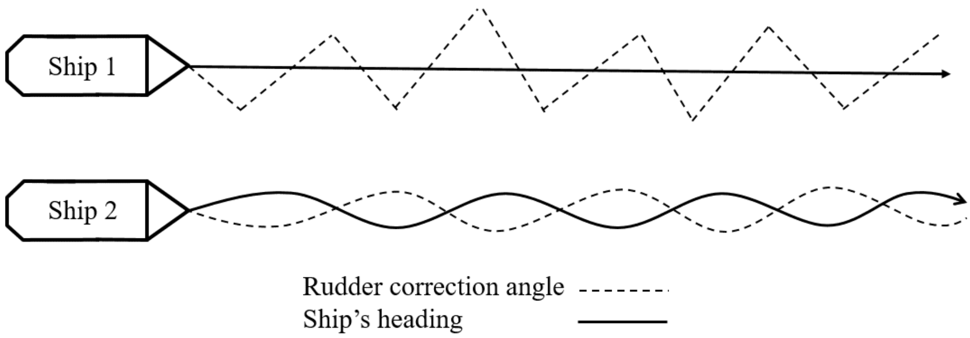


*Figure 2-7 PID and adaptive autopilot systems, Source: adapted from (DNV-GL, GLOMEEP, 2014)*

The measure is mostly cost-free for ships installed with linear autopilot systems integrated with system configuration adjustment. However, the cost for fully adaptive autopilot suitable for directionally unstable ships or heavy weather conditions may cost more than 20,000$ (ABS, 2015). The potential savings differs from 0.25 to 1.55 % fuel savings depending on the shipping route, ship loading and weather conditions within these routes (DNV-GL).

### *2.4.2 Ballast optimization*

The second IMO GHG study defined the ballast optimization as determining optimal ballast by avoiding unnecessary ballast. However, it highlighted the importance of taking into consideration ballast effect on the ship safety, crew comfort, and trim optimization (Second IMO GHG study 2009). The concept also includes the execution of ballasting operation in a more energy efficient way by using various techniques such as gravity assisted ballast exchange and sequential ballast exchange as it requires less water to displace (Bannstrand, Jonsson, Karlsson, & Johnson, 2016).

In a specific case study by DNV-GL of tanker operations, a saving of 0.6% of the ship fuel consumption was estimated for both trim and ballast optimization. Higher figures may be only relevant for a particular ship type that carries significant ballast during most of its operation time (Second IMO GHG study 2009).

### *2.4.3 Hull roughness management*

The marine biofouling was always a great challenge for both economic and environmental perspectives to the efficient ship operations. Hard-shelled fouling can cause a significant rise in the ship's frictional resistance, and hence its fuel consumption. Therefore, Marine coating paints are used to improve and maintain the hull surface smoothness, and if combined with a proper cathodic protection system it may prevent corrosion from ship's hull (Demirel, Turan, & Incecik, 2017). According to FoulXSpel project, the use of antifouling coatings provided globally a $60 billion of fuel saving and 384 million tonnes reduction in carbon dioxide emissions annually (FoulXSpel).

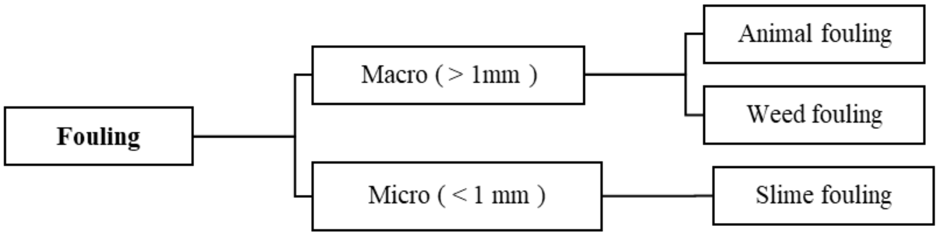


*Figure 2-8 Biofouling organisms, adapted from, (Demirel, Khorasanchi, Turan, & Incecik, 2013)*

The number of marine organisms' types may exceed 25000. Some of them can attach to ship's hull, settle and grow. These species are classified by size into micro and macro as shown in **Figure 2-8** (Demirel, Khorasanchi, Turan, & Incecik, 2013)**.**

The ship's hull fouling has an extended effect on the ship operational performance (**Figure 2-9**). The increased drag resistance of the ship's hull will cause a higher fuel consumption to achieve the normal speed. The severely fouled hull leads to ship's speed reduction to avoid the main engine's overload and a shorter drydock intervals, which will increase the ship maintenance cost. Environmentally, the ship while in operation is transferring the attached spices to its hull to foreign territories and could cause extensive damage to the aquatic ecosystem and marine biodiversity.

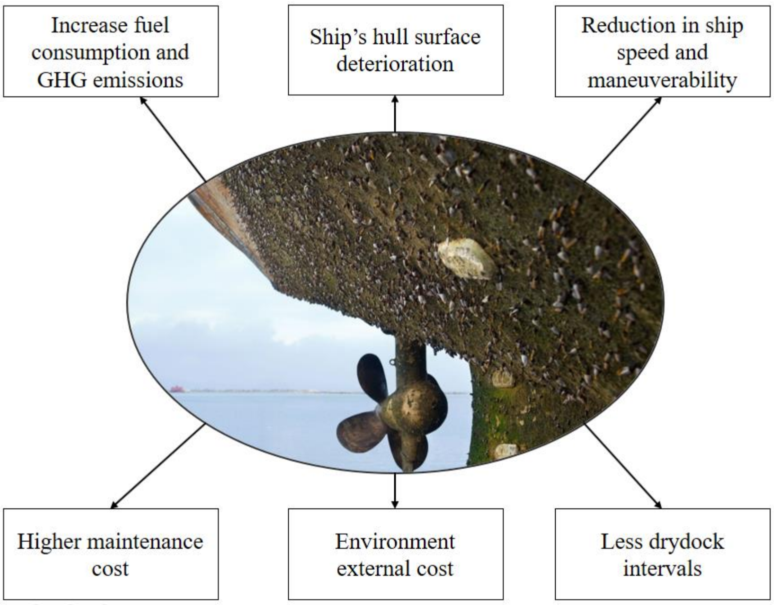


***Figure 2-9*** *Biofouling effect on ships operation*

Finally, applying a good hull management was always an evidence of the ship performance good practice. Now with the need to maximize the ship's energy efficiency, hence the need to adopt such measures becomes more imperative. Especially, with the potential fuel savings from applying an appropriate antifouling coating with a suitable hull cleaning which can achieve an average reduction of 4% of the ship's fuel consumption. While re-coating a rough hull can yield 10 to 12 % reduction in fuel costs (ABS, 2015).

## *2.5 Chapter summary*

In this chapter, different EEOMs has been analyzed with their potential fuel savings guided by the second IMO GHG study. The study had estimated a 50% possible fuel savings with the application of the EEOMs combined, which seems to be misleading and lacks the needed accuracy. The study estimation was based on the assumption of a slow steaming scenario with at least 10% ship's speed reduction. Contrary as discussed in **section 2.2.3**, ship's operational speed mainly governed the market demand and the ship's bunker prices, i.e., the economic concerns. Some of the proposed energy efficient operation measures, like slow steaming and hull cleaning, were historically well-established by ship's operators to reduce ship's operation cost far before the propagation of the energy efficiency concept. Consequently, counting on the application of these two measures as an indication of the industry response to the new energy efficiency requirements sounds disingenuous.

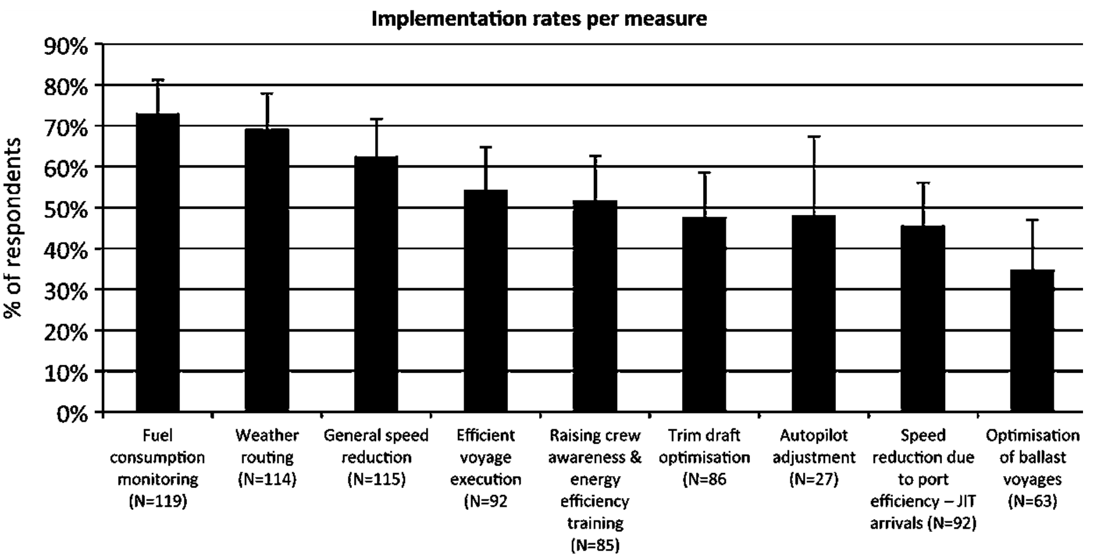


***Figure 2-10** Cost-effective operational measures average implementation rate, Source: (Rehmatulla & Smith, 2015)*

Moreover, (Rehmatulla & Smith, 2015) found after measuring the implementation the rate of the energy efficiency measures that had been implemented in the industry, that the average implementation rate of cost-effective operational measure is 50% of their sample respondents. The study further accounted the reasons for the low implementation rate of measures like trim and ballast optimization to the lack of available practical information of the potential gain, the high level of uncertainty of the applicability, and the split incentives among the shipping stakeholders. Besides, the DNV-GL studies (2014,2015) showed that only minority of shipping companies had set and accomplished their ambitious targets for maximizing their fleet energy efficiency (DNV-GL, 2015).

Therefore, the author is highly confident that the barriers that slow down the implementation of energy efficiency measures, must be overcome to perceive a noticeable improvement in the industry's energy efficiency collectively. Thus, providing a Decision Support System (DSS) based on the ship's operational data that can predict, assess and optimize the operation of the energy efficiency measures is beneficial and provide a step forward with the needed momentum to achieve a better energy efficiency implementation rate shortly.

## *Chapter 3.*

# *Development of the methodology for energy efficiency ship operation*

## *3.1 The research methodology*

Traditionally, the prediction of the ship performance in calm water had been the focus of many types of research in the past. The still water resistance is usually estimated according to the classical method of (Holtrop & Mennen), which is an approximate procedure that was popularly used at the initial design stage of the ship (Holtrop & Mennen, 1982). However, when a ship advances in a seaway, she faces additional resistance caused by the actual sea state condition. The extra power is usually accounted for by a Sea Margin of the total engine power with a value of 15% is usually used as previously explained in **Section 2.3.2.** The added resistance and ship motion problem in waves had widely studied through several approaches from experiments, statistical, numerical simulations using potential flow theory to the computational fluid dynamics CFD (Kim, Hizir, Turan, Day, & Incecik, 2017).

However, one of the research goals is to use a non-classical approach to predict the ship's propulsion power, and hence its fuel consumption. Therefore, the adaptation of the Artificial Neural Network in forecasting the ship's performance in seaway confirms the novelty of the proposed methodology.

**Figure 3-1** illustrates the method that employed (ANN) in forecasting the ship's power based on a set of input variables. The input variables in the proposed system include:

- The Ship's Speed over ground (SOG)
- The ship's course
- Seawater Depth
- Weather hindcast data (Wind, Wave, Current, and swell parameters)

Ideally, the ANN could include more variables that may reflect the ship behavior such as ship's mean draft or ship's trim. However, for the scope of this dissertation, the mentioned variables were only considered due to the data limitation. The ANN can accommodate more inputs as long as its relevant to the network output, which will be discussed in detail in Chapter 4.

The developed ANN model should be able to predict the ship's propulsion power. Then, the propeller RPM and engine S. F. C. can be estimated by fitting in the ANN output to Multiple Regression M.R analysis models.

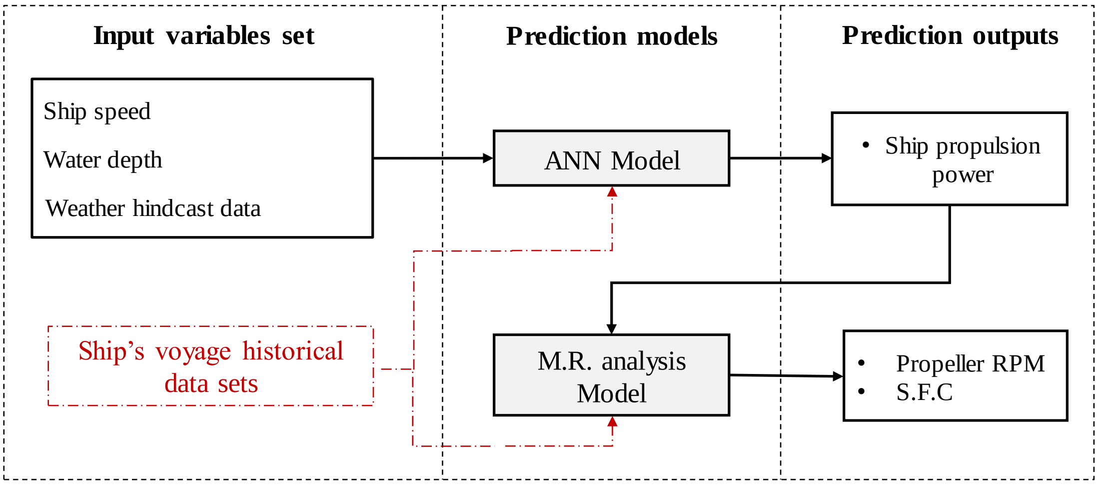


***Figure 3-1*** *Proposed operation performance assessment method*

Still, it is critical to understand the nature of ANN and M.R analysis, and their characteristics befoe discussing how the models have been built.

## *3.1.1 The Artificial Neural Network (ANN)*

### *3.1.1.1 The origin*

The Artificial Neural Network is relatively a new approach that mainly had been derived from neurobiology science. Humans and other animals are able to process the information through their neural networks. These networks are contained trillions of neurons (nerve cells) that exchanging brief electrical pulses called action potentials. Computer algorithms that mimic these biological structures are formally called Artificial Neural Networks. The ANN field has been grown gradually from the modeling of simple processing elements or neurons to massively parallel neural networks, which paved the way to advanced artificial intelligence and machine learning applications.

ANN could be practically defined as a group of interconnected neurons that progressively has learned from their environment (data) to obtain linear and nonlinear trends in complex data. It is flexible enough to reliably predict for new situations containing noisy or even partial information. Neurons are the core computing units that perform local data processing inside a network. These neurons form massively parallel networks, whose function defined by the network structure (i.e., how neurons organized and linked to each other), the connection strengths between neurons, and the processing performed at neurons. Neural networks perform a variety of tasks, including prediction or function approximation, pattern classification, clustering, and forecasting (Samarasing, 2006, p. 12).

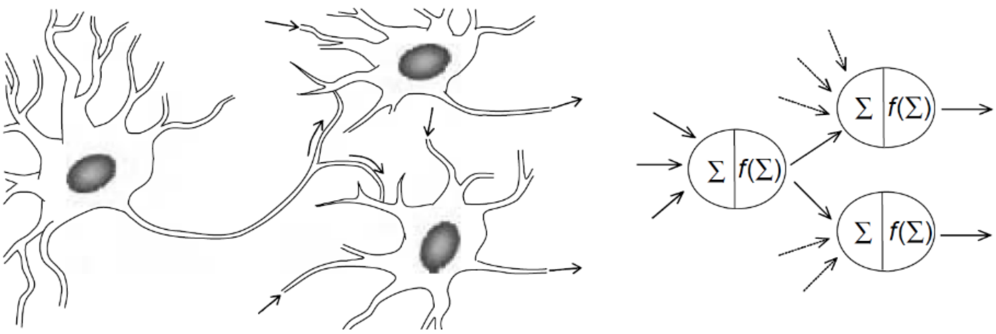


***Figure 3-2*** *Communication between biological and artificial neurons, Source: (Samarasing, 2006)*

### *3.1.1.2 How does it work?*

ANN is a computing system that was made with some highly connected neurons. These neurons are processing information, operate in parallel and are connected in a network shape through weights ($\boldsymbol{w}$). ANN can learn by acquiring the knowledge of the data in the process, which is then reflected on the weight values to capture the essential features of the problem and minimize the error. **Figure 3-3** shows an ANN structure with ($\boldsymbol{n}$) input variables ($\boldsymbol{x_n}$). Each neuron receives inputs $\boldsymbol{x_1}, \boldsymbol{x_2}, \boldsymbol{x_3}, \ldots . \boldsymbol{x_n}.$, attached with a weight $\boldsymbol{w_{ij}}$ which indicates the connection strength for a particular input for each connection. Then it multiplies every input by its corresponding weight of the neuron connection. A bias ($\boldsymbol{b_i}$)can be defined as a type of connection weight with a constant nonzero value added to the summation of inputs and corresponding weights (Bal Besikci, Arslan, Turan, & Olcer, 2016) (Samarasing, 2006) (Smith S. W., 1997)

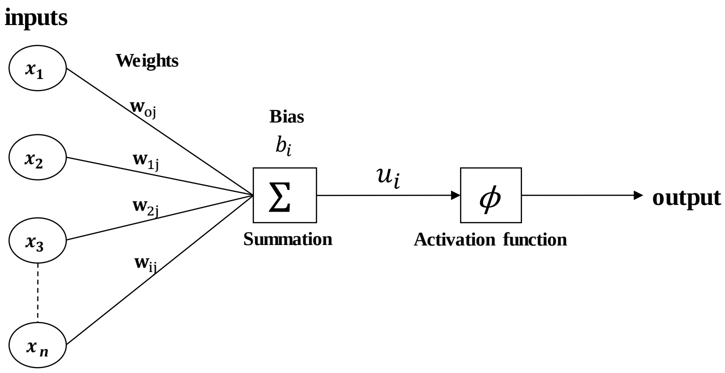


***Figure 3-3*** *Basic Artificial Neural Network structure*

Then, the neuron's network inside activity ($u_i$)can be expressed as following:

$$u_i = \sum_{j=1}^{n} w_{ij} x_j + b_i \tag{2}$$

Where, $w_{ij}$ is the weight value of the i layer, $x_j$ is the output value of the j layer, and n is the number of the neurons. Then, the neuron output will be processed through a nonlinear activation function ϕ to obtain the output $y_i$.i.e the output $y_i$can be mathematicaly expressed as follows:

$$y_i = \phi\,(u_i) = \phi \sum_{j=1}^{n} [w_{ij}x_j + b_i] \tag{3}$$

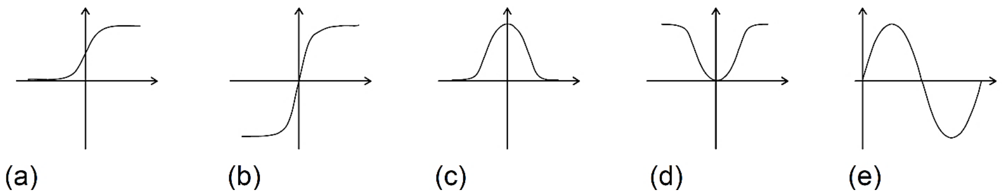


***Figure 3-4*** *Nonlinear neuron activation functions: (a) logistics, (b) hyperbolic tangent, (c) Gaussian, (d) Gaussian complement, (e) sine function, Source: (Samarasing, 2006)*

The neurons activation function could take different shapes as illustrated in Figure 3-4. The activation functions with its nonlinearity makes it possible for neural networks to do the nonlinear mapping between inputs and outputs (Samarasing, 2006, p. 73).

### *3.1.1.3 Multilayer feedforward neural networks*

The ANN structure differs according to the nature of the problem to be solved. A simple problem may require a simple single layer feed forward network with only one layer of neurons as shown in **Figure 3-3**. For more complicated problems that require a significant number of neurons to solve, and the complex nonlinear relation between its multiple inputs, a multilayer feedforward neural network seems more suitable for more accurate results (Samarasing, 2006, p. 113).

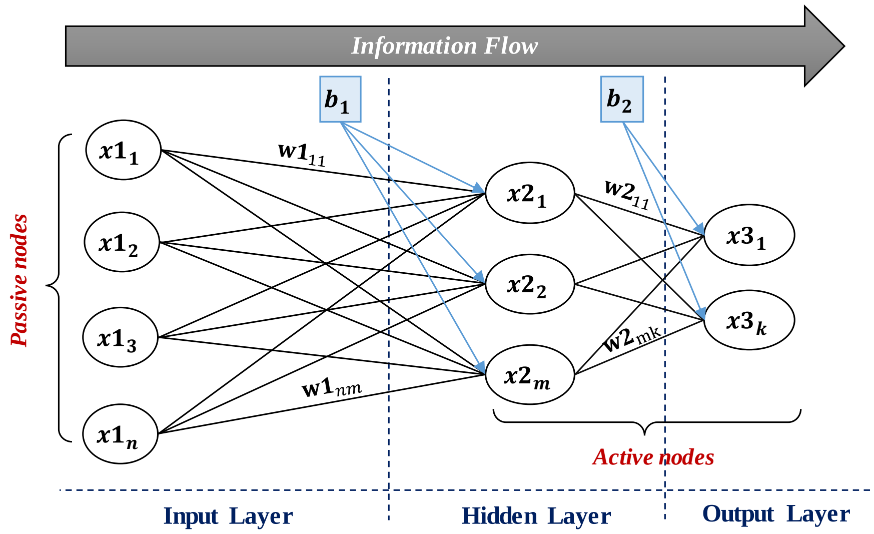


***Figure 3-5*** *Multilayer feed-forward neural network, adapted from several sources*

Each layer can apply a different activation function to the previous layer to produce a linear transformation output followed by a squashing nonlinearity. Such complex calculations smoothed by nonlinearity in hidden neurons whose features are controlled by the network weights.

**Figure 3-5** shows the most commonly used ANN structure. The network has three layers, called the input layer, hidden layer, and output layer. Each layer consists of one or more neuron, the lines between the nodes indicate the information flow from one neuron to the next. In this type of network, the information flows from the input to the output, other types of neural networks may have more complicated connections with feedback paths.

The variables: $\boldsymbol{x_1}$ are representing the input nodes, and they are passive, which means that they don't modify their values, while hidden layer nodes are active. the values entering a hidden node are then multiplied by weights, a set of predetermined numbers stored in the program. The weighted inputs are then added to produce a single number. The first layer weights $\boldsymbol{w_1}$could be expressed as following:

$$w1 = \begin{bmatrix} w1_{11} & w1_{21} & w1_{n1} \\ w1_{12} & w1_{22} & w1_{n2} \\ \vdots & \vdots & \vdots \\ w1_{1m} & w1_{2m} & w1_{nm} \end{bmatrix} \quad (4)$$

Before leaving the node, this single number has to pass through the first layer bias $\boldsymbol{b_1}$, and the nonlinear function.

The variables $\boldsymbol{x2}$ represent the outputs from the hidden layer: Just as before, each of these values $\boldsymbol{x2_1}$**, to** $\boldsymbol{x2_m}$ are multiplied by weights and bias then applied to the next layer. The active nodes of the output layer combine and modify the data to produce the two output values of this network, $\boldsymbol{x3_1}$ and $\boldsymbol{x3_k}$

Similarly, to (*4*), the second layer weights w2 could be expressed as follows:

$$w2 = \begin{bmatrix} w2_{11} & w2_{21} & w2_{m1} \\ w2_{12} & w2_{22} & \vdots \\ \vdots & \vdots & \vdots \\ w2_{1k} & w2_{2k} & w2_{mk} \end{bmatrix} \quad (5)$$

Neural networks can have any number of layers, and any number of nodes per layer. Most applications use the three-layer structure with a maximum of a few hundred input nodes (Samarasing, 2006) (Smith S. W., 1997)

### *3.1.1.4 ANN training and Back Propagation algorithm*

The weights values needed for a neural network to perform a particular task can be obtained by a learning algorithm. The term "learning" is widely used in the neural network field to explain this process. However, a more precise description might be: determining an optimised set of weights based on the statistics of the data set (Smith S. W., 1997). The most commonly used training algorithm for the multilayer perceptron (MLP) is a back-propagation algorithm (BPA). Multilayer ANN trained with BP usually is chosen because of its proven ability to model any function.

The algorithm proceeds by iterations through multiple epochs. Epoch can be referred to as a completed iteration of the training procedure. With each epoch, the training results are submitted to the network and predicted target compared with actual values, and the error is then calculated. Both the error and error surface gradient is used to optimize the weights values, and hence the training repeated, and error minimized. The initial ANN weight values are random, and the training stops when epochs lapse or when the error stops improving (Electronic Statistics Textbook, 2013). The back-propagation algorithm has become the most popular one for training the multilayer perceptron. It is compositionally very efficient. (Samarasing, 2006). (Basheer & Hajmeer, 2000)

### *3.1.1.5 ANN application in ship's performance prediction*

Since (McCulloch and Pitts, 1943) had formed their computational model for neural networks based on mathematical algorithms, the neural network's research paved the way through to many applications. Applications like machine learning, quantum chemistry, medical diagnosis, data mining, e-mail spam filtration, face identification, gaming, financial and business applications had widely used ANN for building models that helped to solve many problems that couldn't be solved with traditional methods.These applications have a broad range of diversity mainly because of the ANN ability to model nonlinear processes as discussed in the above section (Basheer & Hajmeer, 2000).

However, only tow studies were found in the literature that employed ANN as a non-classical methodology to forecast the ship performance. Starting with (Pedersen & Larsen, 2009) which were the first to test the ANN methodology to predict a full-scale propulsion power. In their study, they had used onboard measurement, Noon report data, and hindcast weather data. The study also compared between different linear and non-linear methods with the ANN method and found that ANN has a significantly better performance over other tested methods. Then, (Bal Besikci, Arslan, Turan, & Olcer, 2016) study that employed the ANN to predict the ship fuel consumption to develop a decision support tool. The study counted on the ship's noon data with seven input variables to their ANN model. The study concludes with ANN can learn the relationship between input variables and ship fuel consumption accurately. Furthermore, the study highlighted the ANN superior performance when compared to the results derived using an M.R model.

However, the ANN training dataset used in the mentioned studies based on Noon reports, which are logged in by ship's crew in 24 hours intervals. Such a log data only reflects a time capture or mean values of the ship's parameters and doesn't represent the ship's operational behavior realistically. Despite the fact that it was an excellent attempt, the alternative should be a high-frequency data that indicates the ship's operational changes during its voyage through an automatic data acquisition system.

ANN models by nature are susceptible to the training dataset quality to identify the correlation between input variables and the output. Therefore the obtained highly intensive dataset may satisfy the former argument, also it will provide an opportunity to validate the ANN model with an entirely different voyage dataset that wasn't used for training the model. Such a validation should increase the confidence level of the used methodology.

## 3.1.2 Multiple Regression analysis (M.R) methods

"The regression analyses" as Pearson first used it as a term in 1908, aims to analyze the correlation between several independent or predictor variables. Multiple regression disciplines are widely used in scientific research. In this section, only linear and Polynomial regression methods are described as they have been employed to develop an M.R model.

### 3.1.2.1 Linear regression analysis method

If a set of data of two variables (x) and (y) plotted in a scatterplot, then one of the variables (x) represents an independent, while the other variable (y) accounts for a dependent. The line in two-dimensional space could be represented by the following equation:

$$y = a + bx \qquad (6)$$

Where *(a)* is a constant number, sometimes referred to as the intercept, while *(b)* relates to the regression coefficient (β) or the line slope. When there is more than one independent variable, i.e., a multivariate case, then the multiple regression analysis could be expressed by the following linear equation:

$$\mathrm{y} = \beta_0 + \beta_1 \mathrm{x}_1 + \beta_2 \mathrm{x}_2 \ldots \ldots + \beta_n \mathrm{x}_n \qquad (7)$$

The resulted regression line represents the best prediction concerning the given equation to a variable (y) at a given variable (x), however usually there is a substantial variation of the actual points around the fitted regression line. That deviation of a particular point from regression line is called the residual value. The coefficient of determination, also known as $R^2$, is commonly used in statistics to evaluate the model fit and its value lays between 0 and 1. To determine the $R^2$ value, the ratio of residual variability is subtracted by 1. Thus, the $R^2$ value of 1 means that there is no residual variance and the ratio of variance would be 0.0, i.e., it indicates that the regression function have been accounted for almost all of the variability with the model specified variables (Electronic Statistics Textbook, 2013).

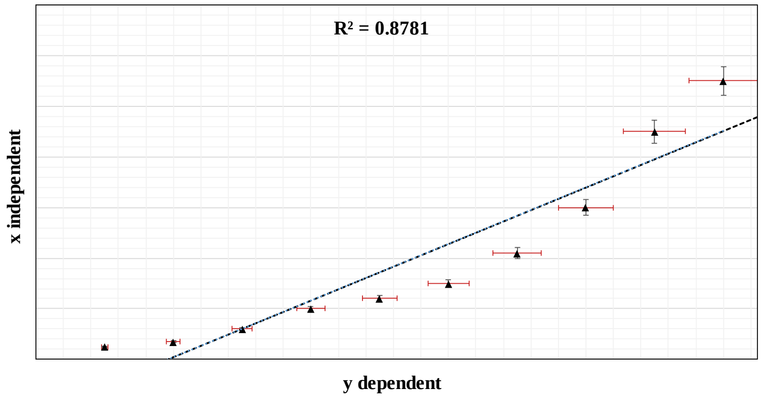


***Figure 3-6*** *Linear regression example*

**Figure 3-6** illustrates a linear regression example between two variables x and y. the linear regression equation as found by Microsoft excel was:

$$y = -2126.7 + 1113.9x$$

With the intercept (a) value = -2126.7 and regression coefficient (β) = 1113.9 and ($R^2$) = 0.88, which means that only 12% of residual variability were left.

### *3.1.2.2 Polynomial regression analysis method*

The polynomial method is a regression analysis method that suits a nonlinear correlation between the independent variable (x) and the dependent variable (y). The model formed by multiple degree polynomials in (x). Additionally, polynomial regression as a statistical evaluation problem is linear as the regression function is linear in the unknown parameters that calculated from the data, which explains why polynomial regression is considered a special case of M.R analysis (Electronic Statistics Textbook, 2013). The resulted function could be expressed by the following equation:

$$y = f(x) = \beta_0 + \beta_1 x_1 + \beta_2 x^2 + \beta_3 x^3 + \cdots + \beta_n x^n \qquad (8)$$

With the application of the previous function to the example illustrated in section 3.1.2.1, the obtained results showed in **Figure 3-7** with a highest $R^2$ value had been found at $n = 3$.

The curve equation is then:

$$y = -66.7 + 608.9\,x + 105.6\,x^2 + 15.8\,x^3$$

$R^2$ = 0.999, which means that only 0.6% of residual variability were left, thus the polynomial method had fitted a more accurate curve for the given variables set.

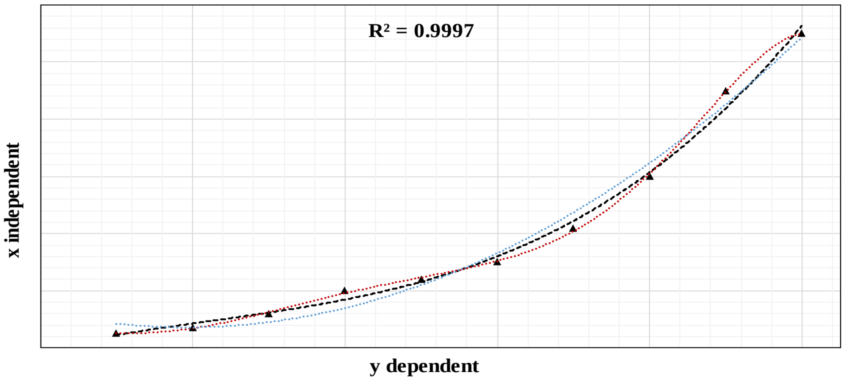


***Figure 3-7*** *Polynomial regression example*

### *3.1.2.3 Error analysis*

For the error estimation and model quality analysis, the following formulas used:

1. **Mean Absolute Error (MAE):** which is a measure of the difference between two continuous variables.

$$MAE = \frac{1}{m}\sum_{i=1}^{m} |y_i - \tilde{y_i}| \qquad (9)$$

2. **Mean Square Error (MSE):** measures the average of the squares of the errors or deviations.

$$MSE = \frac{1}{m}\sum_{i=1}^{m} (y_i - \tilde{y_i})^2 \qquad (10)$$

3. **Root Mean Square Error (RMSE):** is the distance, on average, of a data point from the fitted line, measured along a vertical line.

$$\text{RMSE} = \sqrt{\frac{1}{m}\sum_{i=1}^{m}(y_i - y_i^{\sim})^2} \tag{11}$$

## *3.2 Operational Decision Support System (DSS)*

Energy efficiency measures, in general, can be categorized into operational based and design based measures (Second IMO GHG study 2009). In the previous chapter, available OEEMs discussed in details with its potential energy savings. The DNV-GL (2015) survey of shipping companies implementation of energy efficiency measures had shown the shipping companies favourability of reducing their fleet's fuel consumption through operational measures rather than the adoption of new technology investments of energy efficiency designs (DNV-GL, 2015). However, some of the operational measures need a decision support system (DSS) that provides several alternatives necessary to support the ship's navigators to achieve the potential savings targets safely.

The advisory system should be able to sense the actual sea state variables and analyzes their effect on the ship's performance. Also, it has to forecast the propulsion power needed throughout the voyage route's conditions. Then the system should assess the ship's fuel consumption of the various decision alternatives. Furthermore, it should advise the ship operator with the optimum values of the operational parameters achieve optimum performance in a real-time voyage condition. The success of such a system requires a comprehensive, validated performance prediction model integrated with a reliable performance optimization model.

**Figure 3-8** manifests the components of the proposed Operational Decision Support System (DSS) illustrating the interaction between system's elements. The system tends to achieve voyage optimisation management (VOM) by utilizing certain energy efficiency measures as should be decided by the operator preferences.

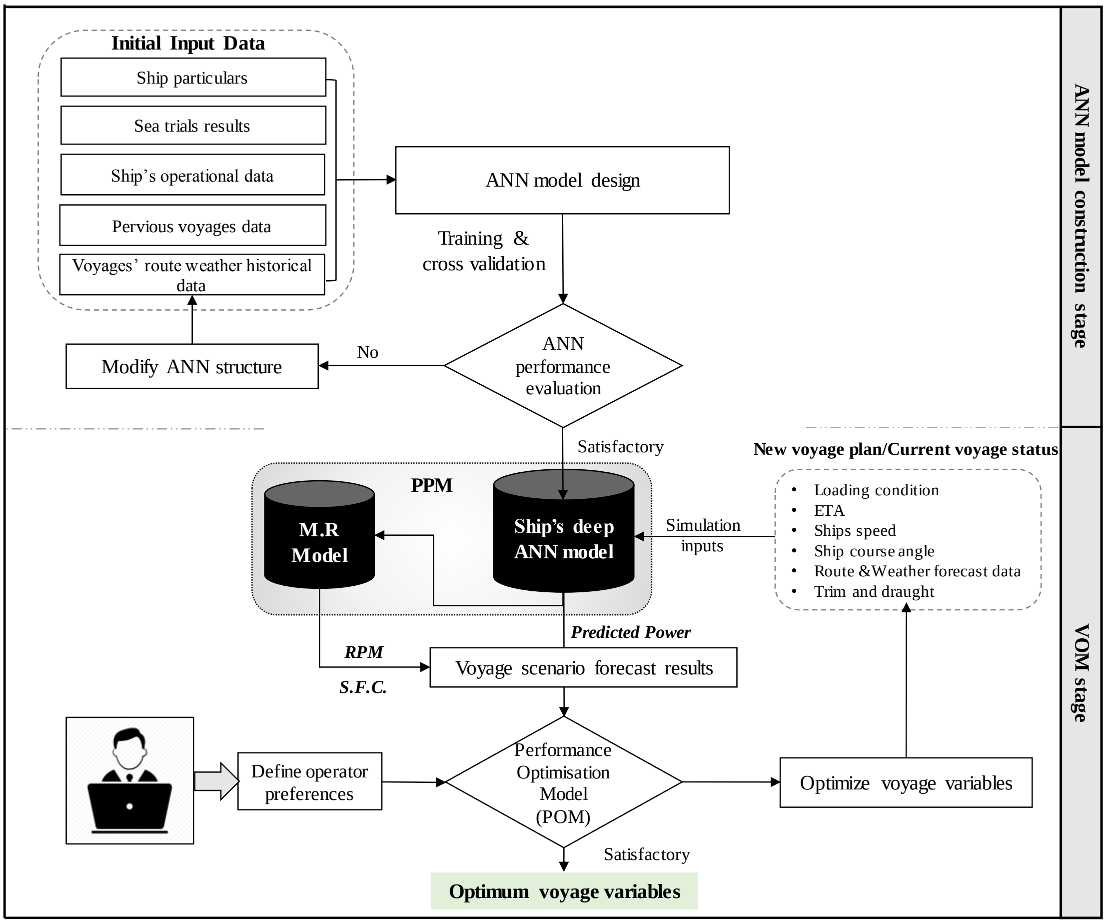


***Figure 3-8*** *The Proposed operational Decision Support System (DSS)*

The system mainly consists of two major models, the ship operational performance prediction model (PPM) and the ship performance optimization model (POM). Both models should be designed to run on a particular ship with its specific preferences. The PPM model includes two ANN and M.R sub-models to estimate the ship's power, B.S.F.C, and RPM. The PPM when initially designed should employ the ship's specifications with its historical voyage dataset to line up with the proposed methodology. Such a dataset should be used to train the ANN model to build up its knowledge about the ship behavior in different operational scenarios.

Additionally, the PPM can update itself automatically with the ship performance degradation as the ANN has the power to learn from the training data pattern. For example, if the ship's performance deteriorated due to the hull fouling effect, the model as continuously fed with the ship performance data, the ANN model can recognize the ship performance new trend.

The PPM after validation can be exploited to predict the ship response to a particular voyage scenario or during the voyage itself to assess several available alternatives to improve the voyage's performance. To achieve such an objective, the performance optimization model (POM) should be fed with the performance forecast results to supply the needed advice to the ship's master.

The nature of the POM depends on the optimization problem's nature. For the scope of this dissertation, only single-objective optimization model was valid.

After setting up the POM with the operator's preferences, the model should be able to evaluate the results according to the set criteria. If the criteria not met, the model will change the available voyage variables, and the results should be obtained spontaneously from PPM till the required criteria met.

Finally, the system as illustrated is dynamic and requires a full integration between its components for an efficient running.

Chapter 4.

# *The Decision Support System modeling*

## *4.1 Dataset*

Ship performance-related studies traditionally collect data either through Noon reports or onboard high-frequency automatic data acquisition systems. Onboard Data logging had been developed in the recent years to become more computerized with client-server software that replaced logbooks with electronic operational reports received continuously from shore's side. Furthermore, many classification societies in cooperation with software solutions providers had offered real-time monitoring systems with an automatic feature voyage reports creation. **Figure 4-1** (NAPA), (DNV-GL). The current technology development in monitoring the ship performance during sea voyage had provided ship's operators with massive real-time data that should be efficiently exploited.

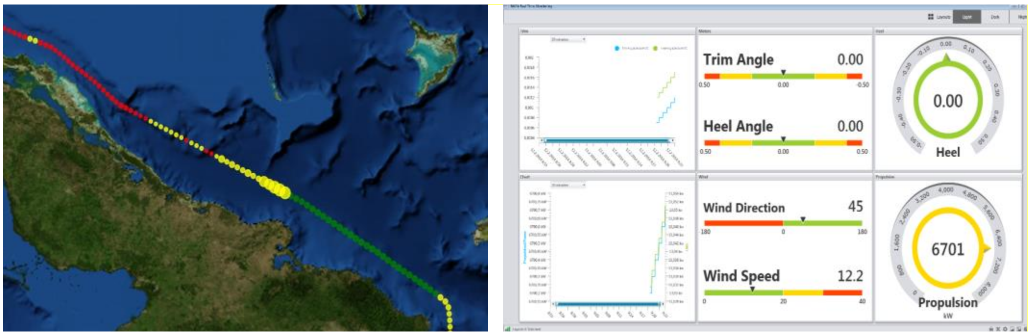


***Figure 4-1*** *Class NK and NAPA joint ship Green monitoring tool, Source: www.napa.fi*

However, the question arises about the certainty and reliability level of automatic Continuous Monitoring systems (CM) and traditional Noon Reporting (NR) method. (Aldous, T.Smith, R.Bucknall, & P.Thompson, 2015) Conducted a study of the uncertainty level of ship performance monitoring, and presented a method to quantify the overall uncertainty in a ship performance indicator. The study results indicated the substantial uncertainty benefit of CM data over NR data; up to 90% decrease in the uncertainty level. In other words, the CM data has much more reliable and reflects the ship behavior pattern during the sea voyage.

### *4.1.1 Data description*

The case studies in this dissertation are based on the operational data of two sea voyages of M/T ORTHIS, a double-hulled VLCC, built at the end of 2011. More details of the ship particulars shown in **Table 4-1**. The study data contains two files obtained from NAPA in excel sheet format demonstrate the operational and weather hindcast condition of two sea voyages at the same loading condition (DWT-mean draught).

***Table 4-1*** *Study case ship particulars, Source: IMO website*

| ***VESSEL'S NAME:*** | **ORTHIS** |
|---|---|
| *IMO NUMBER:* | 9480837 |
| *DATE DELIVERED:* | 1-Dec-11 |
| *BUILDER (WHERE BUILT):* | DMSE, Okpo, Korea |
| *TYPE OF VESSEL:* | Oil Tanker |
| *TYPE OF HULL:* | Double Hull |
| *LENGTH OVERALL (LOA):* | 333.00 m |
| *LENGTH BETWEEN PERPENDICULARS (LBP):* | 320.00 m |
| *EXTREME BREADTH (BEAM):* | 60.00 m |
| *DRAFT (LOADED)* | 21.03 m |
| *FREEBOARD* | 6.14 m |
| *DISPLACEMENT* | 337354.50 mt |
| *DEADWEIGHT* | 293415.80 mt |

The company declared that it is currently cooperating with Tidtech for the weather forecast and VesselTracker as the AIS data provider. The given voyage dataset includes operational values, like ship's speed, propeller RPM, brake power, instant fuel consumption at each sampling point. It additionally contains route and weather hindcast related information such as water depth, wind, wave, swell and current absolute values (**Figure 4-2**)

| | | | | | | | | | |
|---|---|---|---|---|---|---|---|---|---|
| *Index* | *Time stamp* | *Latitude* | *Longitude* | *Speed Over Ground* | *Rpm* | *Brake Power* | *Fuel MassFlow* | *Wind Speed* | *Wind Direction* |

| | | | | | | | | |
|---|---|---|---|---|---|---|---|---|
| *Wave Significant Height* | *Wave Significant Period* | *Wave Direction* | *Swell Significant Height* | *Swell Significant Period* | *Swell Direction* | *Sea Current Speed* | *Sea Current Direction* | *Water Depth* |

***Figure 4-2*** *Dataset variables as obtained from NAPA*

The obtained data were extracted from the ship's automatic continuous monitoring system, the AIS and weather hindcast information with an intensive samples pattern. However, The data sample points have uneven time intervals. This may occur due to the shortage of AIS and weather forecast coverage in some areas along the voyages. From **Figure 4-3**, can observe the sampling frequency in the first voyage is better distributed along ship's route than the second voyage.

**Figure 4-3** and **Table 4-2** reviews both voyages general information, while **Figure 4-4** is showing the SOG histogram for both voyages. The graph shows the average speed difference between the two voyages. The first voyage had an average speed of 12.47 kn, whereas the second voyage had a mean speed of 11.90 kn with the exclusion of the drifting period. The average speed difference is mainly due to the voyage routes variances. The second voyage route as shown in **Figure 4-3** had many maneuvering passages that require speed reduction for the ship navigation safety. It is worth mentioning that both voyages had the same loading condition, i.e., the same DWT of 298762 mt and same mean draft of 21 m.

***Table 4-2*** *Case study voyages overview*

| *Voy. No* | *Departure Port* | *Arrival Port* | *No. of data samples* | *V. time (dd:hh:mm)* | *Route length (nm)* | *Total Fuel Cons. (mt)* | *F.Cons (mt/nm)* |
|---|---|---|---|---|---|---|---|
| **(1)** | *Sultan Qaboos* **(Oman)** | *Ain Sukhnah* **(EGY)** | 1142 | 09:03:34 | 2801 | 367.9 | 0.131 |
| **(2)** | *Sidi Kerir* **(EGY)** | *Rotterdam* **(NTH)** | 2562 | 12:14:21 | 3215 | 437.7 | 0.136** |

*** Drifting period excluded from the calculations*

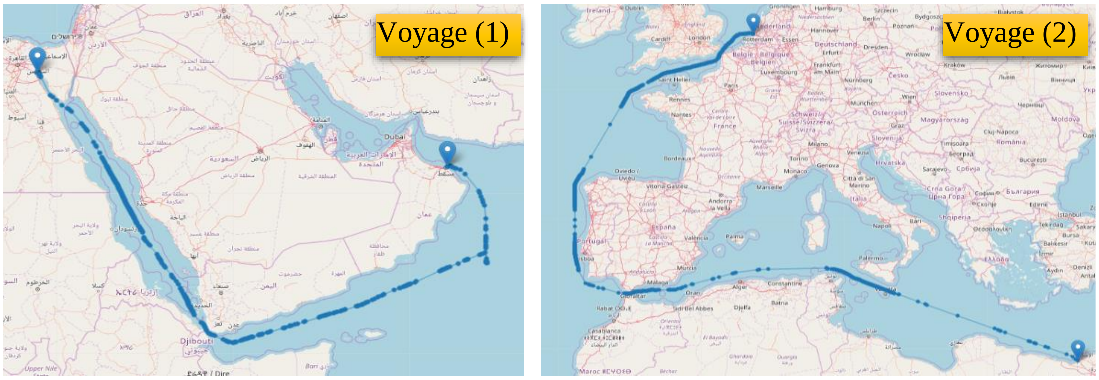


***Figure 4-3** Sea voyages route illustration*

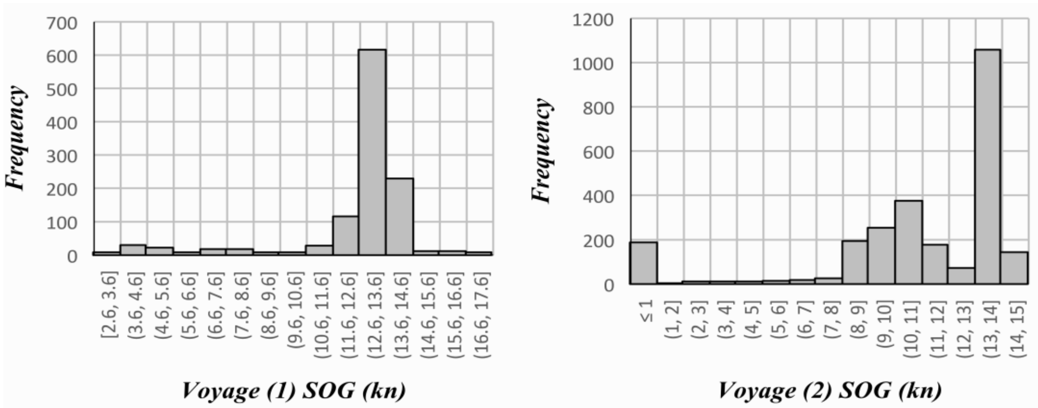


***Figure 4-4** SOG Histogram for both voyages*

### *4.1.2 Data analysis*

The second voyage dataset was chosen to be used in designing the structure of the ANN and M.R models, mainly because it has a larger dataset. However, the second voyage has one day drifting before the arrival to Rotterdam for waiting for the berthing instructions (note **Figure 4-4** for second voyage SOG histogram, as it shows 200 samples with < 1 kn speed), which caused a high noise in the dataset during that period. Thus, the drifting period data set excluded from ANN training dataset to reflect the actual voyage sea time.

## *4.2 Weather modeling*

Many calculations had been carried out on the voyages dataset to understand the effect of the voyage variables, especially the effect of the sea state on the ship's performance. The first step was to obtain the true values of the apparent wind speed, wave, swell and current on ship's direction. The steps used for processing weather was as follows:

1. **Ship's heading ($\boldsymbol{\theta_s}$):**

$$\theta_s = tan^{-1}2\,(sin\,\Delta\lambda * cos\,\varphi_2, cos\,\varphi_1 * sin\,\varphi_2 - sin\,\varphi_1 * cos\,\varphi_2 * cos\,\Delta\lambda) \qquad (12)$$

Where $\varphi_1$, $\lambda_1$ are the start point's Lat and Long, while $\varphi_2$, $\lambda_2$ are the end point's Lat and Long, and $\Delta\lambda$ is the difference in longitude. For excel, DEGREE(ATAN2) function used with the radian Lat and Long coordinates. The results examined against online map service and the used formula showed high accuracy (Veness, 2017) (Bukaty & Morozova, 2013).

2. **The true wind angle ($\boldsymbol{\theta_{tw}}$):**

$$\theta_{tw} = |\theta_w - \theta_s| \qquad (13)$$

Where, $\theta_w$ is the wind angle.

Then, the following excel argument used to contain the true wind angle between (0-180) range instead of (0-360) range as studying the wind effect on ship's power will not be affected if the wind is heading from the port or starboard side of the ship:

$\boldsymbol{\theta_{tw`}}$ =IF($\theta_{tw}$>180,ABS($\theta_{tw}$-360),IF($\theta_{tw}$<-180,ABS($\theta_{tw}$+360),ABS($\theta_{tw}$)))

Similarly, the relative angle for waves, sea current, and the swell has been found. Meanwhile, **Figure 4-5** illustrates the correlation between the wind and wave angles in both voyages. The figure shows a high correlation between both variables. It is well known from fluid dynamic principles the high correlation between wind and wind-generated waves in a sense that justifies the high correlation factors found in the mentioned graph (Wright, Colling, & Park, 1999). Thus, only one angle was used to represent both the wave and wind angles, usually denoted in the dissertation with Wind/Wave encounter angle.

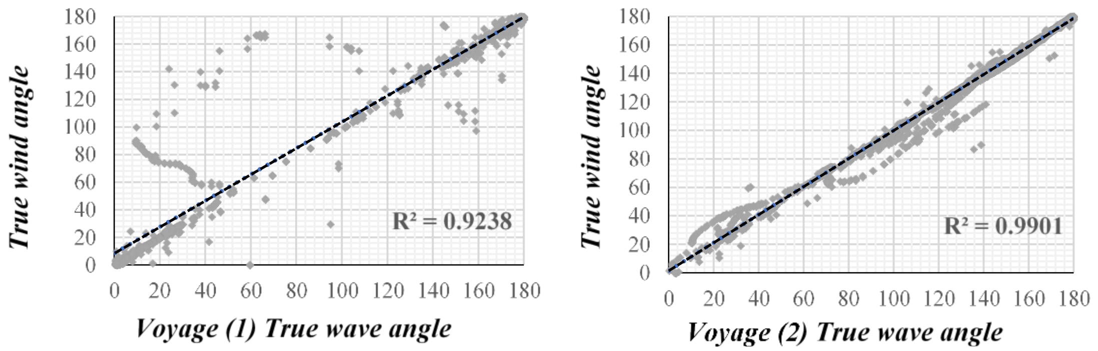


***Figure 4-5*** *Wind and wave angles correlation*

**3. The Apparent wind angle ($\theta_{Aw}$):**

$$\theta_{Aw} = [180 * tan^{-1}\{(sin\left(\pi * \frac{\theta_{tw}}{180}\right) * S_w)/(SOG + cos\left(\pi * \frac{\theta_{tw}}{180}\right) * S_w\}]/\pi \qquad (14)$$

Where (SOG) is the ship speed over ground, and ($S_w$) refers to the wind speed in m/s and ($\pi$) refers to the ratio of a circle's circumference to its diameter, equals a constant value of 3.1416.

**4. The apparent wind speed ($S_{Aw}$):**

$$S_{Aw} = \sqrt{\left[sin\left(\pi * \frac{\theta_{tw}}{180}\right) * S_w\right]^2 + \left[SOG * cos\left(\pi * \frac{\theta_{tw}}{180}\right) * S_w\right]^2} \qquad (15)$$

**5. The apparent wind speed on ship's heading ($S_{AH}$):**

$$S_{AH} = S_{Aw} * cos(\theta_{Aw} * \frac{\pi}{180}) \qquad (16)$$

## *4.2.1 Beaufort number and sea state:*

The Beaufort scale was initially established by Sir. Francis Beaufort in the early 19th century. The scale estimates the wind strength without measurement, and it still currently in use for the same purpose to indicate the weather condition such as wind strength, sea state, wave height with a simple figure. The used BF.No scale excel argument was based on the (National Oceanic and Atmospheric Administration (NOAA), 2015) and (Wright, Colling, & Park, 1999) as follows:

BF.No=IF($S_w \geq 32.7$,12,IF($S_w \geq 28.5$,11,IF($S_w \geq 24.5$,10,IF($S_w \geq 20.8$,9,IF($S_w \geq 17.2$,8,IF($S_w \geq 13.9$,7,IF($S_w \geq 10.8$,6,IF($S_w \geq 8$,5,IF($S_w \geq 5.5$,4,IF($S_w \geq 3.4$,3,IF($S_w \geq 1.6$,2,IF($S_w \geq 0.3$,1,0))))))))))))

To understand the wind effect on the ship's performance, we have to analyze the wind direction whether it was heading, beam or on the ship's tail. The following excel argument used for analysis

**Win_dir** =IF($\theta_{tw}$<=60, "Head",IF($\theta_{tw}$<=120, "Beam",IF($\theta_{tw}$<=180,"Tail","error!")))

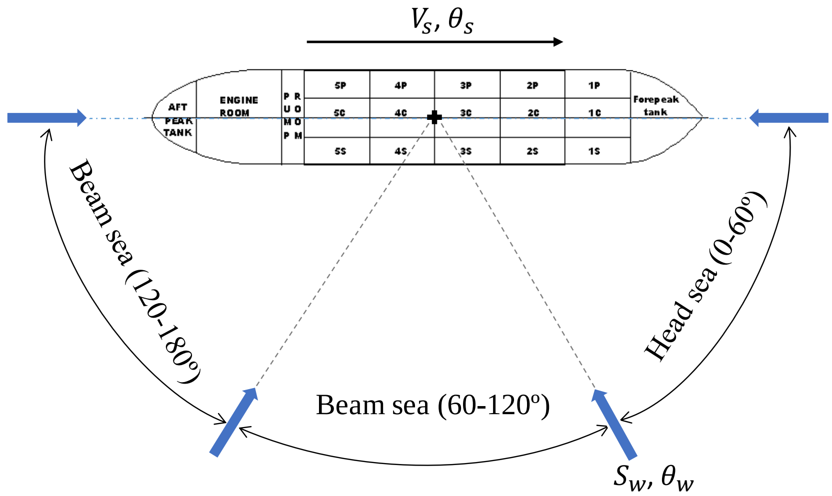


***Figure 4-6*** *The classification of Wind/Wave direction with reference to ship's heading*

Finally, for the sea state number, the following values were used as a reference (Lu, Turan, Boulougouris, Banks, & Incecik, 2015):

***Table 4-3*** *Sea state scale's reference values*

| ***Sea state*** | ***Wind speed (m/s)*** | ***Wave significate height (m)*** | ***Wave significant period (s)*** |
|---|---|---|---|
| **0** | *0* | *0* | 0 |
| **1** | 0.9 | 0.1 | 1.22 |
| **2** | 2.3 | 0.4 | 2.44 |
| **3** | 4.4 | 0.8 | 3.45 |
| **4** | 6.7 | 1.5 | 4.73 |
| **5** | 9.4 | 2 | 5 |
| **6** | 12.6 | 3 | 6.67 |
| **7** | 15.5 | 4.5 | 8.19 |

### *4.2.2 The weather effect on ship's performance*

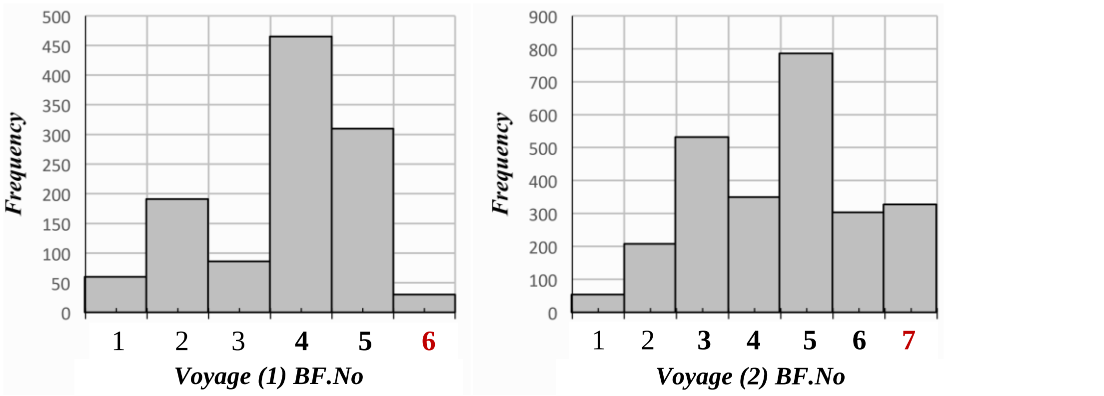


***Figure 4-7*** *The histogram for both voyages Beaufort number*

**Figure 4-7** illustrates histograms for both voyages Beaufort number. The chart clearly shows that the second voyage had rougher weather as the ship was exposed to BF.No 3,5, 6 and 7 for the more extended period. While voyage (1), the ship went through BF.No 4 and 5 for the most of the voyage time. However, to understand the effect of the wind on the ship performance, we have to analyze the wind direction whether it was heading, beam or on the ship's tail. The illustration in **Figure 4-6** was used for this analysis, and the analysis results are shown in Error! Reference source not found.**.**

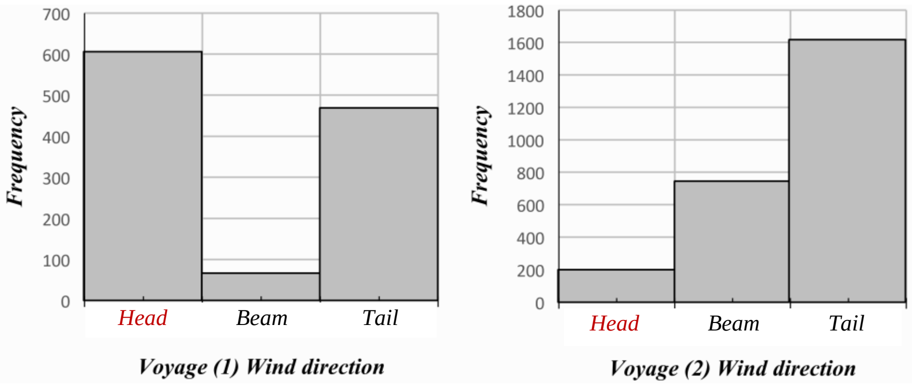


***Figure 4-8*** *The histogram of the Wind/Wave direction to ship's course*

Notwithstanding the ship was exposed to a tougher weather condition in the second voyage as concluded before, the highly correlated wind and wave directions were mostly on tail during that voyage as illustrated in **Figure 4-8**. Thus, the weather condition, in that case, maybe in favor of reducing the ship fuel consumption.

However, to clearly understand the dynamic sea states effect, the ship performance at different sea states and different directions need further analysis.

Therefore, the ship's speed was plotted against the ship's propulsion power at various weather circumstances. **Figure 4-9** shows the trend lines of the three classified wind/wave directions in different sea states. The Ship's power consumption while the wind/wave direction to the tail has a marginal less power consumption for a certain speed. The figure also shows that the weather effect on ship performance raises as the ship speed increases.

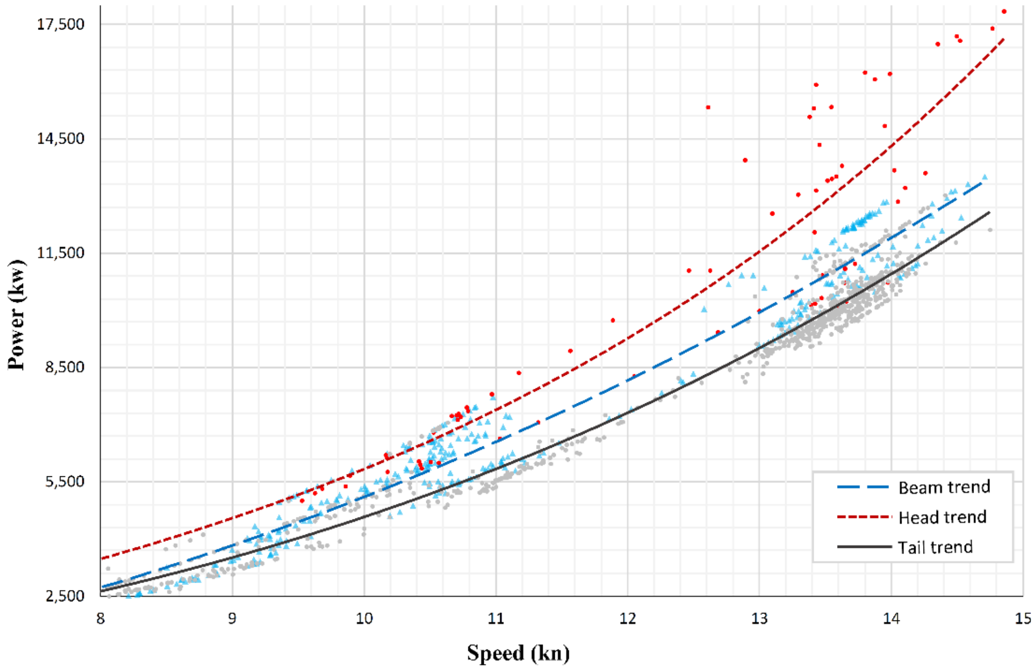


***Figure 4-9*** *Ship's speed-power relationship at different wind/wave encounter angles*

Further analysis has shown in that the ship may consume less at tougher weather conditions if the ship is heading in the right direction relative to the wind/wave encounter angle. For example, the voyage data shown in **Figure 4-10** illustrates the ship performance at different sea states only with the wind/wave direction to the ship's tail. From the graph, if the ship sails at 12.5 kn speed with sea state (1), the delivered propulsion power was around 8800 kw, while in sea state (5) was 7950 kw. Thus, the power difference represents 9.66% although the ship was sailing in harsher weather environment, it was to the favor of the ship's movement.

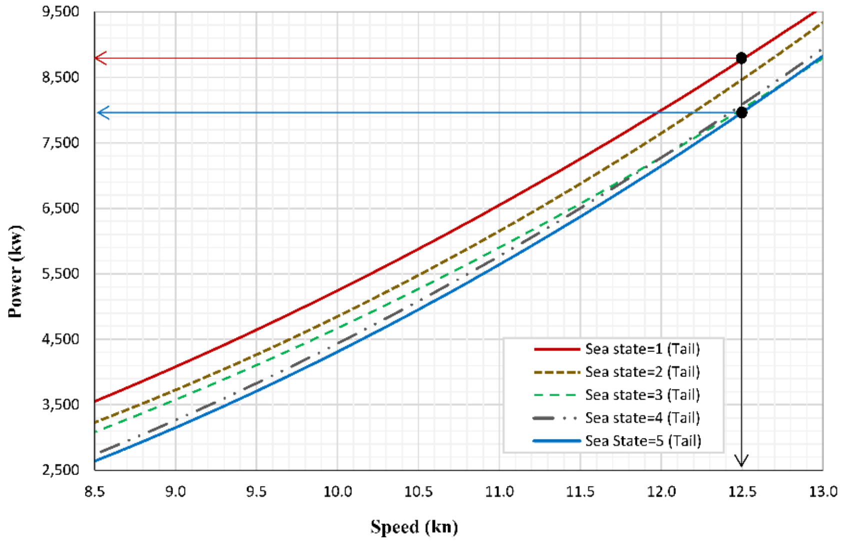


***Figure 4-10*** *Ship's speed-power relationship at different sea states with wind/wave in tail direction*

Finally, **Figure 4-11** comparing the ship's performance at sea state (1) with beam/head wind/wave direction and sea state (4) with tail wind/wave direction. The propulsion power consumed at sea state (4) with tail direction is marginally less than sea state (1) at beam/head direction.

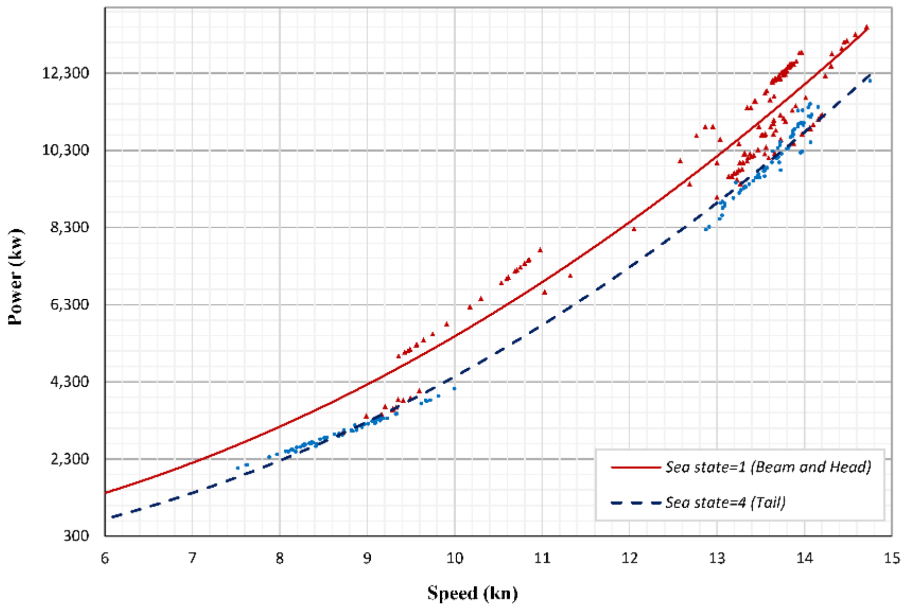


***Figure 4-11*** *Comparison of the ship performance at sea state 1 & 4 with different wind/wave direction*

To sum up, the previous examples verify the potential energy savings of the weather routing as discussed in **section 2.3.2.** Still, The main challenges if the measure to be used in optimization scenarios for voyage planning is the accuracy of the forecast weather data, the quality of the vessel performance model, and the availability of alternative route especially in short voyages or navigation restricted seaways.

## *4.3 Fuel consumption calculations*

To accurately assess the ship performance model, the ship fuel consumption must be calculated at each sampling point. The obtained sampling points as **Figure 4-12** shows, an example of the dataset fuel consumption. The entries divided into patterns as the figure shows.

| Index | Time stamp | Lat | Long | sample time | Time from departure | Sample distance (nm) | distance travelled (nm) | course | Speed (knots) | Rpm | Brake Power (kw) | Fuel Mass Flow (kg/sec) | S.F.C g/kw.hr |
|---|---|---|---|---|---|---|---|---|---|---|---|---|---|
| 1 | 3/8/2017 4:27 | 23.67 | 58.63 | 00:00 | 00:00:00 | 0 | 0 | 45.28 | 3.44 | 16.22 | 247.867 | 0.0131 | 190.7815 |
| 2 | 3/8/2017 4:32 | 23.67 | 58.64 | 00:05 | 00:00:05 | 0.33 | 0.33 | 45.28 | 3.44 | 16.20 | 246.75 | 0.0131 | 190.7821 |
| 3 | 3/8/2017 4:32 | 23.67 | 58.64 | 00:00 | 00:00:05 | 0.00 | 0.33 | 39.42 | 5.17 | 23.28 | 706.2946 | 0.0374 | 190.5028 |
| 4 | 3/8/2017 4:36 | 23.68 | 58.64 | 00:03 | 00:00:09 | 0.30 | 0.64 | 39.42 | 5.17 | 23.21 | 699.6607 | 0.0370 | 190.5069 |
| 5 | 3/8/2017 4:36 | 23.68 | 58.64 | 00:00 | 00:00:09 | 0.00 | 0.64 | 36.90 | 6.87 | 30.18 | 1509.929 | 0.0797 | 190.0138 |
| 6 | 3/8/2017 4:41 | 23.68 | 58.65 | 00:05 | 00:00:14 | 0.63 | 1.26 | 36.90 | 6.87 | 30.17 | 1509.384 | 0.0797 | 190.0141 |
| 7 | 3/8/2017 4:41 | 23.68 | 58.65 | 00:00 | 00:00:14 | 0.00 | 1.26 | 35.05 | 8.29 | 36.04 | 2548.185 | 0.1340 | 189.3808 |
| 8 | 3/8/2017 4:47 | 23.70 | 58.66 | 00:06 | 00:00:20 | 0.83 | 2.09 | 35.05 | 8.29 | 36.05 | 2550.946 | 0.1342 | 189.3791 |
| 9 | 3/8/2017 4:47 | 23.70 | 58.66 | 00:00 | 00:00:20 | 0.00 | 2.09 | 35.57 | 9.32 | 40.24 | 3521.401 | 0.1847 | 188.7862 |
| 10 | 3/8/2017 4:51 | 23.70 | 58.66 | 00:03 | 00:00:24 | 0.52 | 2.62 | 35.57 | 9.32 | 40.24 | 3523.37 | 0.1848 | 188.785 |
| 11 | 3/8/2017 4:51 | 23.70 | 58.66 | 00:00 | 00:00:24 | 0.00 | 2.62 | 41.24 | 10.40 | 44.48 | 4711.605 | 0.2461 | 188.0567 |

***Figure 4-12*** *(Part-1) Dataset Fuel consumption illustration*

The pattern changes with each ship's course value change (green highlighted) with a new set of values (note that the new data row has the same time and location but different ship parameters like speed and power). For fuel consumption calculations, the Brake Specific Fuel Consumption (B.S.F.C) calculated at each power point as follows:

$$B.S.F.C = F.R_{fuel} * \frac{3600}{B.P*1000} \qquad (17)$$

Where ($F.R_{\text{fuel}}$) is the fuel flow rate in kg/sec, while (B.P) is the Brake power in kw and (B.S.F.C) in gr/kw.hr.

| Actual Engine Revolution <rpm> | Actual Brake Power <kW/hr> | SFC gr/kw.hr | Comsumed energy <kw> | sample F.C (mt) |
|---|---|---|---|---|
| 16.22 | 247.87 | 190.78 | 0.0 | 0.00E+00 |
| 16.20 | 246.75 | 190.78 | 23.9 | 8.78E-03 |
| 23.28 | 706.29 | 190.50 | 0.0 | 0.00E+00 |
| 23.21 | 699.66 | 190.51 | 41.0 | 1.23E-02 |
| 30.18 | 1509.93 | 190.01 | 0.0 | 0.00E+00 |
| 30.17 | 1509.38 | 190.01 | 137.5 | 3.51E-02 |
| 36.04 | 2548.18 | 189.38 | 0.0 | 0.00E+00 |
| 36.05 | 2550.95 | 189.38 | 255.8 | 5.76E-02 |

***Figure 4-13*** *( Part-2) Dataset Fuel consumption illustration*

Then, the fuel consumption at each sampling row calculated with simple math by calculating the sample time and the consumed energy during this period (**Figure 4-12** and Error! Reference source not found.)

| Actual Engine Revolution <rpm> | Actual Brake Power <kW/hr> | SFC gr/kw.hr | Comsumed energy <kw> | sample F.C (mt) |
|---|---|---|---|---|
| 16.22 | 247.87 | 190.78 | 0.0 | 0.00E+00 |
| 16.20 | 246.75 | 190.78 | 23.9 | 8.78E-03 |
| 23.28 | 706.29 | 190.50 | 0.0 | 0.00E+00 |
| 23.21 | 699.66 | 190.51 | 41.0 | 1.23E-02 |
| 30.18 | 1509.93 | 190.01 | 0.0 | 0.00E+00 |
| 30.17 | 1509.38 | 190.01 | 137.5 | 3.51E-02 |
| 36.04 | 2548.18 | 189.38 | 0.0 | 0.00E+00 |
| 36.05 | 2550.95 | 189.38 | 255.8 | 5.76E-02 |

***Figure 4-13*** *( Part-2) Dataset Fuel consumption illustration*

## *4.4 The Dataset correlation analysis*

In this section, the dataset parameters analyzed by regression analysis to obtain their correlation factors and to deeply understand the interrelationship between them.

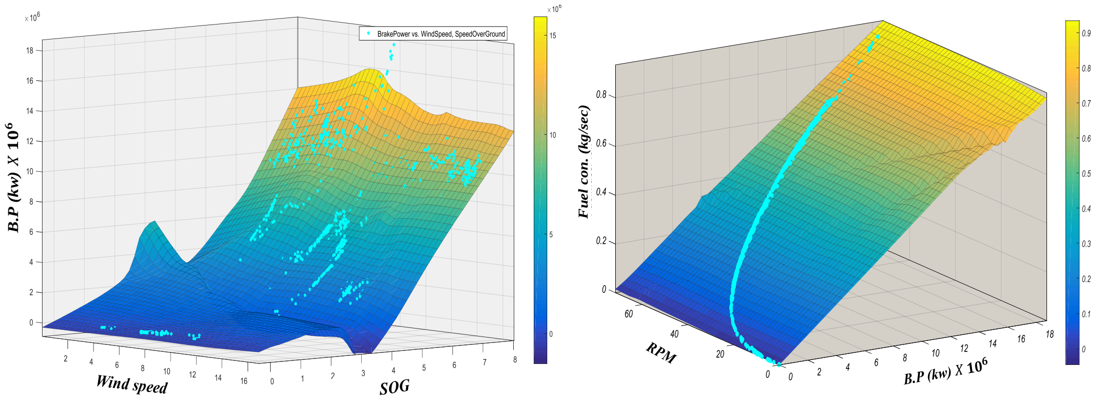


***Figure 4-14*** *Sample of dataset analysis*

The correlation analysis results contained in ***Table 4-4*** with color code from green to red. Green values reflect a positive correlation between their variables, while red values indicate a negative correlation. The ship's speed has a correlation factor of (0.90) with the engine's brake power (B.P) which will certainly benefit the inclusion of the SOG as an ANN input. Both the engine (S.F.C) and Propeller revolutions (RPM) have a linear correlation with the Brake power (B.P) with correlation factors of 0.99 and 0.90 respectively. Such a relation could justify the use of M.R analysis for both values (S.F.C & RPM) to estimate their values from the Engine Brake Power (B.P). As a result, the initial multiple regression results for both RPM and B.S.F.C with the Engine B.P are shown in **Figure 4-15**.

***Table 4-4*** *Data variables correlation factors*

| | Vs | D | Saw | Hws | Tw | ϴen | Hss | Ts | ϴs | Sc | ϴc | RPM | BP | SFC |
|---|---|---|---|---|---|---|---|---|---|---|---|---|---|---|
| Vs | 1.00 | | | | | | | | | | | | | |
| D | 0.43 | 1.00 | | | | | | | | | | | | |
| Saw | 0.13 | 0.34 | 1.00 | | | | | | | | | | | |
| Hws | 0.15 | 0.33 | 0.35 | 1.00 | | | | | | | | | | |
| Tw | 0.12 | 0.24 | 0.34 | 0.98 | 1.00 | | | | | | | | | |
| ϴen | 0.25 | 0.16 | -0.29 | 0.45 | 0.43 | 1.00 | | | | | | | | |
| Hss | 0.16 | 0.13 | 0.16 | 0.51 | 0.56 | 0.08 | 1.00 | | | | | | | |
| Ts | 0.19 | 0.08 | 0.16 | 0.57 | 0.61 | 0.13 | 0.88 | 1.00 | | | | | | |
| ϴs | -0.04 | -0.29 | -0.32 | -0.16 | -0.18 | 0.04 | 0.08 | 0.16 | 1.00 | | | | | |
| Sc | -0.04 | -0.08 | 0.24 | -0.25 | -0.23 | -0.26 | -0.22 | -0.19 | -0.20 | 1.00 | | | | |
| ϴc | 0.35 | 0.29 | 0.12 | -0.23 | -0.27 | -0.12 | -0.27 | -0.49 | -0.25 | 0.15 | 1.00 | | | |
| RPM | 0.99 | 0.42 | 0.16 | 0.11 | 0.08 | 0.18 | 0.15 | 0.18 | -0.06 | 0.01 | 0.37 | 1.00 | | |
| BP | 0.90 | 0.53 | 0.27 | 0.07 | 0.04 | 0.09 | 0.06 | 0.01 | -0.22 | 0.02 | 0.53 | 0.90 | 1.00 | |
| SFC | 0.62 | 0.12 | 0.05 | 0.09 | 0.08 | 0.07 | 0.19 | 0.27 | 0.02 | 0.01 | 0.13 | 0.66 | 0.38 | 1.00 |

***Vs:*** *ships speed;* ***D:*** *water depth;* ***Saw:*** *App. Wind speed on ship dir;* ***Hws:*** *Wave significant height;* ***Tw:*** *Wave Significant period;* ***ϴen:*** *Wave/Wind encountre angle;* ***Hss:*** *Swel significant height;* ***Ts:*** *Swel significant period;* ***ϴs:*** *Swel true angle;* ***Sc****: Current speed;* ***ϴs:*** *Swel true angle;* ***RPM:*** *propeller revolutions per miutes;* ***B.P:*** *Brake Power;* ***SFC:*** *Specific Fuel Consumption*

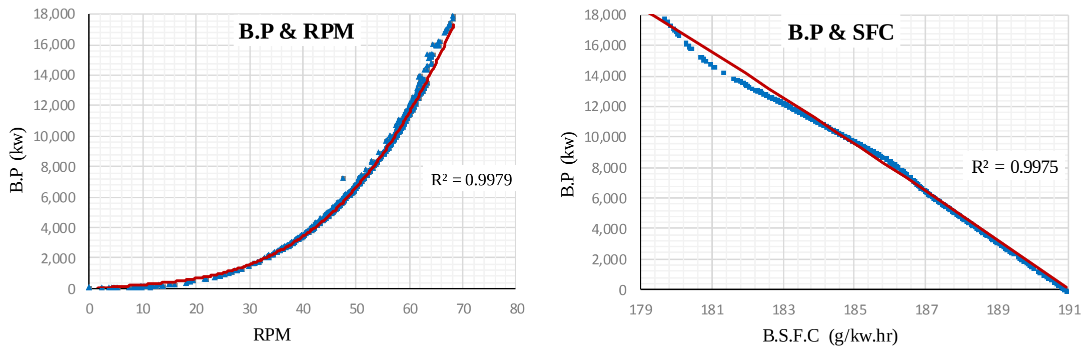


***Figure 4-15*** *Initial M.R analysis between RPM and B.S.F.C with Engine RPM*

Meanwhile, The ship Various SOG values plotted against engine brake power illustrated in **Figure 4-16-(a).**

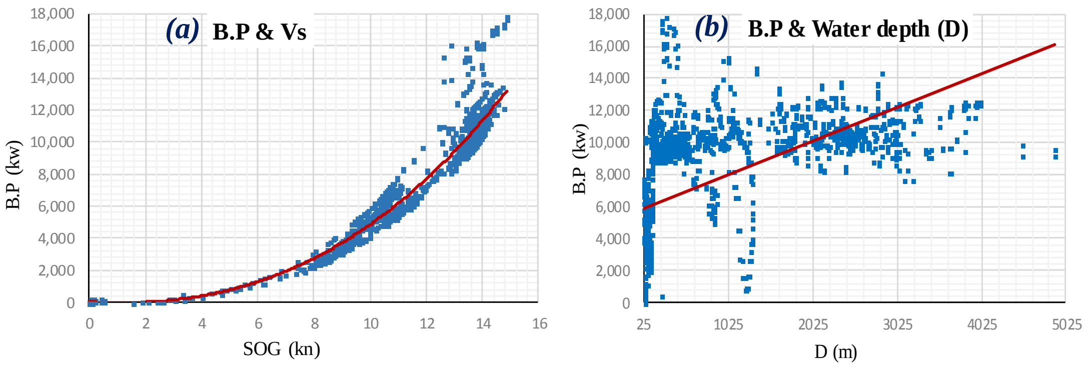

***Figure 4-16** (a) Ship speed and (b) Water depth relation with Engine brake power*

**Figure 4-16 (part-a)** demonstrates the high variation of B.P values with the SOG while its values increases. This variation can be justified by the weather influence as it rises when the ship's speed increases. Additionally, the figure at **(part-b)** shows the sea water depth high correlation factor of 0.53 with the ship's power. It can be explained by the fact that the ship while sailing is usually slowing down as it approaches the restricted waterways (low-depth) and speeds up as the ship commences to the deep sea passage. Besides, the shallow water causes the squat-effect which is a combination of parallel sinkage and trim. Also, it increases the total resistance of the ship (viscous and wave-making resistance) which lead to a speed drop and less propulsion efficiency. The effect is limited to a certain value usually referred to the ratio between the wave height and wavelength to be less than 1/20. After that limit, the effect of the seawater depth vanishes (Havelock, 1922).

However, as the ANN gathers its knowledge by detecting the patterns and relationships in the dataset, therefore water depth addition to the ANN model input variables will be advantageous due to its high correlation factor with the ANN output, i.e., the B.P.

## *4.5 The Performance Prediction Model (PPM)*

One of the study goals was to maximize the benefit of the obtained dataset to enhance the outcome results as much as possible. **Figure 4-17** summarizes the data classification process to build the Performance Prediction Model (PPM). The figure also shows that part of the data used for different purposes, like calculating the Beaufort number or the sea state number to analyze the weather effect.

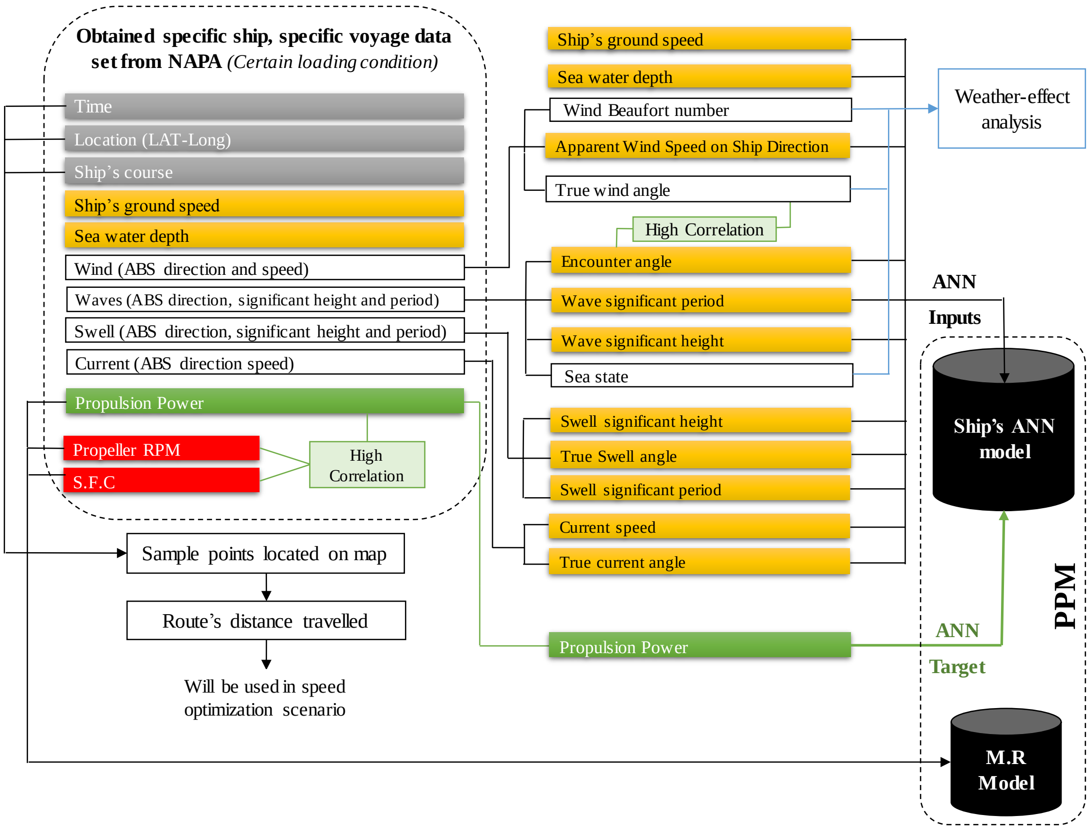


***Figure 4-17*** *Dataflow*

In this section, the procedure used to build the PPM will be thoroughly explained with its two sub-models, the ANN model, and M.R model.

### *4.5.1 The Artificial Neural Network (ANN) model*

The ANN model in this study mainly aims to predict the ship B.P in different seaway conditions from a set of input variables. As discussed in **section 3.1.1**, ANN can take several structures based on the complexity of the dataset and the level of accuracy to be obtained from the model. In this study, the ANN model has one hidden layer with 16 neurons as illustrated in **Figure 4-18**.

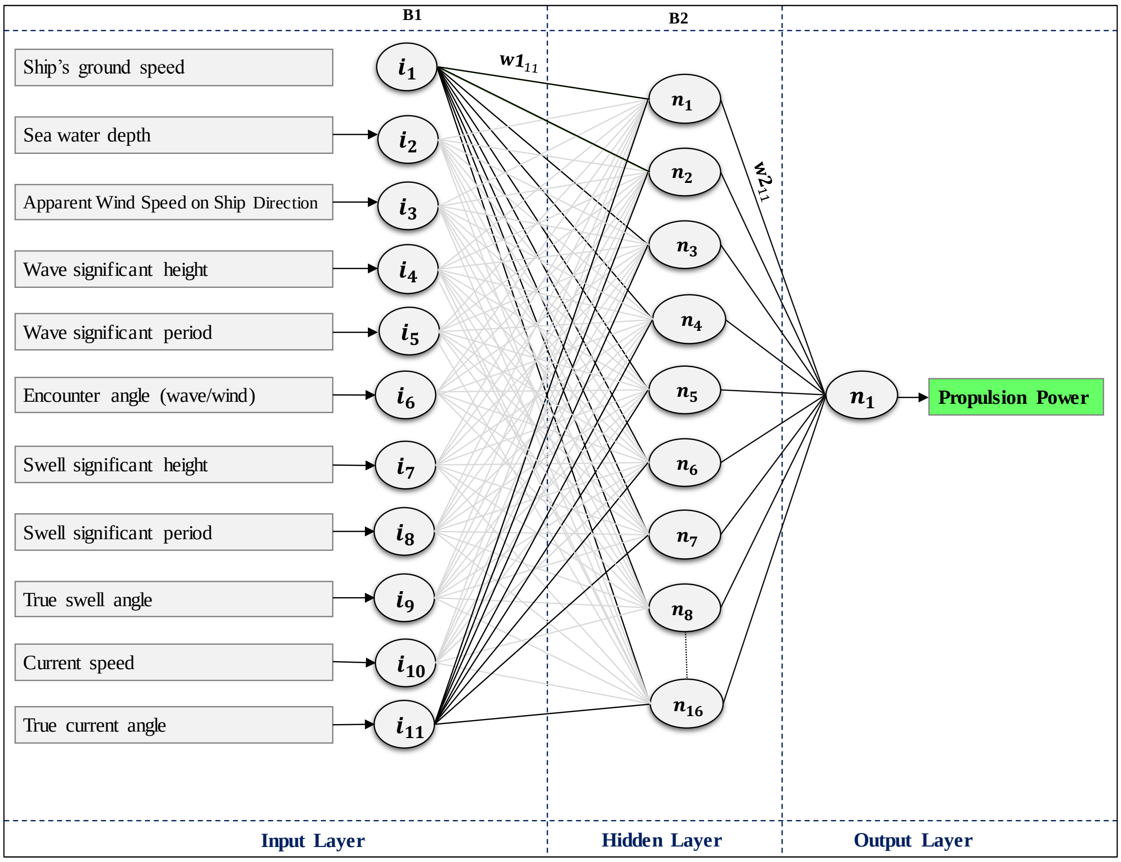


***Figure 4-18** ANN model structure layout*

The ANN model input variables include 11 variables as :

- Ship's speed
- Seawater depth
- Apparent wind speed on ship's direction, which is highly correlated to the ship heading angle.
- Wave parameters (Three inputs)
- Swell parameters (Three inputs)
- Sea current (Two parameters)

Therefore, any change in the ship's heading angle will influence the values of inputs number 3, 6, 9, and 11. It is important that the architecture of this model based on the literature and try and trial of the results.

A feed-forward backpropogation type network selected with a training function that updates weight and bias values according to Levenberg-Marquardt optimization. **Figure 4-19** shows the ANN model structure with the transfer functions for layers 1 and 2 of logistic and hyperbolic tangent functions respectively.

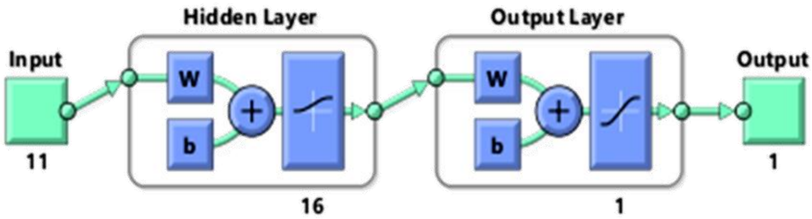


***Figure 4-19*** *Screenshot of the ANN structure*

The ANN input variables normalized to be within the range of [0,1], as illustrated in **Table 4-5**. The second voyage dataset used to train and validate the structured model.

***Table 4-5*** *ANN model input variables range values*

| | $i_1$ | $i_2$ | $i_3$ | $i_4$ | $i_5$ | $i_6$ | $i_7$ | $i_8$ | $i_9$ | $i_{10}$ | $i_{11}$ |
|---|---|---|---|---|---|---|---|---|---|---|---|
| **Min** | 0.122 | 0.001 | 0.0 | 0.0 | 0.002 | 0.0 | 0.0 | 0.0 | 0.0003 | 0.005 | 0.0 |
| **Max** | 0.851 | 0.98 | 0.921 | 0.974 | 0.664 | 0.9 | 0.823 | 0.849 | 0.854 | 0.658 | 0.937 |

### *4.5.2 ANN-model performance*

The model has used the cross-validation method with a random division of the dataset to 70% for training, 15% for validation, and 15% for testing. Furthermore, one of the case studies was dedicated to testing the model accuracy by predicting the first voyage B.P values as will be shown in the next chapter. The ANN model performance assessed by the regression analysis and the mean squared error (MSE) of the results. The ANN model trained for 556 iterations with the best-achieved validation performance at epoch 456 with an MSE value of 8.97e-6, and overall R-square value of 0.99 as shown in **Figure 4-20.** The blue line represents the training data MSE, the green line for the validation data MSE, while the red line represents the test data MSE against the epochs count number.

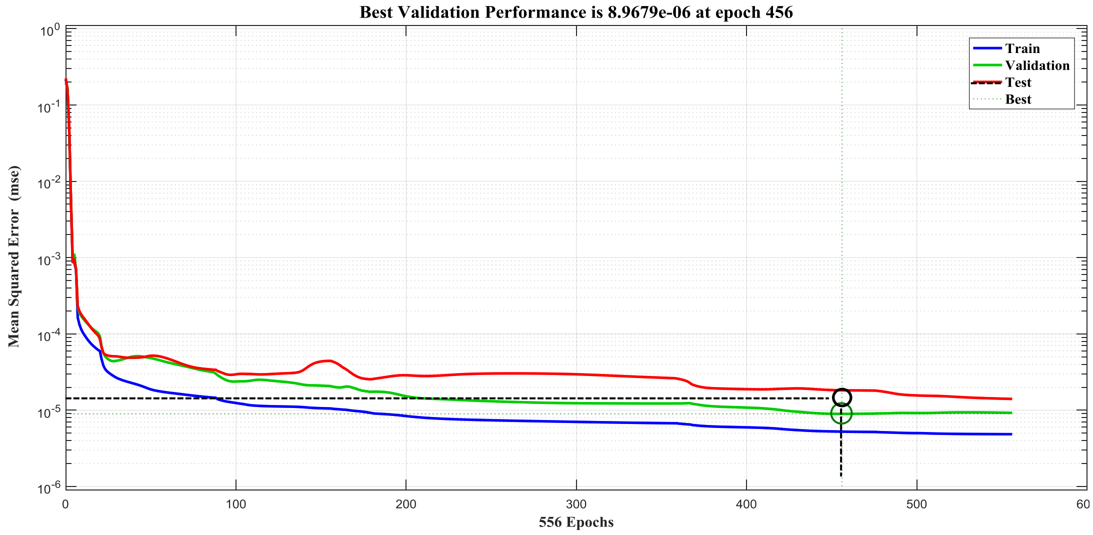


***Figure 4-20*** *ANN model performance*

## *4.5.3 The Multiple Regression (M.R) models*

For this model, the Matlab curve fitting tool had been used to identify the regression function that suits the highly correlated brake power with RPM and B.S.F.C. The second voyage related data fed to the tool, then several functions had been tested to achieve the highest R-square value with minimum RMSE (**section 3.1.2.3.).** Finally, the first voyage data used to validate the selected function.

### *4.5.3.1 The Brake power (B.P) - RPM function*

The Matlab curve fitting tool contains several fitting functions, the best results obtained with the power function as following:

$$RPM = f(x) = a \times x^b + c \qquad (18)$$

***Table 4-6*** *Coefficients of RPM M.R function*

| *(x)* | *(a)* | *(b)* | *(c)* |
|---|---|---|---|
| B.P variables | 3.263 | 0.3161 | −2.742 |

The selected function validated with the first voyage dataset to predict the RPM values corresponding to B.P values. By recalling Equation ( 16 ) and (17), The validation results are as follows:

***Table 4-7*** *Goodness to fit and prediction results for RPM M.R model*

| *Case* | *SSE* | *R-Square* | *RMSE* | *Residuals (g/kw.hr)* | | |
|---|---|---|---|---|---|---|
| | | | | *Mean err* | *Min err* | *Max err* |
| **Voyage (2)** | 262.7 | 0.9985 | 0.3339 | 0.26 | 4.14E-05 | 2.39 |
| **Voyage (1)** | 438.61 | 0.9964 | 0.619735 | 0.51 | 7.42E-04 | 2.46 |

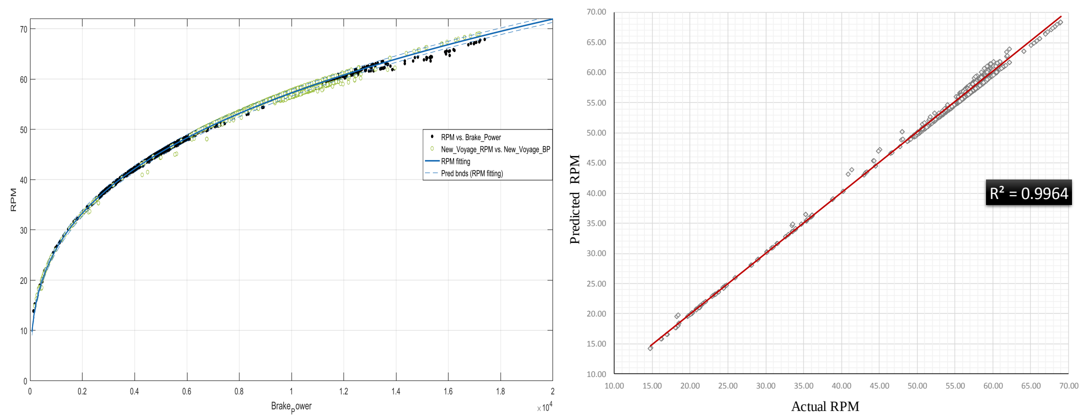


***Figure 4-21*** *Voyage (1) RPM fitting and prediction regression analysis*

### *4.5.3.2 Brake power – B.S.F.C function*

The B.S.F.C best fitting function achieved with the Polynomial function to the power seven.

$$B.S.F.C = f(x) = \beta_0 + \beta_1 x + \beta_2 x^2 + \beta_3 x^3 + \beta_4 x^4 + \beta_5 x^5 + \beta_6 x^6 + \beta_7 x^7 \quad (19)$$

Where *(x)* is normalized by the mean value of 7847 and an std. Deviation value of 3276, while ($\beta_n$) coefficients are as follows:

***Table 4-8*** *B.S.F.C Polynomial function coefficients*

| $\beta_0$ | $\beta_1$ | $\beta_2$ | $\beta_3$ | $\beta_4$ | $\beta_5$ | $\beta_6$ | $\beta_7$ |
|---|---|---|---|---|---|---|---|
| 186.3 | -1.929 | -0.2785 | -0.1988 | 0.04687 | 0.03975 | -0.00263 | -0.00208 |

The selected function validated with the first voyage dataset to predict the B.S.F.C values corresponding to B.P values. The results are illustrated in **Table 4-9**

***Table 4-9*** *Goodness to fit and prediction results for B.S.F.C results*

| *Case* | *SSE* | *R-Square* | *RMSE* | *Residuals (g/kw.hr)* | | |
|---|---|---|---|---|---|---|
| | | | | *Mean err* | *Min err* | *Max err* |
| **Voyage (2)** | 1.9168 | 0.9998 | 0.0285 | 0.05 | 5.58E-03 | 0.67 |
| **Voyage (1)** | 1.5394 | 0.9995 | 0.0367 | 0.06 | 3.63E-03 | 0.18 |

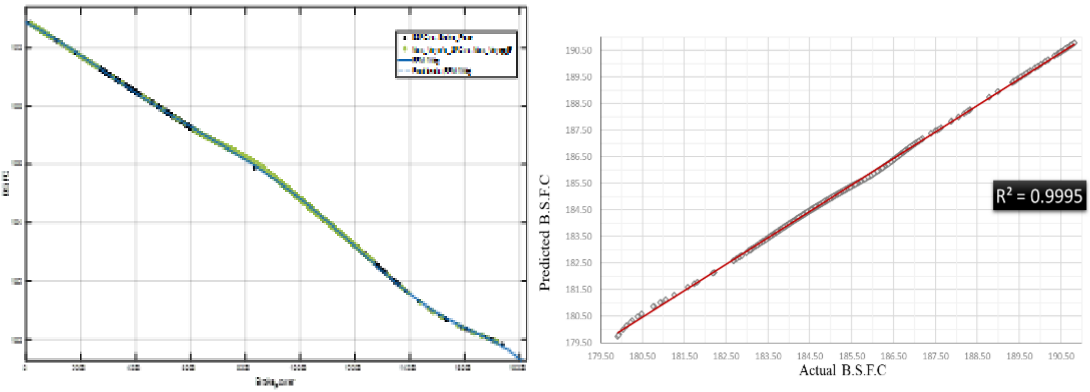


***Figure 4-22*** *Voyage (1) B.S.F.C fitting and prediction regression analysis*

From the previous results, the B.S.F.C estimation showed a higher accuracy with an average error of o.o6 g/kw.hr through 1142 of the first voyage sampling points, while the RPM calculation results had 0.51 mean error within the same sampling points. Both models showed excellent results that can be count on the DSS model.

## *4.6 The Performance Optimization Model (POM)*

Majority of maritime-related problems include multiple conflicting criteria for selecting the optimum choice; therefore marine designers are required to have the utmost careful consideration of these criteria conflict (Parsons & Scott, 2004). Nevertheless, the aim of this dissertation only focused on operational measures with the energy efficiency criteria as a reference. For a more representative result, future developed models should include the ship safety aspect with a higher level decision-making tool. Thus, the optimization in this model will focus only on a single objective approach with two optimization variables, ship's speed, and ship's heading angle to the best energy efficient ship operation. The ship operator then has to compromise (trade-off) between them to achieve better results.

The proposed POM employed the Oracle Crystal Ball add-in software to Excel. The tool could be used when planning for a new voyage with its simulation tool. The software has the capability of performing a random simulation based on a probabilistic approach with a user-defined probability fit function and correlation coefficients between the variables (the second case study).

For the single-objective optimization problem, the software incorporates the OptQuest tool. The tool uses a form of adaptive memory to remember which solutions worked well before and recombines them into new, better solutions. Initially, the tool requires the user to define the optimization model by setting the problem decision variables. Optionally, if the problem requires a probabilistic simulation, then additional assumption variable cells need to be identified with a defined or random probability fit function. Then the tool requires the user to determine the optimization problem by defining the objective and the problem's constraints.

The tool invokes the optimization model to evaluate random or user-defined sets of decision variable values. Then the tool assesses the predicted variables and analyzes them with previous simulation run results, and specify new decision variable values to be evaluated by iteration. Consequently, not all value sets improve the objective, but it provides a solid trajectory to a better solution (Oracle, 2017)

# *Chapter 5.*

# *Case studies*

In this chapter, three case studies are presented to demonstrate the proposed DSS applicability as a support tool that allows enhancing the voyage performance. ***The first case study*** simply employed the developed PPM to forecast a full ship voyage fuel consumption. ***The second case study*** assessed the potentiality of JIT measure if applied in the second voyage. Model simulation supports the results joined with a simple benefit analysis. Finally, ***the third case study*** examines the DSS ability to solve a single-objective voyage optimization problem with various approaches.

## *5.1 (Case study – 1) Voyage Performance forecast*

The developed PPM is used to predict the first Voyage fuel consumption and the results validated with the actual measured values. The ANN model results of Brake Power prediction showed high accuracy with an R-square value of 0.9734 and a mean error value of 333.75 kw as illustrated in **Figure 5-1** and **Figure 5-2**.

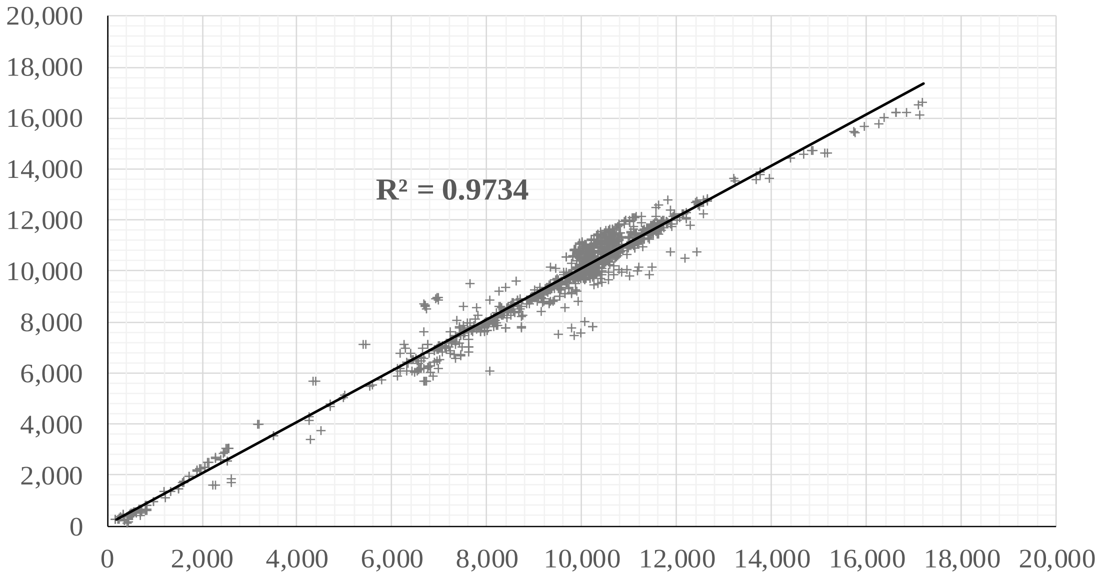


***Figure 5-1*** *Voy (1) ANN model performance regression (Actual B.P against Predicted B.P)*

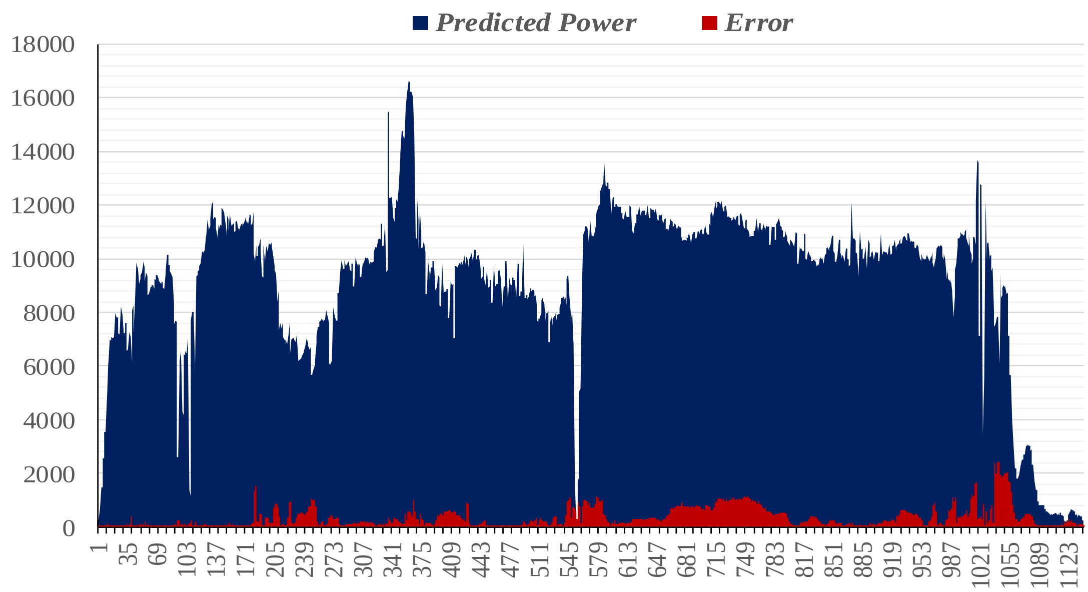


***Figure 5-2*** *Error histogram of Voyage (1) ANN model power prediction*

The predicted B.P values are then fed to the M.R model to obtain RPM and B.S.F.C values at 1124 sampling points. The results showed consistently high accuracy with R-square values of 0.98 and 0.97 for RPM and B.S.F.C respectively.The overall voyage performance prediction summarized in **Table 5-1** showing high total fuel consumption precision with 99.7 % accuracy.

***Table 5-1*** *Voyage performance prediction rsults*

| | **Actual** | **Prediction** | |
|---|---|---|---|
| *Total route distance* | 2801.12 | | *nm* |
| *Sailing time* | 09:03:34 | | *dd:hh:mm* |
| *Average ship speed* | 12.47 | | *knots* |
| *Total energy consumed* | 1,982.7 | 1,978,4 | *MW* |
| *Total voyage fuel consumed* | 367.9 | 366.8 | *mt* |
| *Total $CO_2$ emissons* | 1166.243 | 1162.756 | *ton* |
| *Total voyage fuel Cost (349.99$/mt)* | 128,761.3 | 128,376.3 | *$* |
| *Average propulsion power* | 9067.72 | 9177.00 | *kw.hr* |
| *Average B.S.F.C* | 185.35 | 185.20 | *g/kw.hr* |
| *Average RPM* | 53.77 | 54.18 | |
| *Daily fuel consumption* | 41.14 | 40.09 | *mt/day* |
| *Fuel consumption per nm* | 0.131 | 0.131 | *mt/nm* |

In **Figure 5-2** the B.P prediction error was plotted against the predicted B.P values. The overall results showed an accurate performance. However, the error variation (red color) along the sampling points fluctuated and showed high values at sampling points ranges 681-783 and 1021-1055. This can be justified that the ANN model is trained by the variables of the second voyage dataset. As discussed before in **section 3.1.1**, it is essential for the ANN to train itself with sufficient wide spectrum of the dataset variables. If the test dataset contains a different pattern that the ANN has not been trained by, then the error values increases (**Figure 4-7** shows the dataset variation in both voyages' Beaufort number). Finally, it is important to stress that both voyages had the same loading condition.

## 5.2 (Case study – 2) Slow steaming scenario based on JIT assumption

In this section, the developed prediction tool is used to assess the Just In Time (JIT) potential energy savings for the second voyage, if applied. By evoking the analysis of **Figure 4-4** and **section 4.1.2**, it was shown that the ship had to drift for one day waiting for port authority berthing instructions. The scenario is built on the assumption that the ship operators have given the latest berthing time instructions before commencing the voyage, and hence a new voyage plan designed with a new average speed and new ETA. The second assumption that the ship sails in the same route positions (Lat-Long) through the same weather conditions to use the original dataset. The new ship speed is estimated with the navigational considerations of slowing down at restricted seaways as shown in **Figure 5-3.**

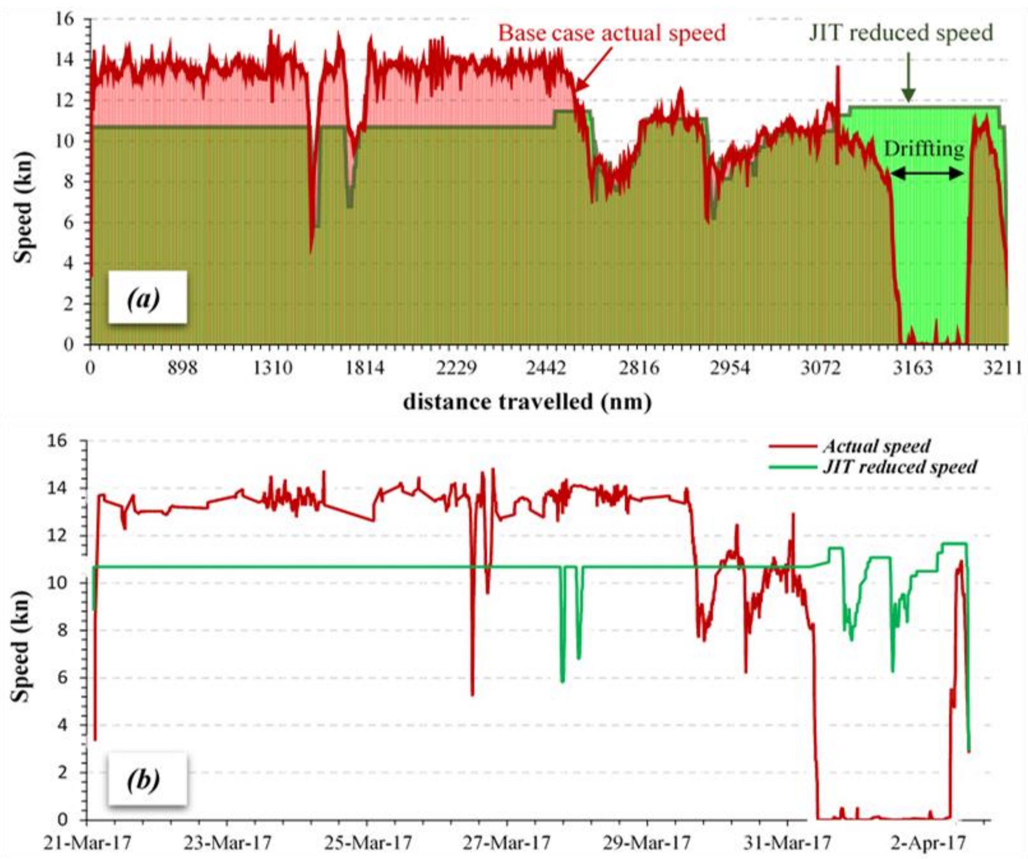


***Figure 5-3 (a)****- Slow steaming with JIT scenario at the same route conditions,*
***(b)****- JIT scenario time-series*

The forecast results of the potential operational energy efficiency benefit of JIT scenario as specified is summarized in table **Table 5-2.**

***Table 5-2*** *JIT scenario forecast results*

| *Criteria* | *Base Case* | *JIT scenario* | *unit* |
|---|---|---|---|
| *Total route distance* | 3215.50 | | *nm* |
| *Sailing time* | 11:13:00 | 12:14:20 | *dd:hh:mm* |
| *Driftting time* | 01:01:20 | 0.0 | *dd:hh:mm* |
| *Total voyage time* | 12:14:20 | 12:14:20 | *dd:hh:mm* |
| *Average ship speed* | 11.9 ** | 10.57 | *knots* |
| *Average propulsion power* | 7928.9 ** | 5720.9 | *kw.hr* |
| *Average B.S.F.C* | 186.04 ** | 187.43 | *g/kw.hr* |
| *Average RPM* | 51.99 ** | 47.04 | *revs* |
| *Daily fuel consumption* | 34.51 ** | 24.38 | *Mt/day* |
| *Fuel consumption per nm* | 0.135 | 0.097 | *mt/nm* |
| *Total energy consumed* | 2,355.8 | 1,669,57 | *Mw* |
| *Total voyage fuel consumed* | 434.8 | 312.8 | *mt* |
| *Speed reduction percentage* | 11.16% | | *%* |
| *Total $CO_2$ emissons savings* | 380.16, *(28.1%)* | | *Ton, %* |
| *Total voyage fuel cost savings (349.99$/mt)* | 42,686.6, *(28.1%)* | | *$, %* |

*** Values calculated with a drifting period exclusion for realistic evaluation.*

The results have shown high consistency level with the potential energy saving of slow steaming analysis discussed in **section 2.2.1.** The model has predicted that with a speed reduction of 11.16%, the fuel consumption dropped by 28.1% and 380 ton of $CO_2$ emissions is eleminated. However, and as discussed before, the improvement of ship's operation energy efficency requires the cooperation and involvement of the various key players, ship's operator (or the charter), ship's master, port authorities and the pormotion of energy awareness amongst all parties.

## *5.3 (Case study – 3) Voyage optimization Management*

The main goal of the case study is to assess the proposed DSS explained in **Chapter 3** to solve simple operational optimization problems. The proposed system is diagrammatically illustrated in the following figure; the figure shows the data flow through different system component platforms.

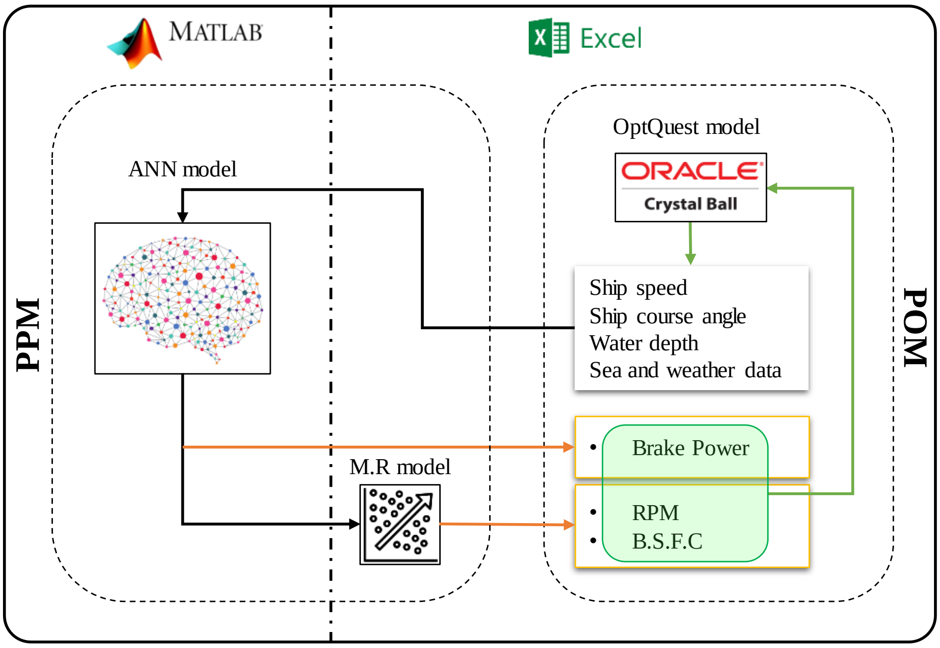


***Figure 5-4*** *Proposed-DSS information flow*

The designed Performance Prediction Model (PPM) and Performance Optimization Model (POM) are integrated and run simultaneously with each other. The system functionality is assessed against two scenarios. The first is a simulation scenario, while the second scenario aims to deterministically optimize the ship performance in a defined sea state by finding the optimum course direction and/or ship speed within the scenario conditions.

### *5.3.1 Scenario-a A voyage Monte Carlo simulation*

The simulation used the Monte Carlo simulation to simulate different sea conditions (from Beaufort number one to three) by probabilistic functions limited by the scenario parameters range shown in **Table 5-3**. The related cells identified as assumption variables, with uniform fit function and their correlation coefficient set as previously found in **Table 4-4**. The aim is to simulate the ship performance in different probabilistic sea conditions and to validate the system ability to forecast the ship performance under these circumstances. Additionally to validate the system ability to recognize the pattern between various variables and to produce the results accordingly. **Table 5-4**. summarizes the obtained forecast results 95% certainty level after 1000 iterations.

***Table 5-3*** *The simulation scenario variables range*

| *Variables* | *Upper value* | *Lower value* | unit |
|---|---|---|---|
| *Ship speed* | Constant (11.2) | | *kn* |
| *Ship course* | 359 | *0* | *deg* |
| *Wind/Wave direction* | 359 | *0* | *deg* |
| *Wind speed* | 5 | *0.79* | *m/s* |
| *Wave significant height* | 1.05 | *0.9* | *m* |
| *Wave significant period* | 3 | *1* | *s* |
| *Swell significant height* | 0.6 | 0.3 | *m* |
| *Swell significant period* | 4.5 | 1 | *s* |
| *Swell true angle* | 359 | 0 | *deg* |
| *Current speed* | 0.25 | 0.1 | *m/s* |
| *Current true angle* | 359 | 0 | *deg* |

**Figure 5-5** shows a noticeable variation in the consumed power at the same loading condition and ship speed, mainly because of weather effect disparity.

***Table 5-4*** *Probabilistic scenario simulation results summary*

| *Output* | *Minimum* | *Maximum* | *Mean* | *Std div* | *unit* |
|---|---|---|---|---|---|
| *Brake power* | 6063.9 | 8223.5 | 6778.3 | 420.3 | *Kw* |
| *B.S.F.C* | 185.98 | 187.21 | 186.81 | 0.24 | *g.kw.hr* |
| *RPM* | 48.47 | 53.64 | 50.28 | 1.03 | *revs* |
| *Fuel consumption/day* | 27.25 | 36.7 | 30.39 | 1.84 | *mt/day* |

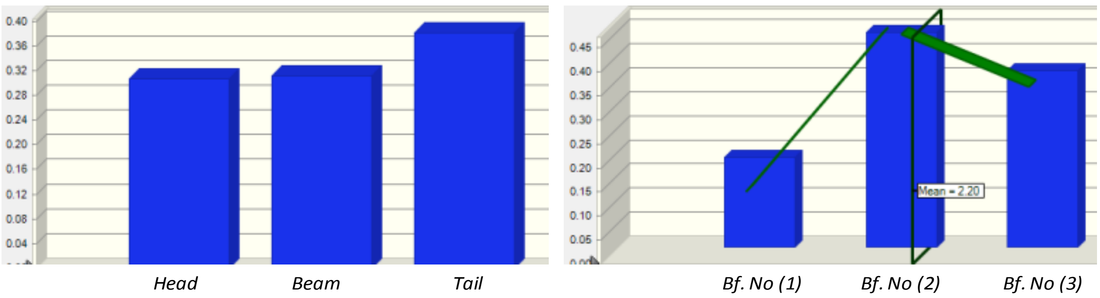


***Figure 5-5*** *The Simulation scenario weather state histogram*

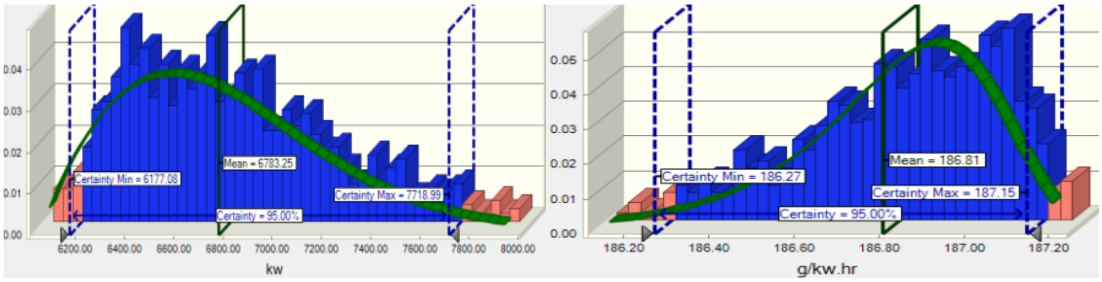


***Figure 5-6** The simulation scenario B.P and B.S.F.C forecast result*

Meanwhile, The sensitivity analysis of brake power showed highest correlation with the ship heading, wind direction and wind speed respectively. Finally, the fuel consumption analysis has shown (with 90% certainty) that its value will be 30 to 33 mt/day within the specified scenario conditions.

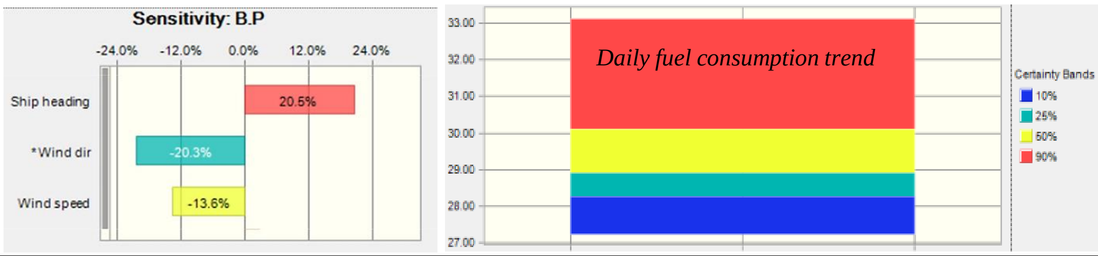


***Figure 5-7** Predicted brake power sensitivity analysis and fuel consumption trend.*

To sum up, the previous scenario results supported the proposed DSS ability to investigate and to provide a comprehensive analysis outcomes of the ship performance at several simulated sea state conditions. Moreover, If the weather forecast data of the ship future's voyage available, then the system can accomplish a precise prediction analysis with high confidence level, which then could lead to the final step, the optimization.

### *5.3.2 Scenario-b Voyage performance optimization*

Now, the DSS will be used to optimize the voyage performance. The voyage performance standard varies with the ship operator priority preferences. In some situations, the preference may oscillate to gain extra ship speed to arrive in time, while in other circumstances it may be preferable to operate the ship in a more energy-efficient way. In both situations, the ship operators have to trade off between both objectives to achieve their aim.

The scenario has been divided into two parts; ***the first part*** has the main objective set to minimize the ship brake power and is constrained by a minimum ship speed in a certain voyage conditions. In ***the second part***, the objective is traded to maximize the ship speed, but with a constraint of a particular brake power in the identical voyage conditions. The voyage base-case conditions set as follows:

***Table 5-5*** *Base-case voyage conditions*

| *Parameter* | *Base case Value* | *unit* |
|---|---|---|
| *Ship speed* | 11 | kn |
| *Ship course* | 00.00 | deg |
| *Brake power* | 8787.62 | kw |
| *RPM* | 54.84 | revs |
| *B.S.F.C* | 185.6 | g/kw.hr |
| *Fuel consumption* | 39.15 | Mt/day |
| *Beaufort no.* | 7 | |
| *Wind speed* | 14 | m/s |
| *Wind/Wave angle* | 348 | deg (Heading) |
| *Water depth* | 1387.98 | m |

### 5.3.2.1 Part-1 "Minimize the ship brake power" objective

- Run preferences: Deterministic optimization (without simulation)
- Number of iterations: 201
- Requirement: maintain ship speed at 11 kn
- Constraints: Ship's heading as a decision variable with 20 deg range (discrete with 0.1 deg step)

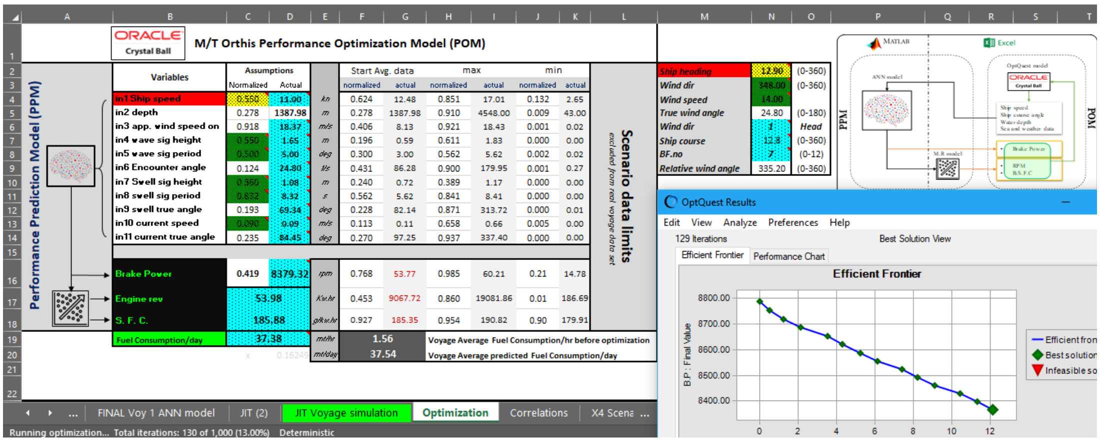


*Figure 5-8 Optimization process screenshot while running*

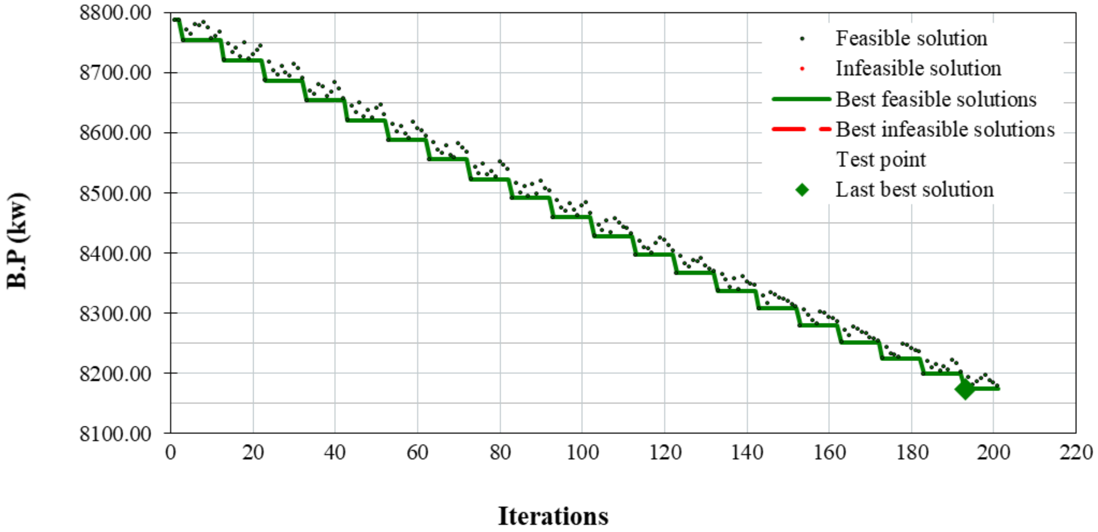


***Figure 5-9 Part-1*** *optimization performance*

The simulation ran for 2 minutes, and the attained optimization results as follows:

***Table 5-6 Part-1*** *optimization results summary*

| ***Obj. best results rank*** | ***Heading angle*** | ***Objective B.P (kw)*** | ***B.P diff (kw)*** | ***B.P savings %*** | ***Fuel Cons. (mt/day)*** |
|---|---|---|---|---|---|
| Base Case | 0.00 | 8787.62 | --- | | 39.27 |
| 01 (best) | 19.20 | 8173.83 | 613.8 | 6.98% | 36.53 |
| 02 | 18.20 | 8198.91 | 588.7 | 6.70% | 36.64 |
| 03 | 17.30 | 8224.98 | 562.6 | 6.40% | 36.76 |
| 04 | 16.30 | 8251.96 | 535.7 | 6.10% | 36.88 |
| 05 | 15.10 | 8279.75 | 507.9 | 5.78% | 37.00 |
| 06 | 14.30 | 8308.27 | 479.4 | 5.45% | 37.13 |
| 07 | 13.10 | 8337.46 | 450.2 | 5.12% | 37.26 |
| 08 | 12.10 | 8367.25 | 420.4 | 4.78% | 37.39 |
| 09 | 11.30 | 8397.57 | 390.1 | 4.44% | 37.53 |
| 10 | 10.40 | 8428.38 | 359.2 | 4.09% | 37.66 |
| 11 | 9.10 | 8459.62 | 328.0 | 3.73% | 37.80 |
| 12 | 8.20 | 8491.24 | 296.4 | 3.37% | 37.95 |
| 13 | 7.40 | 8523.21 | 264.4 | 3.01% | 38.09 |
| 14 | 6.10 | 8555.49 | 232.1 | 2.64% | 38.23 |
| 15 | 5.20 | 8588.05 | 199.6 | 2.27% | 38.38 |
| 16 | 4.30 | 8620.85 | 166.8 | 1.90% | 38.52 |
| 17 | 3.50 | 8653.86 | 133.8 | 1.52% | 38.67 |
| 18 | 2.10 | 8687.07 | 100.6 | 1.14% | 38.82 |
| 19 | 1.20 | 8720.45 | 67.2 | 0.76% | 38.97 |
| 20 | 0.50 | 8753.97 | 33.7 | 0.38% | 39.12 |

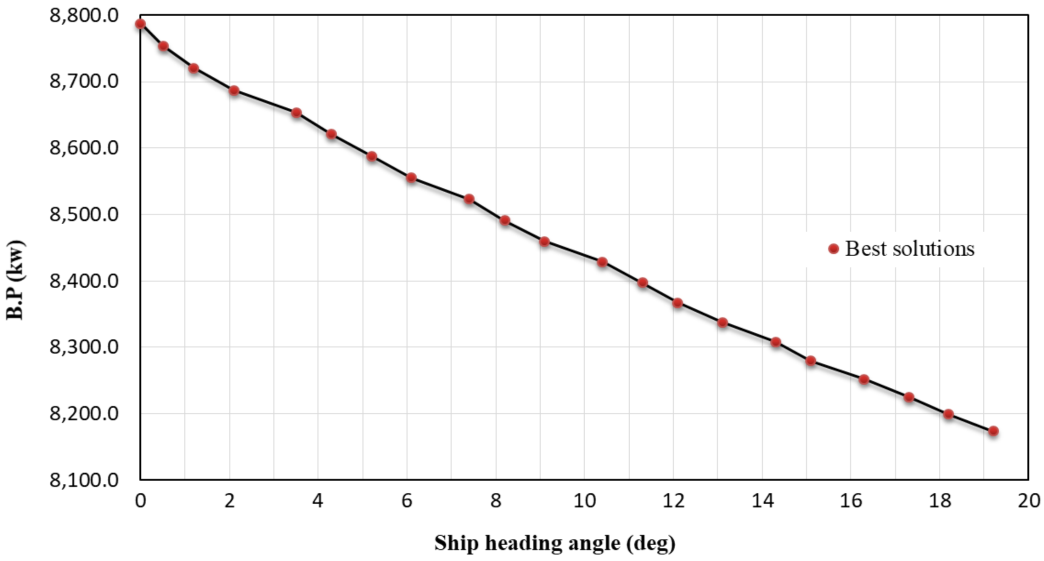


***Figure 5-10** Part-1 optimization results*

The results exposed a semilinear relationship between the obtained power saving and ship's heading adjustment to the starboard side as shown in Figure 4 14. The wind/waves were heading the ship with an encounter angle of 12 degrees. As the ship course alters, the wave/wind encounter angle increases and the wave relative direction changes to the ship's beam, which reduces the additional ship's resistance. However, the results are only representing the particular scenario conditions.

To conclude, the previous example showed the potentiality of weather routing as discussed before in chapter 2 with a fuel savings up to 7% under the terms of this particular scenario.

#### *5.3.2.2 Part-2 "Maximize the ship speed" objective*

- Run preferences: Deterministic optimization (without simulation)
- Number of iterations: 3000
- Requirement: maintain the brake power less than or equal to 8800 kw. In other words, any fuel savings obtained from heading angle change to be traded with a ship speed gain.
- Constraints: Ship's heading as a decision variable with 20 deg range (discrete with 0.1 deg step)

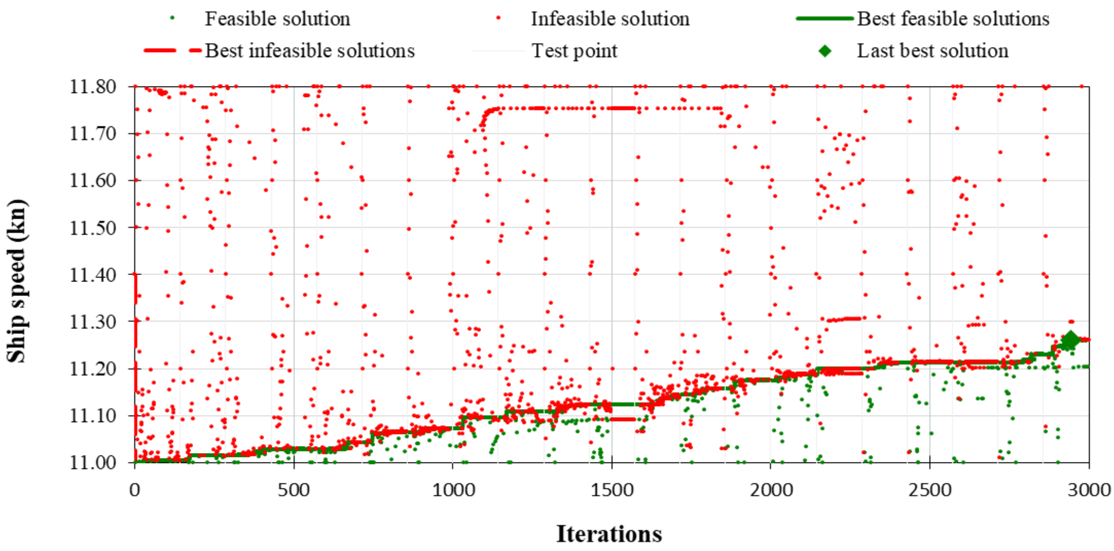


***Figure 5-11*** *Part-2 optimization performance*

The simulation ran for 37 minutes, and the attained optimization results as follows:

***Table 5-7*** *Part-2 optimization results summary*

| *Objective best results rank* | *Heading angle* | *Objective Vs (kn)* | *B.P (kw)* | *Vs gain %* | *Fuel Cons. (mt/day)* |
|---|---|---|---|---|---|
| **Base Case** | **00.00** | **11** | **8787.62** | | **39.27** |
| **01** | 19.00 | 11.23 | 8747.70 | 2.10% | 39.09 |
| **02** | 14.00 | 11.22 | 8691.98 | 2.00% | 38.84 |
| **03** | 13.00 | 11.21 | 8758.50 | 1.91% | 39.14 |
| **04** | 10.00 | 11.17 | 8790.4 | 1.56% | 39.28 |
| **05** | 01.40 | 11.16 | 8774.15 | 1.50% | 39.21 |

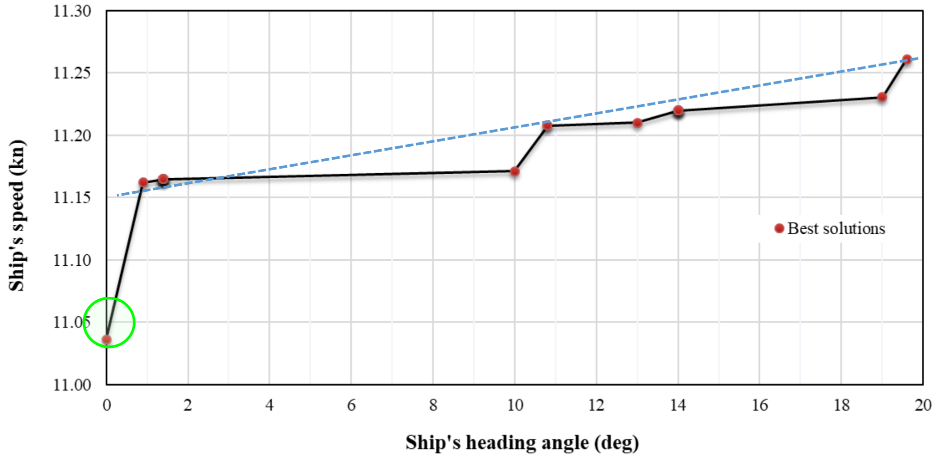


***Figure 5-12*** *Part-2 optimization results*

The results uncovered a nonlinear relationship between the obtained the ship's speed gain and the ship's heading angle adjustment as shown in **Figure 5-12**. The scenario tested for several times, and the results always showed the same trend. The justification may arise due to the different nature of the optimization problem than the Part-1 problem. In this scenario, the brake power requirement argument is set with an upper limit and not as a constant value like the ship speed in the part-1 problem. It is important also to understand that changing the ship heading angle, will change the swell and the current relative angles, which will influence their net effect on the ship resistance. Meanwhile, with the exclusion of the green circled point, the other solution points will have a better common trend (dashed blue line).

Now, concerning the results revealed in **Table 5-7**, the decision-making process has become more challenging than part-1 scenario, especially if this scenario is approached in a real-time domain with multiple alternatives and a short time frame for the decision. Solving such a problem may demand the implementation of a higher rank decision-making method with weights associated with each criterion to address the problem efficiently. Still, for the specific illustration in the table, solution ranked 5 in the table may become favored too as it requires only a change in ship's course by 1.40 degree, while the obtained speed gain represents 1.50% of the base case ship speed combined a slight fuel consumption reduction.Generally, the results showed a high reliability of the developed system.

# *Chapter 6.*

# *Conclusion*

The maritime transport is currently have been accounted for 2.5% of global GHG emissions with a forecast for this share to expand by 50% to 250% in 2050. (Third IMO GHG study, 2014) Thus, The IMO's environmental protection regulations are becoming stricter year after year which justifies the need for a more energy efficient shipping.Consequently, The shipping is currently stacking between the hammer of reducing its GHG emissions in an energy efficient way, and an anvil of being sustainable as it should be.

In the meantime, the technical upgrades are not the only way to achieve improvements in the ship energy efficiency, changing the crew operation behavior on board can gain cost-free energy savings. These potential behavioral savings need to be guided by analyzing the ship operational data and distinguishing the inherent opportunities in the ship dynamic operating environment. However, achieving an optimized energy-efficient performance for ship's operation is an enormous challenge that requires a robust mechanism of decision support system. The advisory system should assess the ship's fuel consumption of the various decision alternatives. Furthermore, it should advise the ship operator with the optimum values of the operational parameters to achieve optimum performance ideally in a real-time voyage condition. The success of such a system requires a comprehensive, validated performance prediction model integrated with a reliable performance optimization model.

The traditional ship's performance prediction methods have been used in the ship design phase with several methodologies applied throughout the years. However, for an effective DSS, there is a need to a prediction model that sense the actual environmental variables and analyzes their effect on the ship's performance. Also, it has to forecast the propulsion power needed throughout the voyage route under its dynamic conditions. Meanwhile, the Artificial Neural Networks has proven its applicability in many fields to forecast systems outputs that have many nonlinear relationships between its components.

All the above have motivated the research to aim to employ ANN as a non-classical methodology to predict the ship performance in seaways and to be integrated to a DSS that supplies the ship operator to maximize the ship energy efficiency during sea voyages.

The study has proposed an operational Decision Support System (DSS) that comprises mainly two primary components, the ship performance prediction Model (PPM) and the ship Performance Optimization Model (POM). Both models have been designed to run on a particular ship with its specific preferences. The PPM model includes two ANN and M.R sub-models to estimate the ship's power, B.S.F.C, and RPM respectively. The PPM is designed to use the ship's specifications with its historical voyage dataset to line up with the proposed methodology. Such a dataset is used to train the ANN model to build up its knowledge about the ship behavior in different operational scenarios. Finally, the proposed DSS has a dynamic nature and requires a full integration between its components for an efficient running.

The dataset used in this dissertation contains two sea voyages of M/T ORTHIS that had been extracted from the ship's automatic continuous monitoring system (CM), the AIS and weather hindcast information in an intensive samples pattern. The dataset correlation analysis results in many useful relations that were beneficial in classifying the dataset to determine the structure of the PPM. Moreover, the dataset has been deeply analyzed to recognize the relationship among its variables, especially the effect of the sea state on the ship's performance. The weather analysis demonstrated the potential cost-free energy savings in executing techniques like weather and route optimization as an operational measure. The given an example showed a 9.66% possible propulsion power gain by adopting a sea state number five to the favor of the ship movement when compared to a calm sea state one but heading the ship movement.

The developed ANN model aims to predict the ship B.P in different seaway conditions from a set of 11 input variables. The ANN input variables included ship's speed, sea water depth, and nine variables representing the weather and sea state environment. The ANN is A feed-forward backpropogation type network selected with a training function that updates weight and bias values according to Levenberg-Marquardt optimization.

The developed PPM can be exploited to predict the ship response to a particular voyage scenario or during the voyage itself to assess several available alternatives to improve the voyage's performance. To achieve such an objective, the performance optimization model (POM) should be fed with the performance forecast results to supply the needed advice to the ship's master.

The nature of the POM depends on the optimization problem nature. For the scope of this dissertation, only single-objective optimization model is aimed. The proposed POM employed the Oracle Crystal Ball add-in software to Excel. The tool could be used when planning for a new voyage with its simulation tool. The software has the capability of performing a random simulation based on a probabilistic approach with a user-defined probability fit function and correlation coefficients between the variables (the second case study). The study also has examined the system capability to perform a Monte Carlo simulation to the voyage environmental variables, and assess the ship propulsion power to the simulated scenario.

**Three case studies are presented in this thesis to demonstrate the proposed DSS applicability as a support tool that allows enhancing the voyage performance:**

1. ***The first case study*** aims to validate the PPM ability for forecast the ship fuel consumption for an entire voyage. The forecast result has shown high accuracy estimation of the consumed fuel. The ANN prediction error is highly related to the

training dataset quality which emphasizes the importance of using the ship continuous monitoring dataset over noon reports.

2. ***The second case study*** was designed to apply a slow steaming scenario based on just in time (JIT) assumption. The main purpose of the case study is to test the system capacity to estimate the fuel savings if such a scenario applied. The result is consistent to the well known the discussed relation between the speed reduction and corresponding fuel saving. The ship was slowed down by 11.16 %, and the PPM predicted the potential fuel savings of 28.1%.
3. ***The third case study*** is presented to demonstrate the DSS applicability as a support tool that assists the ship operator to maximize the ship energy efficiency. The case study also aims To test the ability of the DSS components to perform their functions in full complementarity between them.

   I. **The first scenario** exercised the POM to run a full Monte Carlo simulation to mimic the sea voyage environmental condition. The scenario result shows the DSS ability to investigate and to provide a comprehensive analysis outcomes of the ship performance at several simulated sea state conditions. Moreover, If the weather forecast data of the ship future's voyage available, then the system can accomplish a precise prediction analysis with high confidence level, which then could lead to the final step, the optimization.

   II. **The second scenario** is used to optimize the voyage performance in a predetermined sea state condition. The scenario was divided into two problems with two different objectives,

      a. ***Part-1:*** The objective is set to minimize the ship's brake power while maintaining the ship's speed variable by altering the ship's heading angle variable . However, the heading angle set as a constraint with a maximum value of 20 degrees. The DSS optimization results is ranked relative to the objective. The best result is obtained at heading angle 20 degrees with a power savings of 7%. The problem represents a simple optimization problem that can provide a simple result to the ship's master to enhance the ship voyage performance.

b. ***Part-2:*** The objective is set to maximize the ship's speed while maintaining the ship's brake power less than a certain value. The problem constraint is kept similar to the previous problem. The optimization result this time is more challenging. According to the objective best result, the highest speed gain (2.1 %) is obtained at the largest ship heading angle alteration (19.0 degree). However, the fifth rank result with a small heading angle alteration (1.4 degrees) achieved less speed gain with a narrow margin (0.6 %). Thre result requires a trade-off from the ship's captain to choose the optimum solution according to his preferences. However, there is no trade-off between safety and energy efficiency, as safety standards must be fulfilled first. In this dissertation, weather hindcast data is analyzed regarding its effect on the ship power and fuel consumption. Nevertheless, its effect on the ship safety and ship stability is beyond the scope of this dissertation. Nevertheless, for more holistic results, its influence on ship's stability must take into consideration.

Finally, the methodologies used in this thesis have been successfully applied in many domains, however integrating them together to accommodate the proposed DSS makes the proposed methodology novel. Additionally, the developed methodology has the following features:

1. developed an (ANN) model by using intensive dataset with a higher quality extracted from the ship continuous monitoring system unlike traditional Noon Reports used by previous studies.
2. The proposed (DSS) if integrated properly onboard, can be easily used in a real-time domain, which allows the system to identify the ship performance.
3. The proposed (DSS) can update itself automatically with the ship performance degradation as the (ANN) has the power to learn from the training data pattern. The system as continuously fed with the ship performance data on a real-time basis, the ANN can recognize the ship performance new trend.
4. The proposed DSS can be applied in any other ship regardless its type and size.

## *Recommendations for future work*

The research that has been undertaken for this thesis has highlighted some topics on which further research would be beneficial.

- The dataset in this thesis is limited, however to develop a general performance prediction model, a massive dataset is required to train the model at different loading conditions with the addition of variables like trim and DWT to the (ANN) input variables.
- The addition of new variables like, the ship trim will allow the application of trim optimization with the DSS.
- The second scenario of the third case study has evoked the need to a higher decision-making tool especially, if the safety criterion is added to the system objectives. Then a multi-objective optimization model is needed with a propriate Decision Making Method (DMM).

# Appendixes

1- ANN model performance results

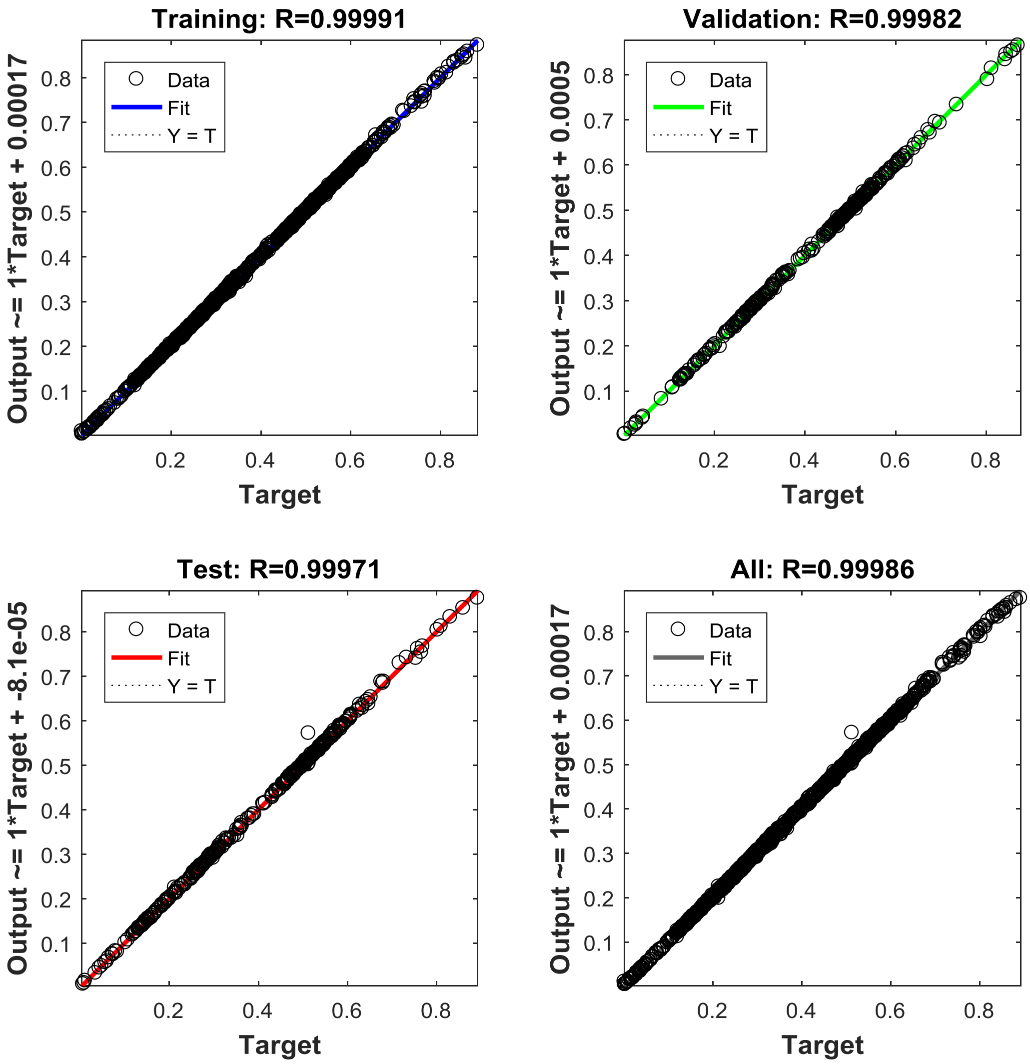

## 2- Screenshot of the JIT scenario evaluation

| sample no | optimized speed DateTime | Sample time hh:mm | Optimized Speed <m/s> | Optimized Speed kn | Time from departure dd:hh:mm | Sample distance nm | distance travelled nm |
|---|---|---|---|---|---|---|---|
| 1 | 3/21/2017 2:05 | 0.00 | 1.7 | 3.30 | 0.00 | 0.00 | 0.00 |
| 2 | 3/21/2017 2:10 | 00:05 | 3.2 | 6.22 | 00:00:05 | 0.20 | 0.20 |
| 3 | 3/21/2017 2:15 | 00:05 | 4 | 7.78 | 00:00:10 | 0.58 | 0.78 |
| 4 | 3/21/2017 2:20 | 00:05 | 4.3 | 8.36 | 00:00:15 | 0.67 | 1.45 |
| 5 | 3/21/2017 2:25 | 00:05 | 5 | 9.72 | 00:00:20 | 0.75 | 2.21 |
| 6 | 3/21/2017 2:30 | 00:05 | 5.3 | 10.30 | 00:00:25 | 0.83 | 3.04 |
| 7 | 3/21/2017 2:35 | 00:05 | 5.5 | 10.69 | 00:00:30 | 0.87 | 3.92 |
| 8 | 3/21/2017 2:40 | 00:05 | 5.5 | 10.69 | 00:00:35 | 0.89 | 4.81 |
| 9 | 3/21/2017 2:45 | 00:05 | 5.5 | 10.69 | 00:00:40 | 0.89 | 5.70 |
| 10 | 3/21/2017 2:50 | 00:05 | 5.5 | 10.69 | 00:00:45 | 0.89 | 6.59 |
| 11 | 3/21/2017 2:55 | 00:05 | 5.5 | 10.69 | 00:00:50 | 0.89 | 7.48 |
| 12 | 3/21/2017 3:00 | 00:05 | 5.5 | 10.69 | 00:00:55 | 0.89 | 8.37 |
| 13 | 3/21/2017 3:05 | 00:05 | 5.5 | 10.69 | 00:01:00 | 0.89 | 9.26 |
| 14 | 3/21/2017 3:10 | 00:05 | 5.5 | 10.69 | 00:01:05 | 0.89 | 10.15 |
| 15 | 3/21/2017 3:15 | 00:05 | 5.5 | 10.69 | 00:01:10 | 0.89 | 11.04 |
| 16 | 3/21/2017 3:20 | 00:05 | 5.5 | 10.69 | 00:01:15 | 0.89 | 11.93 |
| 17 | 3/21/2017 3:25 | 00:05 | 5.5 | 10.69 | 00:01:20 | 0.89 | 12.82 |
| 18 | 3/21/2017 3:30 | 00:05 | 5.5 | 10.69 | 00:01:25 | 0.89 | 13.72 |
| 19 | 3/21/2017 3:35 | 00:05 | 5.5 | 10.69 | 00:01:30 | 0.89 | 14.61 |

| sample no | optimized speed DateTime | Sample time hh:mm | Optimized Speed <m/s> | Optimized Speed kn | Sample distance | Time from departure dd:hh:mm | distance travelled nm | distance travelled nm |
|---|---|---|---|---|---|---|---|---|
| 1 | 3/21/2017 2:05 | 00:00 | 1.7 | 3.30 | 0.00 | 00:00:00 | 0.0 | 0.0 |
| 15 | 3/21/2017 3:15 | 01:10 | 5.5 | 10.69 | 12.47 | 00:01:10 | 11.0 | 10.8 |
| 15 | 3/21/2017 3:15 | 00:00 | 5.5 | 10.69 | 0.00 | 00:01:10 | 11.0 | 27.7 |
| 34 | 3/21/2017 4:50 | 01:35 | 5.5 | 10.69 | 16.93 | 00:02:44 | 28.0 | 53.3 |
| 34 | 3/21/2017 4:50 | 00:00 | 5.5 | 10.69 | 0.00 | 00:02:44 | 28.0 | 133.8 |
| 63 | 3/21/2017 7:15 | 02:24 | 5.5 | 10.69 | 25.84 | 00:05:09 | 53.8 | 145.8 |
| 63 | 3/21/2017 7:15 | 00:00 | 5.5 | 10.69 | 0.00 | 00:05:09 | 53.8 | 185.9 |
| 153 | 3/21/2017 14:45 | 07:29 | 5.5 | 10.69 | 80.18 | 00:12:39 | 134.0 | 191.4 |
| 153 | 3/21/2017 14:45 | 00:00 | 5.5 | 10.69 | 0.00 | 00:12:39 | 134.0 | 191.8 |
| 166 | 3/21/2017 15:50 | 01:05 | 5.5 | 10.69 | 11.58 | 00:13:44 | 145.6 | 210.5 |
| 166 | 3/21/2017 15:50 | 00:00 | 5.5 | 10.69 | 0.00 | 00:13:44 | 145.6 | 215.9 |
| 211 | 3/21/2017 19:35 | 03:44 | 5.5 | 10.69 | 40.09 | 00:17:29 | 185.7 | 316.0 |
| 211 | 3/21/2017 19:35 | 00:00 | 5.5 | 10.69 | 0.00 | 00:17:29 | 185.7 | 335.0 |
| 217 | 3/21/2017 20:05 | 00:30 | 5.5 | 10.69 | 5.35 | 00:17:59 | 191.0 | 337.2 |
| 217 | 3/21/2017 20:05 | 00:00 | 5.5 | 10.69 | 0.00 | 00:17:59 | 191.0 | 347.8 |
| 218 | 3/21/2017 20:10 | 00:05 | 5.5 | 10.69 | 0.89 | 00:18:04 | *191.9* | 362.8 |
| 218 | 3/21/2017 20:10 | 00:00 | 5.5 | 10.69 | 0.00 | 00:18:04 | 191.9 | 517.9 |
| 239 | 3/21/2017 21:55 | 01:45 | 5.5 | 10.69 | 18.71 | 00:19:49 | 210.6 | 643.9 |
| 239 | 3/21/2017 21:55 | 00:00 | 5.5 | 10.69 | 0.00 | 00:19:49 | 210.6 | 651.0 |

| sample F.C MT | Speed kn | Predicted RPM | Predicted Power | Predicted SFC gr/kw.hr | Comsumed energy <kw> | Estiamated Sample F.C <mt> | RPM diff | Power diff | SFC diff | Optimized Speed kn | sample time <hh> | Optimized RPM | optimized Power kw/hr | Predicted SFC gr/kw.hr | Comsumed energy <kw> | Estiamated fuel consumption <mt> | consumed energy diff <kw> | Fuel diff <mt> |
|---|---|---|---|---|---|---|---|---|---|---|---|---|---|---|---|---|---|---|
| 0.00 | 3.32 | 17.10 | 302.10 | 190.71 | 0.00 | 0.00 | 2.51 | 174.54 | 0.07 | 3.30 | 00:00 | 18.24 | 360.2458 | 190.67 | 0.00 | 0.00 | 0.00 | 0.000 |
| 0.28 | 3.32 | 17.32 | 313.00 | 190.70 | 997.65 | 0.19 | 1.22 | 105.72 | 0.02 | 10.69 | 01:10 | 50.10 | 6696.222 | 186.86 | 4116.03 | 0.78 | -3118.37 | -0.515 |
| 0.00 | 13.65 | 58.25 | 10544.07 | 184.36 | 0.00 | 0.00 | 0.53 | 434.11 | 0.32 | 10.69 | 00:00 | 50.07 | 6684.28 | 186.86 | 0.00 | 0.00 | 0.00 | 0.000 |
| 2.51 | 13.65 | 59.14 | 11036.93 | 183.96 | 13356.24 | 2.46 | 0.13 | 54.97 | 0.01 | 10.69 | 01:35 | 48.22 | 5971.581 | 187.27 | 10018.58 | 1.87 | 3337.65 | 0.551 |
| 0.00 | 13.73 | 59.67 | 11340.44 | 183.71 | 0.00 | 0.00 | 0.27 | 17.34 | 0.06 | 10.69 | 00:00 | 47.56 | 5730.048 | 187.40 | 0.00 | 0.00 | 0.00 | 0.000 |
| 3.87 | 13.73 | 59.08 | 11002.02 | 183.99 | 20843.65 | 3.83 | 0.17 | 222.03 | 0.15 | 10.69 | 02:24 | 46.68 | 5419.088 | 187.58 | 13471.01 | 2.53 | 7372.64 | 1.216 |
| 0.00 | 13.23 | 57.20 | 9979.25 | 184.79 | 0.00 | 0.00 | 0.04 | 162.47 | 0.09 | 10.69 | 00:00 | 46.60 | 5390.219 | 187.60 | 0.00 | 0.00 | 0.00 | 0.000 |
| 11.09 | 13.23 | 56.69 | 9711.10 | 184.99 | 59948.90 | 11.08 | 0.23 | 159.10 | 0.18 | 10.69 | 07:29 | 44.93 | 4834.957 | 187.93 | 38341.95 | 7.20 | 21606.95 | 3.565 |
| 0.00 | 12.25 | 52.84 | 7859.36 | 186.19 | 0.00 | 0.00 | 0.38 | 169.78 | 0.23 | 10.69 | 00:00 | 44.94 | 4839.475 | 187.93 | 0.00 | 0.00 | 0.00 | 0.000 |
| 1.40 | 12.25 | 52.70 | 7794.08 | 186.23 | 7672.36 | 1.43 | 0.29 | 149.47 | 0.21 | 10.69 | 01:05 | 45.47 | 5010.329 | 187.82 | 5334.97 | 1.00 | 2337.39 | 0.386 |
| 0.00 | 13.74 | 58.51 | 10688.18 | 184.24 | 0.00 | 0.00 | 0.00 | 90.10 | 0.10 | 10.69 | 00:00 | 45.48 | 5015.029 | 187.82 | 0.00 | 0.00 | 0.00 | 0.000 |
| 5.61 | 13.74 | 57.84 | 10320.84 | 184.53 | 30603.14 | 5.64 | 0.13 | 38.31 | 0.06 | 10.69 | 03:44 | 43.33 | 4340.803 | 188.23 | 17541.06 | 3.30 | 13062.08 | 2.155 |
| 0.00 | 13.09 | 55.30 | 9013.70 | 185.47 | 0.00 | 0.00 | 0.02 | 64.23 | 0.18 | 10.69 | 00:00 | 43.33 | 4340.286 | 188.23 | 0.00 | 0.00 | 0.00 | 0.000 |
| 0.70 | 13.09 | 55.39 | 9054.56 | 185.45 | 3786.81 | 0.70 | 0.04 | 88.04 | 0.19 | 10.69 | 00:30 | 43.51 | 4393.374 | 188.20 | 2183.28 | 0.41 | 1603.53 | 0.265 |
| 0.00 | 13.19 | 55.69 | 9206.26 | 185.34 | 0.00 | 0.00 | 0.03 | 55.00 | 0.15 | 10.69 | 00:00 | 43.50 | 4391.28 | 188.20 | 0.00 | 0.00 | 0.00 | 0.000 |
| 0.06 | 13.19 | 55.70 | 9210.34 | 185.34 | 301.83 | 0.06 | 0.03 | 58.07 | 0.15 | 10.69 | 00:05 | 43.52 | 4397.858 | 188.19 | 366.19 | 0.07 | -64.36 | -0.011 |
| 0.00 | 12.93 | 54.67 | 8707.85 | 185.67 | 0.00 | 0.00 | 0.01 | 61.99 | 0.20 | 10.69 | 00:00 | 43.53 | 4399.388 | 188.19 | 0.00 | 0.00 | 0.00 | 0.000 |

| | | | |
|---|---|---|---|
| Real voyage measured data | Total voyage fuel consumed | 434.8 | mt |
| | Fuel consumption per nm | 0.135 | mt/nm |
| | Daily fuel consumption | 34.51 | mt/day |
| | Total voyage fuel Cost (349.99$/mt) | $152,177.7 | $ |
| | Total energy consumed | 2,355.8 | MW |
| | Average propulsion power | 7928.96 | kw.hr |
| | Average speed | 11.90 | knots |
| | Sailing time | 12:14:20 | dd:hh:mm |
| | Average voyage sfc | 186.04 | g/kw.hr |
| | Total route distance | 3213.0 | nm |
| Voyage NN prediction results | Total fuel consumed | 439.9 | mt |
| | Fuel consumption per nm | 0.137 | t/nm |
| | Daily fuel consumption | 34.92 | t/day |
| | Average propulsion power | 8025.12 | kw.hr |
| | Predicted average voyage sfc | 186.04 | g/kw.hr |

# References


ABS. (2015). *Ship Energy Efficiency Measures.* Houston: TX.

Aldous, L., T.Smith, R.Bucknall, & P.Thompson. (2015). Uncertainty analysis in ship performance monitoring. *Ocean Engineering, 110*, 29-38. doi:https://doi.org/10.1016/J.OCEANENG.2015.05.043

Bal Besikci, E., Arslan, O., Turan, O., & Olcer, A. I. (2016). An artificial neural network based decision support system for energy efficient ship operations. *Computers & Operations Research, 66*, 393-401. doi:https://doi.org/10.1016/j.cor.2015.04.004

Bannstrand, M., Jonsson, A., Karlsson, R., & Johnson, H. (2016). *Study on the optimization of energy consumption as part of implementation of a ship energy efficiency management plan (SEEMP).* London: International Maritime Organization. Retrieved from http://www.imo.org/en/OurWork/Environment/PollutionPrevention/AirPollution/Documents/E-book.pdf#search=ballast%20optimization

Basheer, I., & Hajmeer, M. (2000). Artificial neural networks: fundamentals, computing, design, and application. *Microbiological Methods, 43*(1), 3-31. doi:https://doi.org/10.1016/S0167-7012(00)00201-3

Besikci, E. B., Arsalan, O., & Olcer, A. I. (2014). *Improving Energy Efficiency of Ships through Optimisation of Ship Operations.* Tokyo: IAMU.

Bhattacharyya, R. (1978). *Dynamics of marine vehicles.* New York: Wiley.

Bialystocki, N., & Konovessis, D. (2016). On the estimation of ship's fuel consumption and speed curve: A statistical approach. *Journal of Ocean Engineering and Science, 1*, 156-166.

Bukaty, V. M., & Morozova, S. U. (2013). Determining of the distance of the nearest approach of vessels with using information from AIS of relative ship plotting with a virtual second observation opech . In A. Weintrit, *Marine Navigation* and Safety of Sea Transportation: Advances in Marine Navigation* (pp. 23-26). CRC Press.

Chan, C.-C., & C.-H. C. (2013, August). Energy conservation for international dr ybulk carriers via vessel speed reduction. *Energy Policy, 59*, 710-715. Retrieved August 2017, from http://www.sciencedirect.com/science/article/pii/S0301421513002644?via%3Dihub

Christiansen, M., Fagerholt, K., Nygreen, B., & Ronen, D. (2013). Ship routing and scheduling in the new millennium. *European Journal of Operational Research, 228*, 467-483.

Demirel, Y. K., Khorasanchi, M., Turan, O., & Incecik, A. (2013). On the importance of antifouling coatings regarding ship resistance and powering. *Low Carbon Shipping Conference.* London. Retrieved from https://pure.strath.ac.uk/portal/files/30996372/Demirel_et_al.pdf

Demirel, Y. K., Turan, O., & Incecik, A. (2017). Predicting the effect of biofouling on ship resistance using CFD. *Applied Ocean Research, 62*, 100-118.

DNV-GL. (2015). *Eergy management study.*

DNV-GL. (June, 2017). *Low Carbon Shipping Towards 2050.* DNV-GL. Retrieved August 10, 2017, from https://www.dnvgl.com/maritime/publications/studies-papers.html

DNV-GL, GLOMEEP. (2014). *Autopilot adjustment and use*. (GLOMEEP) Retrieved August 2017, from http://glomeep.imo.org/technology/autopilot-adjustment-and-use/

et.al., N. T. (2014). *Guidelines for energy efficient ships.* Target project.

FoulXSpel. (n.d.). *FoulXSpel*. Retrieved August 2017, from http://www.foulxspel-antifouling.com

Haag, F., Kleverlaan, E., & Dispert, A. (2015). *Estimations of the contribution of international shipping to greenhouse gas emissions.* IMO. Retrieved from https://sustainabledevelopment.un.org/content/documents/636488-Haag-Estimations%20of%20the%20contribution%20of%20international%20shipping%20to%20greenhouse%20gas%20emissions.pdf

Havelock, T. H. (1922). The Effect of Shallow Water on Wave Resistance. *Proceedings of the Royal Society of London. Series A, Containing Papers of a Mathematical and Physical Character, 100*, 499-505. Retrieved August 2017, from http://www.jstor.org/stable/93825

Holtrop, J., & Mennen, G. (1982). An approximate power prediction method. *International Shipbuilding Progress, 29*, pp. 166-171.

International Maritime Organization. (2016). *MEPC-70*. Retrieved from IMO Website: http://www.imo.org/en/MediaCentre/MeetingSummaries/MEPC/Pages/MEPC-70th-session.aspx

ITTC. (2014). *Speed and Power Trials, Part 2, Analysis of Speed/Power Trial Data.* Copenhagen. Retrieved from https://ittc.info/downloads/proceedings/27th-conference-copenhagen-2014/

Kim, M., Hizir, O., Turan, O., Day, S., & Incecik, A. (2017). Estimation of added resistance and ship speed loss in a seaway. *Ocean Engineering, 141*, 465-476. Retrieved from http://dx.doi.org/10.1016/j.oceaneng.2017.06.051

Lu, R., Turan, O., Boulougouris, E., Banks, C., & Incecik, A. (2015). A semi-empirical ship operational performance prediction model for voyage optimization towards energy efficient shipping. *Ocean Engineering, 110 part B*, 18-28.

MAERSK. (2014, May 20). *Building the worlds biggest ship*. (Maersk) Retrieved August 15th, 2017, from http://www.maersk.com/en/hardware/innovation/case-stories/building-the-worlds-biggest-ship

MAN. (2012). *Slow Steaming, Benefiting retrofit solutions from MAN.* Denmark: MAN Diesel & Turbo.

MAN. (n.d.). *Basic Principles of ship propulsion.* Copenhagen: MAN Diesel & Turbo. Retrieved from http://pdf.nauticexpo.com/pdf/man-diesel-se/basic-principles-ship-propulsion/21500-86662.html

NAPA. (n.d.). *NAPA Fleet Intelligence*. Retrieved August 2017, from https://fleetintelligence.napa.fi/

National Oceanic and Atmospheric Administration (NOAA). (2015). Marine Beaufort Scale. United States of America. Retrieved June 2017, from https://www.ncdc.noaa.gov/sites/default/files/attachments/Marine_Beaufort_Scale.pdf

Ø.Buhaug, J.J.Corbett, Ø.Endresen, V.Eyring, J.Faber, S.Hanayama, . . . K.Yoshida. (2009). *Second IMO GHG study 2009.* London: International Maritime Organization (IMO).

Oracle. (2017). *OptQuest*. Retrieved from Crystal Ball: https://docs.oracle.com/cd/E57185_01/CBOUG/ch02s03.html

Parsons, M. G., & Scott, R. L. (2004). Formulation of multicrierion design optimization problems for solution with scalar numerical optimization methods. *Ship Research, 48,* 61-76.

Pedersen, B. P., & Larsen, J. (2009). Prediction of Full-Scale Propulsion Power using Artificial Neural Networks. *8th International Conference on Computer and IT Applications in the Maritime Industries (COMPIT'09).* Budapest, Hungary.

Perera, L. P., & Soares, C. G. (2017). Weather routing and safe ship handling in the future of shipping. *Ocean Engineering, 130,* 684-695. Retrieved July 2018, from http://www.sciencedirect.com/science/article/pii/S0029801816303808

Psaraftis, H. N., & Kontovas, C. A. (April 2009). CO2 emission statistics for the world commercial fleet. *WMU Journal of Maritime Affairs*. doi:10.1007/BF03195150

Rehmatulla, N., & Smith, T. (2015). Barriers to energy efficiency in shipping: A triangulated approach to investigate the principal agent problem. *Energy Policy, 84*, 44-57.

Reichel, M., Minchev, A., & Larsen, N. (2014). Trim Optimisation - Theory and Practice. *The International Journal on Marine Navigation and Safety of Sea Transportation, 8*, 387-392. doi:10.12716/1001.08.03.09

Samarasing, S. (2006). *Neural Network for applied sciences and engineering.* New York: Taylor & Francis Group, LLC.

Smith, S. W. (1997). Chapter 26: Neural Networks. In *The Scientist and Engineer's Guide to Digital Signal Processing* (pp. 451-480). San Diego: California Technical Publishing. Retrieved July 2017, from http://www.dspguide.com/CH26.PDF

Smith, T. W., Jalkanen, J., Anderson, B., Corbett, J., Faber, J., Hanayama, S., . . . Pande, A. (April 2015). *Third IMO GHG study 2014.* London: International Maritime Organization (IMO).

StatSoft, Inc. (2013). Electronic Statistics Textbook. Tulsa: StatSoft. Retrieved June 2017, from http://www.statsoft.com/textbook/

UNCTAD. (2016). *Review of Maritime Transport.* Geneva: United nations publication.

Veness, C. (2017). *Calculate distance, bearing and more between Latitude/Longitude points*. Retrieved from Movable Type Scripts: http://www.movable-type.co.uk/scripts/latlong.html

Wright, J., Colling, A., & Park, D. (1999). *Waves, Tides, and Shallow-water Processes.* Gulf Professional Publishing.